DESIGN AND IMPLEMENTATION OF AN ELECTRONIC FAN REGULATOR FOR REDUCED HARMONICS AND RIPPLE FREE SPEED

Kirielle Koralage Chandika Sudul Kiriella

188508D

Degree of Master of Science

Department of Electrical Engineering

University of Moratuwa

Sri Lanka

November 2021

DESIGN AND IMPLEMENTATION OF AN ELECTRONIC FAN REGULATOR FOR REDUCED HARMONICS AND RIPPLE FREE SPEED

Kirielle Koralage Chandika Sudul Kiriella

188508D

Dissertation submitted in partial fulfillment of the requirements for the degree Master of Science in Electrical Engineering

Department of Electrical Engineering

University of Moratuwa

Sri Lanka

November 2021

DECLARATION

I declare that this is my own work and this dissertation does not incorporate without acknowledgement any material previously submitted for a Degree or Diploma in any other University or institute of higher learning and to the best of my knowledge and belief it does not contain any material previously published or written by another person except where the acknowledgement is made in the text.

Also, I hereby grant to University of Moratuwa the non-exclusive right to reproduce and distribute my dissertation, in whole or in part in print, electronic or other medium. I retain the right to use this content in whole or part in future works (such as articles or books).

Signature: Date:

……. …….

K. K. C. S Kiriella

The above candidate has carried out research for the Masters Dissertation under our supervision.

Signature of the supervisor: Date:

……. …….

Prof. J. P. Karunadasa

Signature of the supervisor: Date:

……. …….

Dr. W. D. A. S Rodrigo

Abstract

A ceiling fan regulator is needed to control the speed of a ceiling fan. With the development of power electronic switching devices, electronic (triac based) fan regulator has been introduced to the market by ceiling fan manufacturers. Compared to old fan controlling methods like inductive and resistive fan controller, this method offers advantages like low power dissipation, compactness, step-less control etc.

Since this electronic fan regulator controls the effective voltage to the ceiling fan by chopping the waveform, it generates current and voltage harmonics. Speed ripples, low power factor issues, humming noises, mechanical oscillations, additional heating of the ceiling fan can be observed because of these low quality waveforms.

This research investigated a suitable power electronic based fan regulator for reduced harmonics and ripple free speed. The study was carried out by choosing 6 different power electronic based single phase motor controlling methods and examining their technical aspects and market competitiveness as a ceiling fan regulator.

Out of these 6 methods, DC chopper fed controller showed comparatively a best possible solution for above mentioned problems. Moreover, the simulation results were validated by implementing a prototype of a DC chopper fed controller. Unlike traditional electronic fan regulator, proposed method feeds the current continuously to the load. Thereby it reduces the speed ripples of the motor. Also FFT results suggests that the input, output current and voltage harmonics are significantly less in the proposed method compared to traditional electronic fan regulator.

Since the production cost of the proposed fan regulator is around Rs. 1870/= (2021 figure), and it involves smart remote controlling facility, the prototype can also be developed as a market competitive product.

Keywords: Ceiling Fan, Fan Regulator, Harmonics, PWM, Speed Ripples

ACKNOWLEDGEMENT

First and foremost, I'd want to thank my supervisor, Prof. J. P. Karunadasa, for his unwavering support during my M.Sc. studies. His extensive knowledge in the field, as well as the assistance and inspiration he provided, really aided me in completing this project. For my M.Sc. research, I could not have asked for a better supervisor.

In addition, I'd like to express my gratitude to Dr. W. D. A. S. Rodrigo, my co-supervisor, for his unwavering support and encouragement. I'd also like to express my gratitude for his informative comments made during the research.

I would also like to thank Prof. I. J. Dayawansa for allowing me to use electronics laboratory in SLIIT Academy for conducting experiments with my prototyped circuit. I highly appreciate Mr. Sumudu Sadees’s dedication on facilitating the experiment environment.

Finally, I would like to express my gratitude to my parents, Disna Wijeweera and Gunatilake Wijeweera, my brother Sameera, my sister Nethmini, and all of my colleagues for their assistance throughout this study.

DEDICATION

Thank you

for your kind affection towards me and all your sacrifices.

Dear Amma and Appachchi,

I would like to dedicate my dissertation

with heart full of happiness to you.

TABLE OF CONTENTS

LIST OF FIGURES

LIST OF TABLES

LIST OF ABBREVIATIONS

Abbreviation	Description
MOSFET	Metal Oxide Semiconductor Field Effect Transistor
FFT	Fast Fourier Transform
IDE	Integrated Development Environment
PWM	Pulse Width Modulation
ISR	Interrupt Service Routine
IGBT	Insulated Gate Bipolar Transistor
RMS	Root Mean Square
PCB	Printed Circuit Board
ESR	Equivalent Series Resistance
EFR	Electronic Fan Regulator
FR	Fan Regulator
SMD	Surface Mount Device
SMPS	Switching Mode Power Supply
AC	Alternating Current
DC	Direct Current
Hz	Hertz
DIAC	Diode for Alternating Current
TRIAC	Triode for Alternating Current
IR	Infrared
CAD	Computer Aided Design

LIST OF APPENDICES

CHAPTER 1

INTRODUCTION

Introduction

Different types of fan regulators can be seen in the market nowadays. Each and every one of them has its own merits and demerits. Although the traditional electronic (triac based) fan regulator offers impressive set of merits like compactness, step-less operation etc., several demerits can be seen because of its lower quality output waveforms.

The aim of this research is to build an affordable electronic fan regulator with higher quality output waveforms. This chapter will provide an introduction to this study by first discussing the study's background, research problem, research aim and objectives, research significance, limitations, and structural outline.

1.1 Background

A ceiling fan can be considered as an air flow controlling device using a mechanical action. In early 1860s and 1870s rotary ceiling fans were introduced in the United States. Those were not operated using electricity at that time, instead steam was used to make the rotation. Philip Diehl invented the first electrically operated ceiling fan in 1882.

As the name depicts, the ceiling fan regulator is an equipment which regulates the speed of the ceiling fan. Almost all of the fan regulators control the voltage across the fan motor and adjust the speed. So, a traditional fan regulator circuit controls this voltage and the user can adjust the speed by turning the rotatable knob of the regulator.

Fan regulators are being used since 1950s. Since early days, assorted switches and other methods were used to switch on the fan and control the speed. There are several types of fan regulators [3], [18].

I. Resistive type fan regulators
II. Capacitive type fan regulators
III. Inductive type fan regulators
IV. Triac based fan regulators (traditional electronic fan regulator)

With the development of the technology, Electronic fan regulators came into the market. Electronic type fan regulators consist power semiconductor components like DIAC and TRIAC. This regulator chops the sinusoidal waveform asymmetrically by electronic means and controls the effective voltage across the ceiling fan motor terminals. This lower quality waveforms generates current and voltage harmonics, speed ripples, low power factor issues, humming noises, mechanical oscillations, additional heating of the ceiling fan.

However, with the development of motor controlling technology, there are numerous ways have been presented in the past to control single phase induction motors [2]-[9] which the ceiling fans use most. Hence, there could be more cost effective and efficient method as a fan regulator design.

Nowadays, the ceiling fan regulator has become a smart module. Remote controllability, touch controls, voice activated features…etc. make it more attractive. Also there is a trend using energy-efficient, remote/app controlled brushless DC motors as ceiling fans nowadays.

1.2 Research Problem

Traditional electronic fan regulator has been used for speed controlling of ceiling fans for decades. However, it generates several problems such as humming noise, vibrations, unwanted heating, shorter lifetime etc. Most of these occur due to lower quality output waveforms [4], [19].

Most of the ceiling fans are single phase induction motors. Although novel methods for these motors are presented in literature[2]-[9], there are no comparative studies carried out by showing power electronic based affordable controllers with quality output waveforms focused for ceiling fan speed regulators.

By carrying out this research, it is possible to find the best suited design for a reliable fan regulator with quality output waveforms with an affordable price.

1.3 Research aim and objectives

Aim of this research is to create an affordable electronic fan regulator with reduced harmonics and ripple free speed. This was achieved by performing technical and cost analysis of novel designs of fan regulators with traditional electronic fan regulator.

Following are the objectives identified for this research:

I. Evaluate adverse impacts due to speed ripples, voltage and current harmonics of traditional electronic fan regulators.
II. Investigate different power electronic based methods to control the speed of ceiling fans
III. Access control methods, design aspects and cost of proposed fan regulator systems
IV. Implement best-suited system and evaluating its performance compared to existing system

1.4 Research significance

By carrying out this study, it is possible to introduce a novel electronic fan regulator with high performing capabilities to an affordable price. Since the aimed fan regulator offers less speed ripples and less humming in low speeds, it can be suitable for places like libraries. Also compared to traditional electronic fan regulator proposed system will reduce the generated heat and increase the durability in the fan by generating quality output waveforms.

1.5 Research limitations

Nowadays, DC operated ceiling fans are available in the market too. However, this research is only focused on regulators for ceiling fans operated with AC mains.

Furthermore, developed hardware for this research is based on Atmega328P microcontroller. Usage of different microcontroller can affect price variations and performance of the product.

1.6 Structural outline

Chapter one of this dissertation is dedicated to present the background of the study, research problem, research aim and objectives, research significance, research limitations and structural outline.

Chapter two provides a literature review of different types of single phase induction motors, single phase motor control methods, commercially available ceiling fan controllers, novel power electronic based single phase motor controllers and outcomes of literature review.

Chapter three presents mathematical modeling of ceiling fan in simulation environment, simulation of novel power electronic based fan regulators, simulation of traditional electronic fan regulator, analysis of technical aspects of fan regulators, cost analysis and filtering out best solution for research problems stated.

Chapter four of this study discusses hardware development of chosen fan regulator by first discussing microcontroller selection followed by implementing complementary switching and dead time, algorithm, active switches, gate drivers and signal power isolation, mitigation of ringing, input filter design and PCB development.

Fifth chapter is dedicated to present research findings. It includes how the experiment setup was formed, comparison of obtained waveforms and FFT results and analysis of obtained waveforms.

Sixth chapter of this study concludes research findings by highlighting how proposed fan regulator met the aim and objective of the research, its importance and recommendation for future work.

CHAPTER 2

LITERATURE REVIEW

Introduction

Ceiling fan regulator is a subcategory of a single phase induction motor controllers. Chapter 2 of this study is dedicated to present the work that has already been carried out with regards to single phase motor controllers. Since the study focused on ceiling fans and their controllers, this chapter describes different types of single phase induction motors, commercially available ceiling fan regulators as well.

2.1 Different types of single phase induction motors

The majority of ceiling fans on the market today use single phase induction motors. There are various types of single phase induction motors available. By investigating on this area, it is possible to acquire which type of single phase motors are mostly used in ceiling fans, their internal construction, torque, speed and power outputs.

2.1.1 Shaded pole induction motors

Shaded pole induction motor (figure 2.1) is one of the single-phase motors which one pole is shaded by a copper ring [25]. Hence the name depicts. This previously mentioned shaded copper ring acts as the secondary winding of the induction motor. This motor can rotate in one direction only.

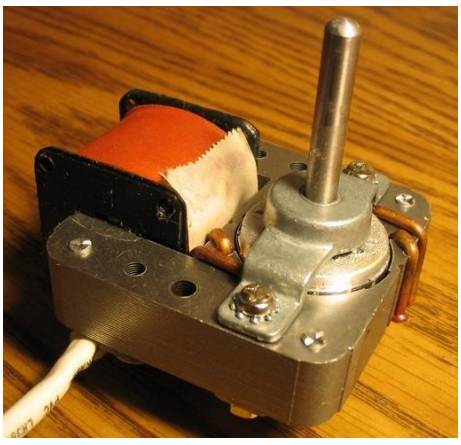

1*Figure 2.1: A shaded pole induction motor*

Power factor of this motor is low in value. Starting torque of these motors are very low compared to other single phase induction motors. However, this motor offers less maintenance and low cost. These motors can be seen in exhaust Fans, refrigerators, projectors, air conditioners, photocopy machines, relays …etc.

2.1.2 Split phase induction motors

This type of motor has a single caged rotor and this motor is known as resistance start induction motor too. Two windings in the stator (figure 2.2), main winding and starter winding (or auxiliary winding) are placed in the motor making a 90-degree electrical angle in between them. Resistance and reactance of these windings are different. Ratio of main winding resistance to reactance is smaller than the ratio of auxiliary winding resistance to reactance.

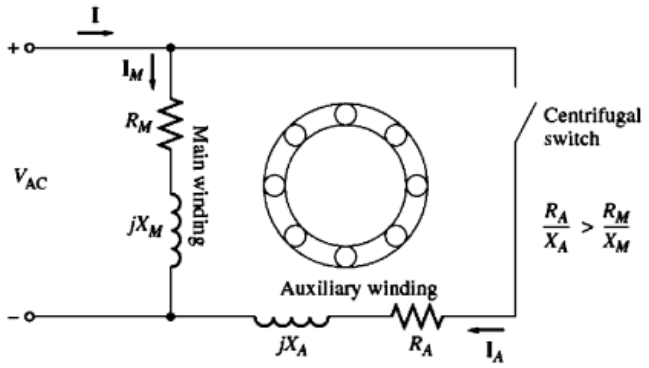

2Figure 2.2: Circuit diagram of a split phase induction motor

There is a centrifugal switch attached in the auxiliary winding to remove that path when the motor is running higher than a set speed. In this way, the motor can create higher starting torque compared to previous method.

2.1.3 Permanent split capacitor induction motors

In this motor, a capacitor is permanently connected (figure 2.3). The capacitor is used to generate a second power supply phase by generating a magnetic field. This operation provides the torque which is required to start the motor. Auxiliary winding and the capacitor are connected in series. Rotor of the motor is a squirrel caged one. This motor is also called as “single value capacitor motor”.

The starting torque of these types of motors are somewhat low since the capacitor is tuned to perform best at running conditions. The operation of the motor

produces very less noise with pure sinusoidal waveforms. This motor type is used in ceiling fan, table fan, exhaust fan and intake fan applications. Typically 1-3 uf split capacitor values are used in market available permanent split capacitor motors.

(a)

Table fan motor with the permanent split capacitor(black colored)

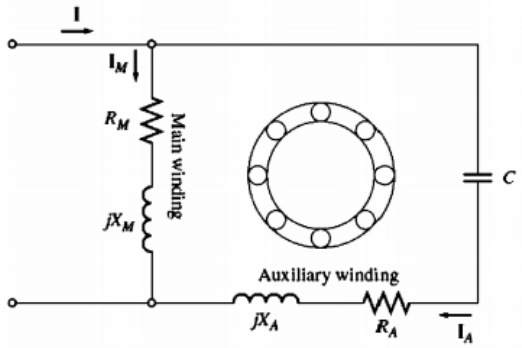

(b)

Circuit diagram of a permanent split capacitor induction motor

3Figure 2.3: A permanent split capacitor motor and its circuit diagram

2.1.4 Capacitor start induction motors

In this type of motors, there is a capacitor connected in series with the auxiliary winding (figure 2.4). It generates a phase difference between main winding and the auxiliary winding. So that, the starting torque can be generated. Main winding current is lagging the auxiliary winding by 90 degrees. Two windings are arranged in the motor to make a 90-degree electrical angle in between them.

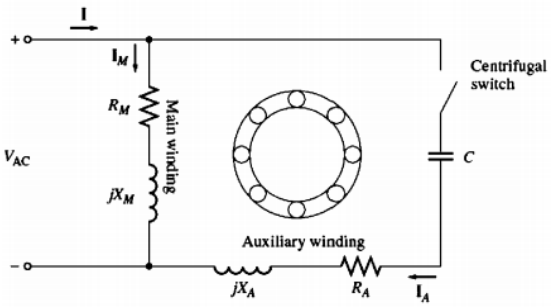

4Figure 2.4: Circuit diagram of a capacitor start induction motor

Since a capacitor is used, starting torque is higher than split phase induction motors and it can be even more than 300% of its rated torque. When the motor reaches its set speed, the capacitor and the auxiliary winding is disconnected by

a centrifugal switch which is operating by using the shaft itself. This type of motors can be seen in air conditioners, pumps, compressors… etc.

2.1.5 Capacitor start – capacitor run induction motors

Two capacitors used in this motor are connected in parallel (figure 2.5). Since a large amount of current is required to start the motor, the reactance of the starter capacitor has to be low in order to make low impedance auxiliary path. As seen in the general equation of the capacitor, $X_c = \frac{1}{2\pi f C}$ to make the reactance low, the capacitance C of the capacitor has to be high. So, the starting capacitor is a high value capacitor (15uf – 300uf).

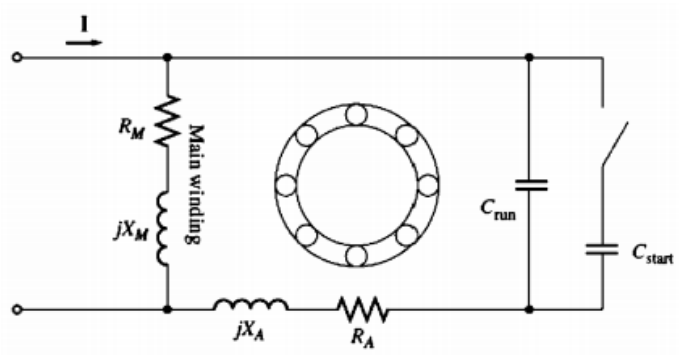

5Figure 2.5: Circuit diagram of a capacitor start – capacitor run induction motor

Typical running capacitor values are ranging from 1 uf to 30 uf. This motor not only produces high starting torque but also comes with impressive running torques as well. However compared to other motors, this motor is costly. Capacitor start – capacitor run motors can be seen in conveyer and compressor applications.

2.2 Speed control of single phase induction motors

After discussing different types of single types of induction motors, the control of single phase induction motors should be analyzed. There are three basic speed controlling techniques are available for squirrel caged type induction motors [1]. Those are,

I. Changing stator frequency
II. Changing number of poles
III. Changing applied terminal voltage

Considering the individual methods, description of each method is given as follows:

2.2.1 Changing stator frequency

Motor speed can be controlled by changing the supply to the motor. Compared to other methods, this method presents wide range of speed values. However, in order to preserve safety one has to use this within motor's voltage and torque limits. Working principle of this method can be explained mathematically as follows:

Synchronous speed of an induction motor $(N_s) = \frac{60f}{p}$……. (1)

Where; p = number of pole pairs

f = frequency of the supply

Slip equation $(s) = \frac{N_s - N_r}{N_s}$ …… (2)

Where; N_r = rotor speed

By using (1) and (2);

$$N_r = \frac{60f(1-s)}{p} \text{……. (3)}$$

According to equation 3, rotor speed can be changed by changing the supply frequency. Variable frequency drivers are used in industry to realize this mechanism with some other impressive features. Also there are a lot of control topologies and control were developed in the literature taking frequency control as the base and some of them were discussed briefly in section 2.4 of this study.

2.2.2 Changing number of poles

By keeping the frequency of the motor as a constant value, the rotor speed can again be altered by changing number of poles (p). However, this time the rotor speed and the number of poles are inversely proportional. So, the speed of the motor can be decreased by increasing the number of active poles which are in the stator. There are three methods to change the number of poles in the stator.

I. Multiple stator winding
II. Consequent pole method
III. Pole amplitude modulation

2.2.2.1 Multiple stator winding

In this method, if two windings are provided at two different pole locations and each winding is energized in different times.

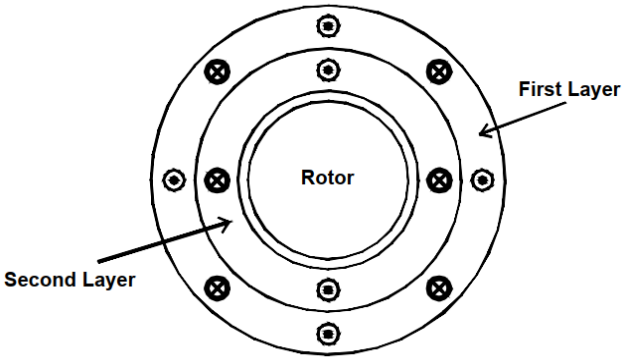

6*Figure 2.6: Multiple stator winding method*

Considering the number of poles in the second stator winding set is 4, and the line frequency is 50 Hz, synchronous speed of the motor will be 1500 rpm. If the first layer is used, synchronous speed will be 750 rpm. Hence the rotor speed will also change.

However, this method not efficient compared to other methods. Since the stator has two layers, it is costly and the setup is heavy.

2.2.2.2 Consequent pole method

For this method, coils are arranged to have a gap in between them. When the current flow is changed in a set of coils, the poles are changed to show same kind of poles. This same kind of poles then automatically induced the opposite pole in the gap by the nearby coil. Those induced poles are called consequent poles. In that manner, if the previous number of poles is 2(figure 2.7), after changing the direction of current, the number of poles will change into 4 with the addition of the consequent poles. By doing so, the motor speed will become half.

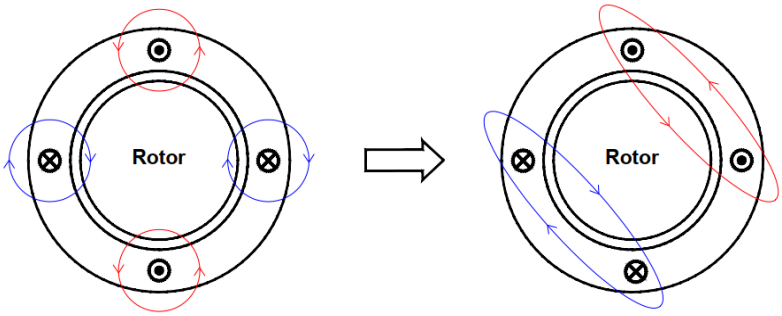

7Figure 2.7: Consequent pole method

2.2.2.3 Pole amplitude modulation

In this case, speed controlling is done using signal modulation technique. This method is carried out by applying waves to different poles separately and by doing so, active poles are neutralized to have less poles. As an example, if there were 8 poles in the stator winding, then after applying a two-pole modulating ware, that 8 active poles can become 6 poles. To perform this action, coil inversion method and omission method are used.

2.2.3 Changing applied terminal voltage

There are several methods are being used like, using a series resister, series inductor, series AC capacitor, auto transformer or using a triac controller. All these methods are field weakening methods. This is done by changing the terminal voltage to the motor. By doing so, torque – speed characteristics can be altered (figure 2.8) and obtain different speed values.

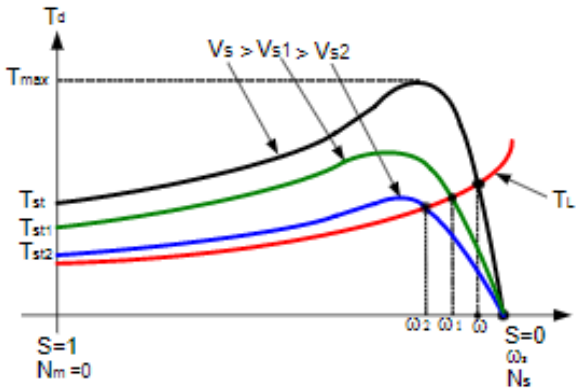

8Figure 2.8: Torque speed characteristics with different terminal voltages (Vs, Vs1, Vs2)

Lots of commercially available fan controllers utilize one of these methods to change the speed of the fan motor.

2.3 Commercially available ceiling fan regulators

Several different types of ceiling fan regulators are available in the market. Subtopics 2.3.1 – 2.3.5 are dedicated to discuss their general arrangement, working principle and advantages and disadvantages.

2.3.1 Resistive type fan regulators

In early stages, the regulator consisted with a set of resistors to adjust the voltage across the motor of the fan. When the rotatable knob aligned with a particular resistor, the voltage across the motor of the fan drops according to the aligned resistance in the regulator. Compared to other methods, this method generates more heat due to resistors.

2.3.2 Capacitive type fan regulators

Here, a set of capacitors are connected to the terminals of the motor. The voltage across the capacitor is inversely proportional to the capacitance of the capacitor. Parts of two market available capacitive fan regulators are shown in figure 2.9.

9*Figure 2.9: Parts of market available capacitive type fan regulators*

Polyester film capacitors (brownish capacitors shown in figure 2.9) are used to reduce the voltage across the fan. This regulator offers hum-less operation. However, these capacitors weaken over time it can cause fire hazards and some intermediate speed steps may not work properly. Cost of this kind of a fan regulator is roughly about Rs. 1000/= (year 2021 figure).

2.3.3 Inductive type fan regulators

This fan regulator has a transformer with multiple tapping. By connecting to each tapping end, the inductive reactance is changed and hence the voltage across the motor is changed. When increased the number of turns in the induction coil connected to the fan, the speed of the fan is decreased. This method is quite costly and bulky and has a low power factor. The advantage in this method is it has low power dissipation compared to resistive type fan regulators.

2.3.4 Triac based fan regulators

In this circuit, motor voltage is controlled by a triac. Figure 2.10 shows circuit diagram a of market available triac based fan regulator (traditional electronic fan regulator).

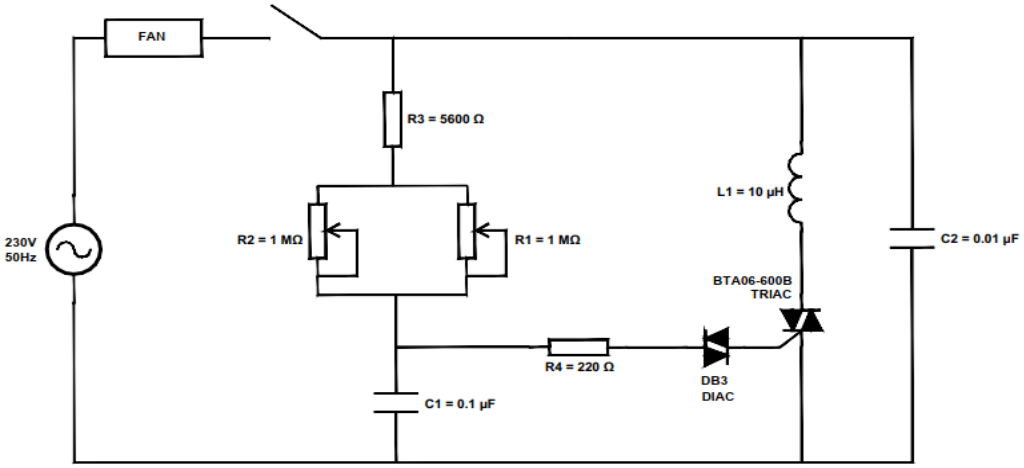

10Figure 2.10: Circuit diagram of a market available triac based fan regulator

When the supply is available C1 capacitor starts charging. After it exceeds diac's breakdown voltage, DB3 conducts and C1 will discharge along R4-> DB3->triac->C1 closed path. As a result triac will be triggered and line current starts flowing through main terminals of the triac. C1 capacitor charge time can be adjusted by varying R1 and R2 resistors. Normally in a commercially available fan regulator, R1 is given to set the minimum speed for fan at the installation. R2 is fixed to the rotatable knob. R4 is used to limit the trigger current to a desired level. Inductor is used to limit di/dt across the triac. 0.01 uf capacitor is used as the snubber capacitor for triac.

Theoretically, this kind of a fan regulator should generate a voltage waveform across the fan like shown in figure 2.11. Effective voltage to the ceiling fan (blue colored portion) can be changed by adjusting variable resistor value. However, practically obtained waveforms have some discrepancies and those are explained in chapter 5 of this research.

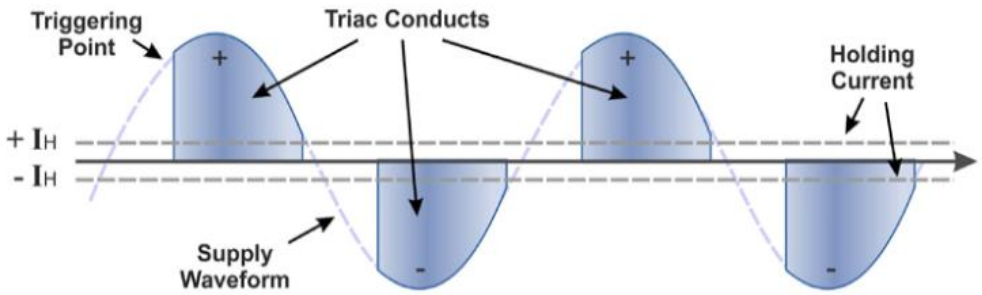

11Figure 2.11: Terminal voltage waveform (theoretical) when utilizing a triac based controller

Traditional electronic fan regulators are compact in size and it costs almost same as capacitive type fan regulators. However it causes some problems like higher speed oscillations of the fan, low input power factor, generation of current and voltage harmonics at low speeds, additional heat generation in the fan motor, humming noise…etc [2], [4], [19].

2.3.5 Smart fan regulators

In those regulators, control is done remotely using IR waves, radio waves or touching the regulator screen. In order to make it remotely operated Wi-Fi and dedicated mobile app is used. By this method, fan can be controlled remotely from anywhere in the world. In those regulators, ESP-32 or other Wi-Fi module is used to transmit and receive the control signals.

(a) Wi-Fi connected regulator

(b) Smart touch controlled regulator

12Figure 2.12: Smart fan regulators

2.4 Novel power electronic based single phase motor controllers

This section of the study is dedicated to examine novel power electronic based motor controllers. By going through various topologies, it is possible to acquire merits and demerits of them and ultimately the possibility of developing them as a ceiling fan controller.

2.4.1 DC chopper fed controller

This topology basically needs a bridge rectifier and an active switch to control the effective voltage across the load. By changing duty cycle given to the active switch this can be realized. However, it is better to add complementary operated active switch and bridge rectifier across the load to compensate the flyback if the load is inductive.

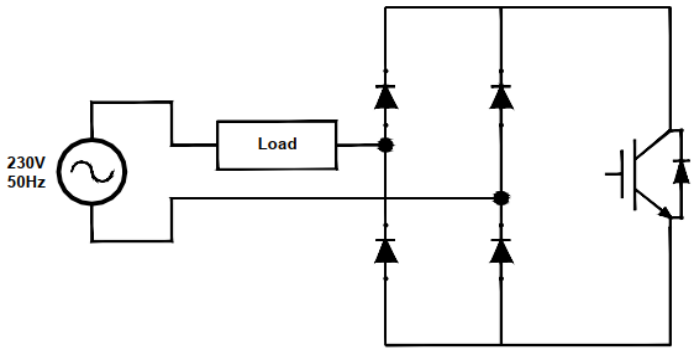

13Figure 2.12: Generalized circuit diagram for DC chopper fed controller

Compared to other controls this method offers cheap, simple control. Also it can reduce low order harmonics. This type of control and topology are recorded in [3] and [4].

2.4.2 Conventional cyclo-converters

Cyclo-converter is a circuit which takes fixed voltage and fixed frequency AC power as input and provides variable frequency and variable voltage AC power as output. This operation is done without a DC link [23], [24]. Conventional cyclo-converters are step down cyclo-converters. There are several types, which are,

I. Single-Phase to Single-Phase
II. Three-Phase to Single-Phase
III. Three-Phase to Three-Phase

Working principle of the above cyclo-converters are almost similar but the number switching circuits are the fact that defines the differences of the circuit types.

Cyclo-converter has two switching circuits on the both sides of the load. One circuit performs at the positive half cycle of the supply power signal and the other circuit performs at the negative half cycle of the power signal. Although switching circuit is represents with thyristors (figure 2.13), modern cyclo-converters use other active switches such as IGBTs, MOSFETs…etc. Switching circuit is operated by a microcontroller. Single phase – single phase, three phase-single phase and three phase – three phase, cyclo-converters have around 8, 12 and 36 active power electronic switches to operate. Cyclo-converters offer intermediate speed range for motor and intermediate control complexity. However, the setup is somewhat bulky.

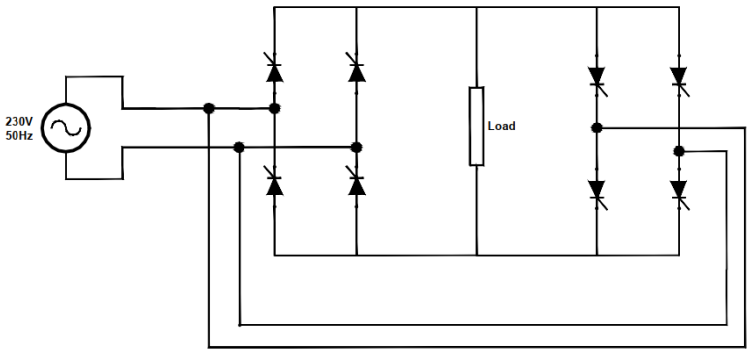

14*Figure 2.13: Single phase – single phase cyclo-converter*

2.4.3 Non-Conventional cyclo-converter

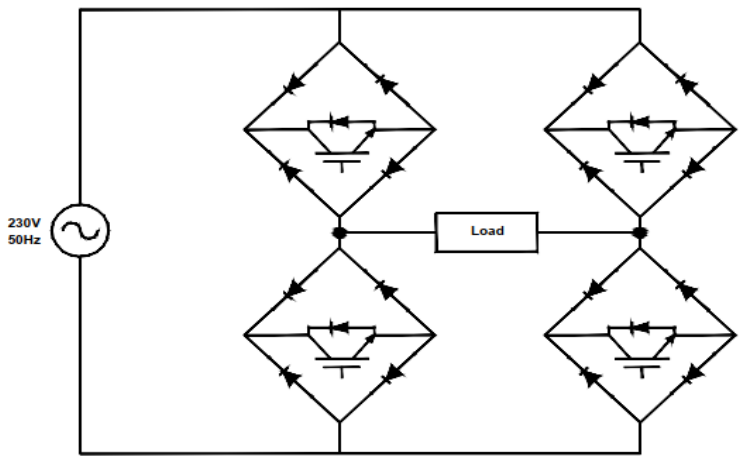

15*Figure 2.14: Non-conventional cyclo-converter*

Figure 2.14 shows a single phase non-conventional cyclo converter. It needs 4 uni-directional active switches and 16 diodes. Diodes are formed as bridge rectifiers for active switches. This can control both voltage and frequency of the ac signal.

Compared to conventional cyclo-converter, bulkiness and cost is low in this topology. Costly DC link capacitors are also absent. However some studies suggest this method has low efficiency and somewhat high THD in low speeds [5]. It also needs a separate switching strategy to supply same frequency of the switching signal generator to the load.

2.4.4 Burst firing method

This is one of the common thyristor firing method. The same can be used as a speed controlling purposes of single phase motors [6]. This is also called the zero-voltage crossover firing. In this method, thyristor gets gate signals only when the voltage through its main terminals is zero. In this case, the thyristor switches on and off at the zero-voltage crossing point of the voltage sine wave (figure 2.15). By the firing circuit, the switch on and off timing is adjusted and set according to the load. This bursting occurs in each half cycle of the sine wave.

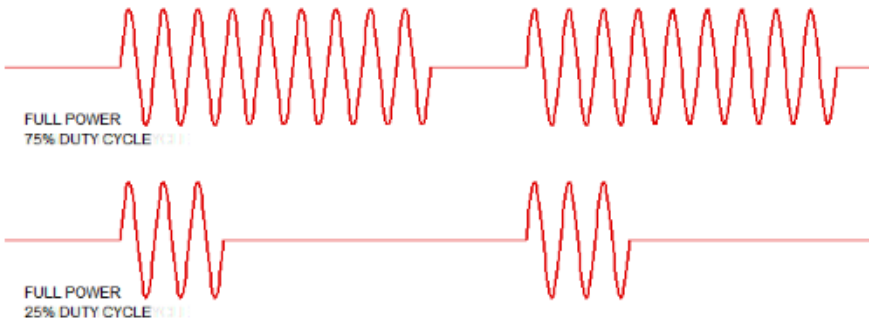

16*Figure 2.15: Voltage across the load when utilizing burst firing method*

Compared to methods discussed in 2.4.2 and 2.4.3, this method is cheaper and less in complex. Although this method offers less interferences to the nearby loads, it generates subharmonics of the power frequency which is bit difficult to filter.

2.4.5 AC-AC buck converter

This is an AC chopper circuit operated using PWM control [20], [21]. Switches S1 and S2 (figure 2.16) can be realized using back to back MOSFETs or IGBTs. These switches have to work in a complementary manner with PWM signals. S1 (main switch) is required to power up the load and S2 (auxillary switch) is required as a freewheeling path to the load.

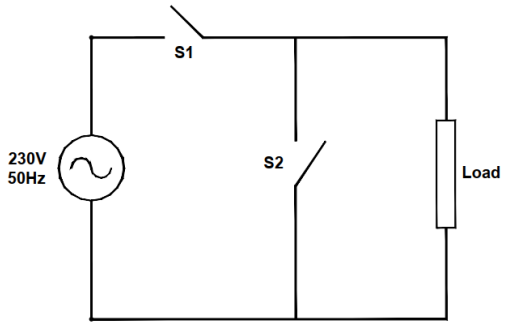

17Figure 2.16: Generalized circuit diagram for AC – AC buck converter

Input harmonics generated in this topology can be filtered out using simple passive filters [7].This also offers simple control, continuous load current for inductive loads and less implementation cost.

2.4.6 Single phase PWM inverter with full bridge rectifier

In this circuit arrangement, a full bridge IGBT based inverter is used. In addition to that, the source is connected through a diode rectifier which is arranged as a full bridge. To supply the reactive power to the motor, a DC link capacitor is used.

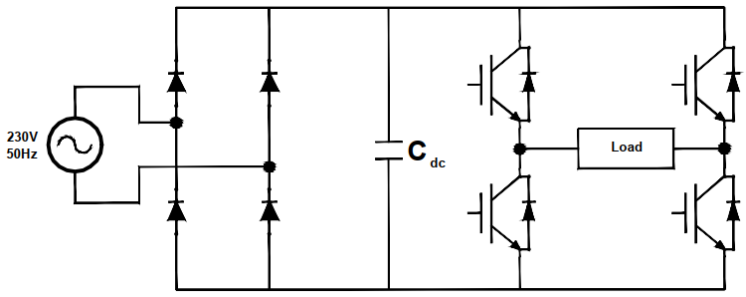

18Figure 2.17: Circuit diagram of PWM inverter with full bridge rectifier

Different control schemes can be implemented on this topology according to the user requirement [2]. Square wave PWM, sinusoidal PWM, regular sampled PWM, harmonic elimination PWM, distortion minimization PWM, voltage

vector PWM, current control PWM are some schemes available for implementation. Also by using this topology, wide speed range can be achieved.

2.4.7 Single phase PWM inverter with half bridge rectifier

This circuit arrangement (figure 2.18) shows a little difference than in the previous one. This time the diode bridge is not a full bridge, it shows a half bridge. Instead of the remaining diodes of the full bridge, there are two capacitors in the positions where diodes were present. Higher value of DC filter capacitors need to be used in order to achieve the same DC voltage bus ripple as previous.

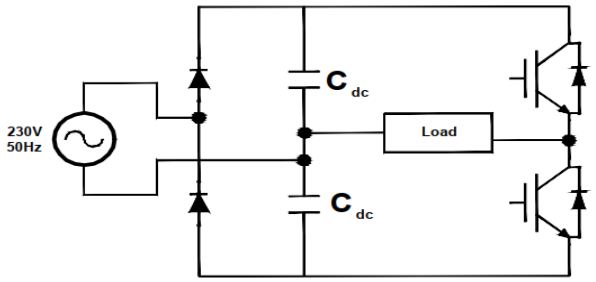

19Figure 2.18: Circuit diagram of single phase PWM inverter with half bridge rectifier

In this case, the half bridge rectifier works to give the two switches in one leg to perform at 50% duty ratio. This operation forms the midpoint of the DC bus [22]. When it happens, the maximum motor terminal voltage becomes half the rectified supply voltage. With this topology, there are advantages like, lower vibrations, lower noise, torque reductions and speed pulse emissions.

2.4.8 Single phase PWM inverter with controlled half bridge rectifier

This is an extension of previously discussed topology. Instead of two diodes, this method uses active rectifiers (figure 2.19). This newly introduced IGBTs is useful to limit THD and increase the utility side power factor. This topology also has regenerative capability.

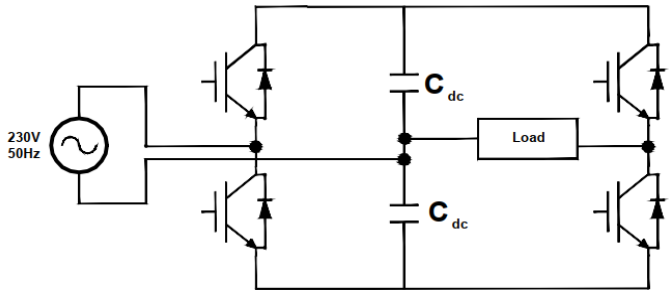

20Figure 2.19: Circuit diagram of single phase PWM inverter with controlled half bridge rectifier

2.4.9 Two-phase full bridge PWM inverter

In this case, two separate H-bridges are used to supply the two windings of the single phase induction motor (figure 2.20) [8]. In the separate two windings, the voltage and the current can be controlled separately. So, the speed and the torque of the motor can be controlled accurately. The control can be done separately aiming each field. Since the main winding and the auxiliary winding is supplied separately, an AC capacitor does not require inside the single-phase induction motor.

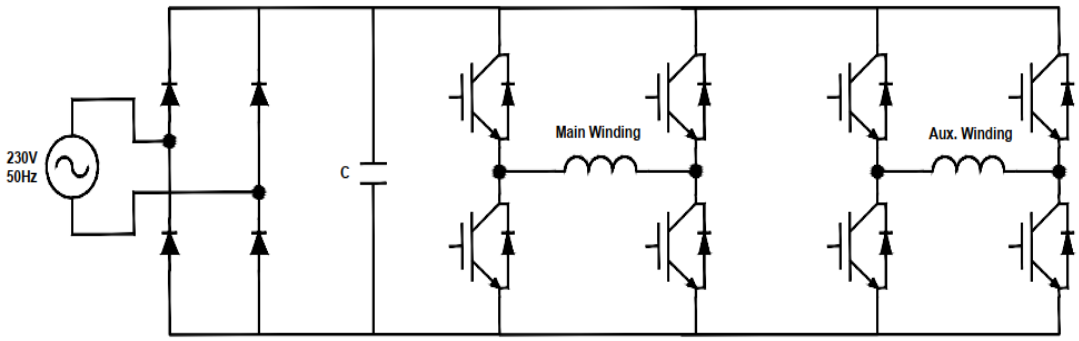

21Figure 2.20: circuit diagram of two phase full bridge PWM inverter

2.4.10 Two-phase half bridge PWM inverter

In this circuit, only four active switches are used for the operation (figure 2.21). Since there are two capacitors connected in series, the motor windings get half of the DC bus voltage. In this manner, the motor will work under the half of the supply voltage. To achieve that, capacitors should be kept balanced to have a balanced voltage across them carefully.

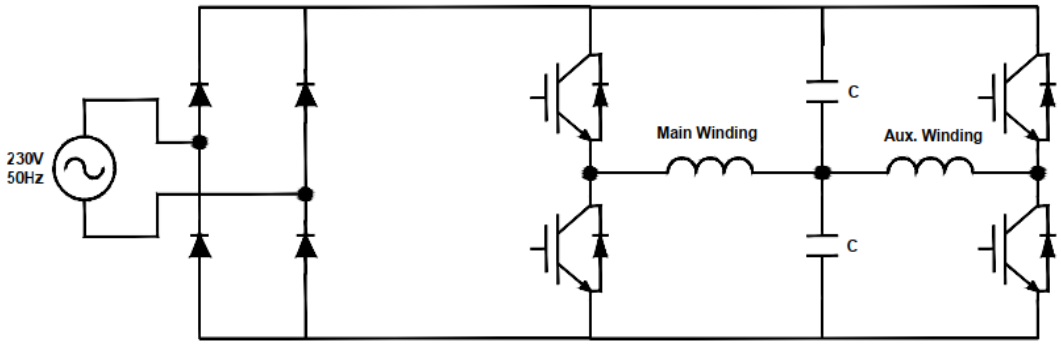

22Figure 2.21: Circuit diagram of two phase half bridge PWM inverter

2.4.11 Two-phase semi full bridge PWM inverter

For this circuit arrangement, 6 IGBTs are taken in to account. Divided DC bus is absent in this method. As in the previous topology, the motor will operate under a half of the rectified input voltage. This inverter can be operated with high efficiency with special PWM techniques. A control method of this technique was discussed in [9].

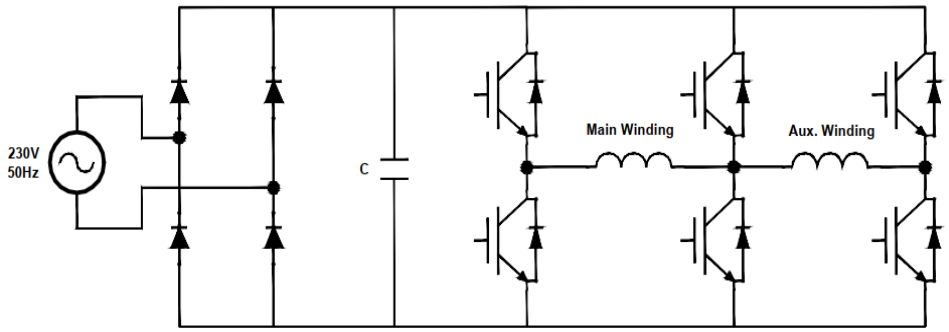

23Figure 2.22: Circuit diagram of two phase semi full bridge PWM inverter

2.4.12 Two-phase PWM inverter with controlled rectifier

As same as the configuration shown in 2.4.8, this method also can control the supply power factor, source current, and THD [12, 13, 15, and 16]. To do that, IGBTs are used. A full rated voltage can be applied across the motor terminals. Special attention should be given to maintain a balanced voltage across DC bus capacitors. Space vector PWM can also be implemented in this topology.

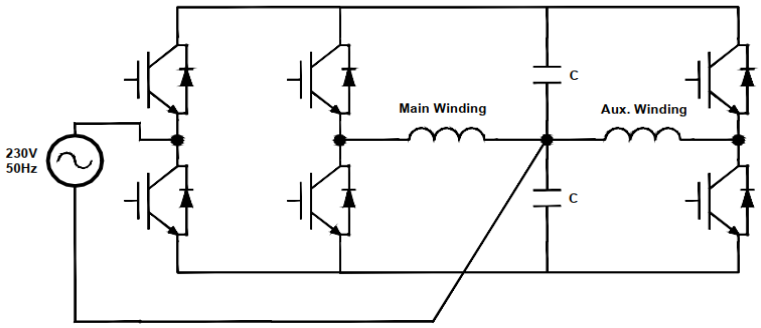

24Figure 2.23: Circuit diagram of two-phase PWM inverter with controlled rectifier

2.5 Summary of literature review

Literature review chapter of this study began by discussing different types of single phase induction motors. According to that, permanent split capacitor typed motors are mostly being used as ceiling fan motors. Generally 1.2uf – 3.5 uf valued AC capacitors are being chosen for the split capacitor.

Cost of the commercially available, traditional fan regulators are roughly in the price range of Rs. 950/= to Rs. 1,250/= (2021 figure). However since the smart fan regulators carry set of impressive features, it costs around Rs. 7,400/= (2021 figure) [32]. These selling costs are important to compare the cost of proposed fan regulator with the existing ones. Also there is a trend using remote controllable facility in fan regulators nowadays.

Subsection 2.4 of this chapter addressed novel power electronic based single phase motor controlling methods. According to that, topologies controlling main and auxiliary currents separately performs better. However, those methods need lots of electronic components and advanced control methods. Hence, analysis should be made considering cost, size, control complexity, size of DC link capacitors, speed range… etc.

CHAPTER 3

SIMULATION AND COST ANALYSIS OF NOVEL FAN REGULATORS

Introduction

Literature review of this study revealed different types of power electronic based single phase motor controlling methods. However, each and every control method given there is not suitable for ceiling fan motor controlling purposes. This chapter is dedicated to evaluate the performance of six shortlisted single phase motor controlling methods with traditional electronic fan regulator circuit. Moreover, a cost analysis has been performed to check whether the proposed solution is viable as a commercial product.

3.1 Load Modeling

Before modeling proposed fan regulators in a software environment, fan motor was modeled and tested. Matlab/Simulink was used to model the load. Importance of modeling the load:

I. Stabilization time of the fan can be obtained
II. On-off behavior of power switches depends on the load
III. Ability to record maximum input current

As described in the literature review, different ceiling fan motor types are available in the market. Lots of manufactures use permanent split capacitor single phase induction motors as the fan motor. Same type was used in the simulation. Motor parameters for fan motor was obtained from [11]. Those are shown in table 3.1 and developed fan motor in Matlab/Simulink is shown in figure 3.1.

1Table 3.1: Ceiling fan motor parameters

Parameter	Symbol	Value
Main winding resistance	r_{1m}	300 Ω
Auxiliary winding resistance	r_{1a}	320 Ω
Rotor resistance	r_2'	290Ω
Main winding leakage reactance	x_{1m}	170 Ω
Auxiliary Winding leakage reactance	x_{1a}	223 Ω
Rotor leakage reactance	x_2'	170 Ω
Magnetizing reactance	x_{mag}	711 Ω
Pole pairs	p	9
Split capacitor value	C	2.5uF

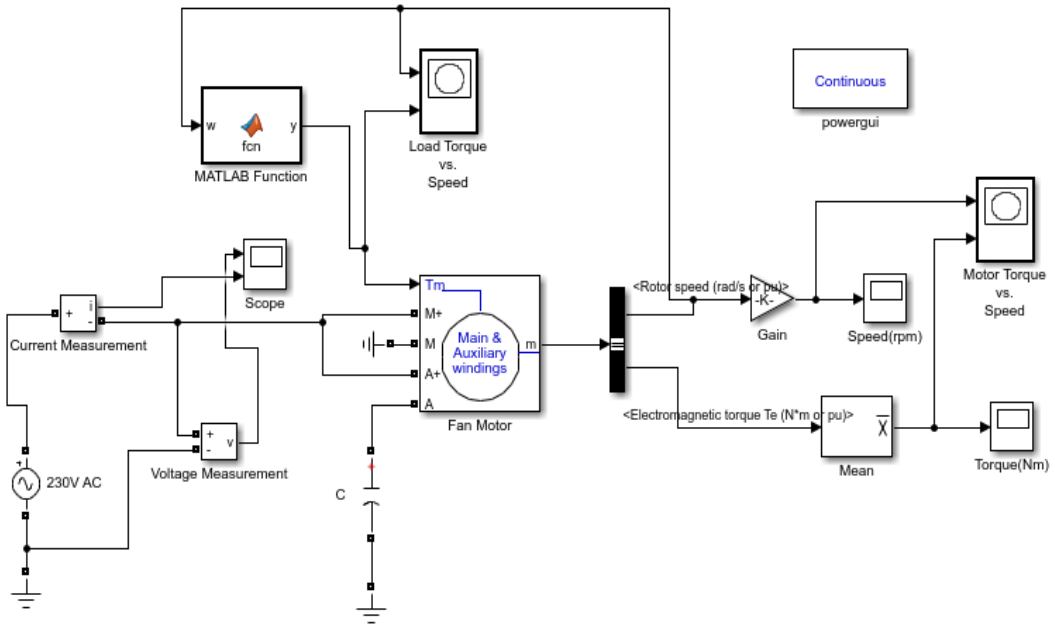

25Figure 3.1Fan motor model

3.2 Verification of fan motor model

Furthermore, the simulated model was tested and verified beforehand. Figure 3.2(a) shows torque vs. speed graph of simulated fan motor. In comparison with figure 3.2(b), which is obtained from [11], the graphs for C=2.5uf are almost same.

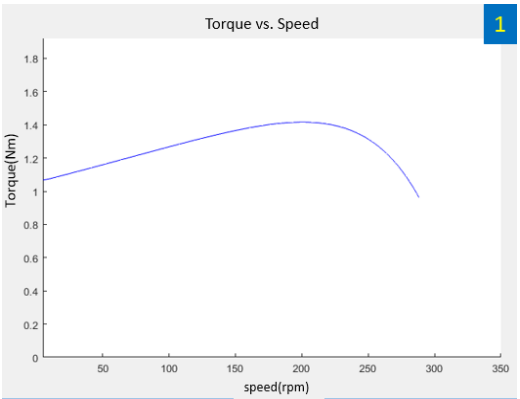

26Figure 3.2(a): Simulated results of fan motor (with loaded condition)

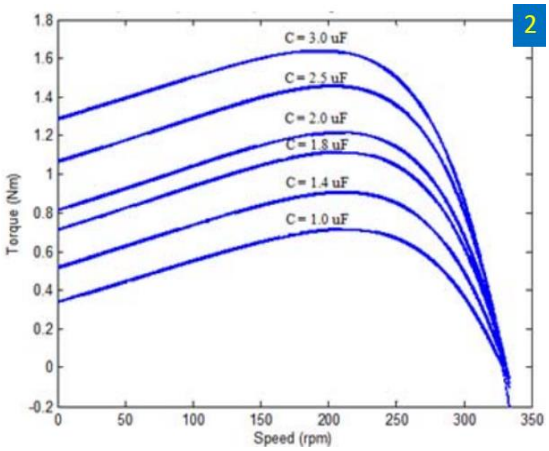

27Figure 3.2(b): Torque-speed characteristics presented in [11]

Moreover, a comparison was done between the simulated model and some experimentally obtained result given in [2] for the same motor model.

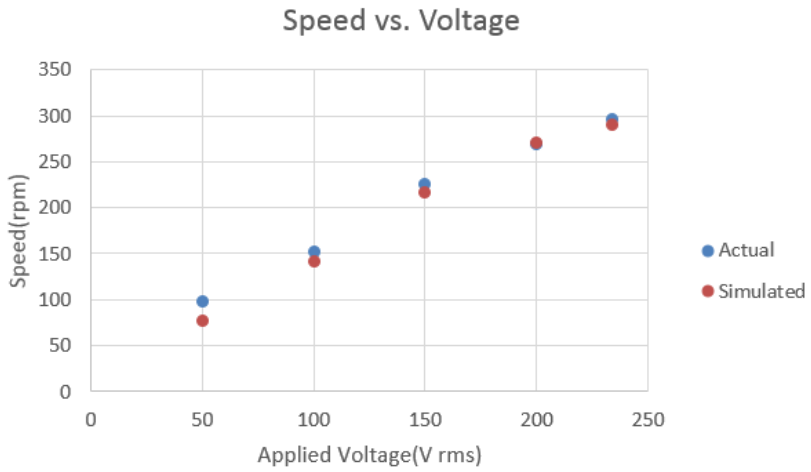

28Figure 3.3(a): Speed (rpm) vs. Voltage (V) graph for experimented fan motor in [2] and simulated results

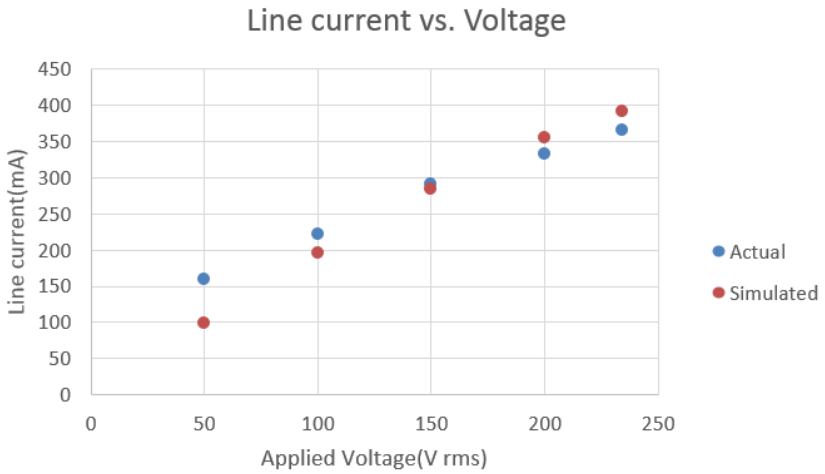

29Figure 3.3(b): Line current (mA) vs. Voltage (V) graph for experimented fan motor in [2] and simulated results

Two scenarios given above verifies the simulated model in Matlab/Simulink. However, some discrepancies can be seen in simulated results and practically obtained results given in [2]. This can be happen due to following reasons;

I. Omission of core loss component from simulated model
II. Omission of windage loss from simulated model
III. Other losses (Ex: losses due to wire resistances…etc.) were not considered when creating the model.

Next, it was used as a load to compare the quality of proposed fan regulators.

3.3 Simulation of different types of novel fan regulators

Various induction motor control methods were discussed in chapter 2. A brief summary of discussed methods is shown in table 3.2

2Table3.2: Comparison of various single phase motor controlling methods

No.	Method of Control	Review
1	DC chopper fed motor control	Cheap, simple control, No DC link capacitor
2	Burst firing method	Less harmonic content, High I_{start} at cycles
3	AC-AC buck converter	Cheap, Ease of harmonic filterization
4	Non-conventional cyclo-converter	Wide speed range, cheap
5	Conventional cyclo-converter	Wide speed range, Intermediate control complexity
6	Single phase PWM inverter with full bridge rectifier	Wide speed range, Different PWMs can be implemented, Large DC link capacitor
7	Single phase PWM inverter with half bridge rectifier	Divided DC bus, reduced torque & speed pulsations
8	Single phase PWM inverter with controlled half bridge rectifier	Active rectifier for current control, regenerative capability, can increase utility side power factor
9	Two phase full bridge PWM inverter	Complex method of controlling, Precise control of speed and torque
10	Two phase half bridge PWM inverter	Motor windings receive half of the supply voltage, need to keep balanced voltage across DC link capacitors
11	Two phase semi full bridge PWM inverter	Complex method of controlling, divided DC bus is absent
12	Two phase PWM inverter with controlled rectifier	Costly, can implement space vector PWM, supply power factor and THD can be controlled

Different topologies have their own merits and demerits. However, proposed method needs to be less complex and affordable in price for ceiling fan control applications. Hence, six methods were shortlisted for simulations. Those are:

I. DC chopper fed controller

II. Burst firing method

III. Non-conventional cyclo-converter

IV. AC-AC buck converter

V. Single phase sinusoidal PWM inverter

VI. Single phase sinusoidal PWM inverter with half bridge configuration

Traditional electronic fan regulator was also designed and simulated in order to compare the performance with proposed novel solutions.

3.3.1 Simulation of traditional electronic fan regulator

Circuit diagram for commercially available traditional fan regulator was presented in figure 2.10 of chapter 2. Function of this circuit was also explained there in detail. Same component values of this circuit were used in the simulation. Since Matlab/Simulink 2017 is not equipped with inbuilt triac and diac models, those were replaced by two back-to-back thyristors and a separate Mathlab function respectively. Developed Matlab code for DB3 diac is given in appendix-A.

Figure 3.4 shows developed traditional electronic fan regulator in Matlab/Simulink. This was used to obtain four different parameters which determines waveform quality and performance of the fan regulator. Those are:

I. Stabilization time(s)
II. Total harmonic current distortion ($THD_I\%$)
III. Total harmonic voltage distortion ($THD_V\%$)
IV. Maximum input current to the fan

Stabilization time stated above is defined as the time taken by fan to reach some specified speed from 0 rpm. The above four parameters were obtained for

five different speed levels of simulated ceiling fan. Obtained results are shown in table 3.3.

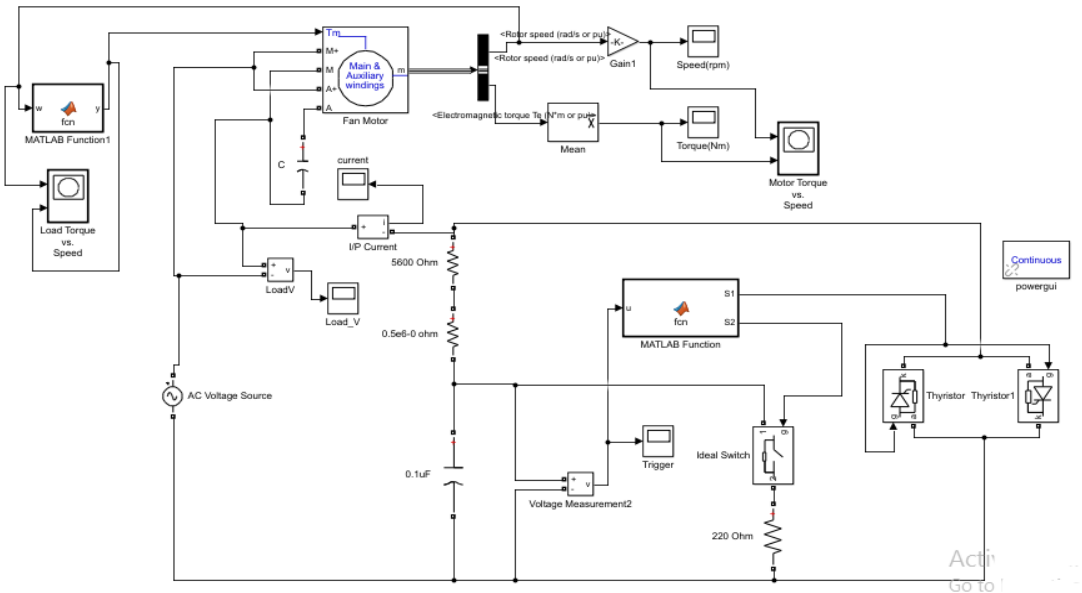

30*Figure 3.4: Block diagram of simulated traditional fan regulator*

3Table 3.3: Performance of traditional fan regulator for different speed levels

No.	Speed(rpm)	Stabilization time(s)	THD_I%	Max. I/P current(mA)	THD_V%
1	170	31	61.25	394	65.18
2	200	25	54.63	422	58.01
3	230	21	49.45	453	42.16
4	260	20	42.37	485	35.04
5	288	9	1.99	423	6.41

Figure 3.5, 3.6 and 3.7 shows simulated load voltage waveform, load current waveform and FFT analysis for load voltage waveform for 260rpm operation of traditional fan regulator. Comparison and analysis of simulation results were discussed in the latter parts of this chapter.

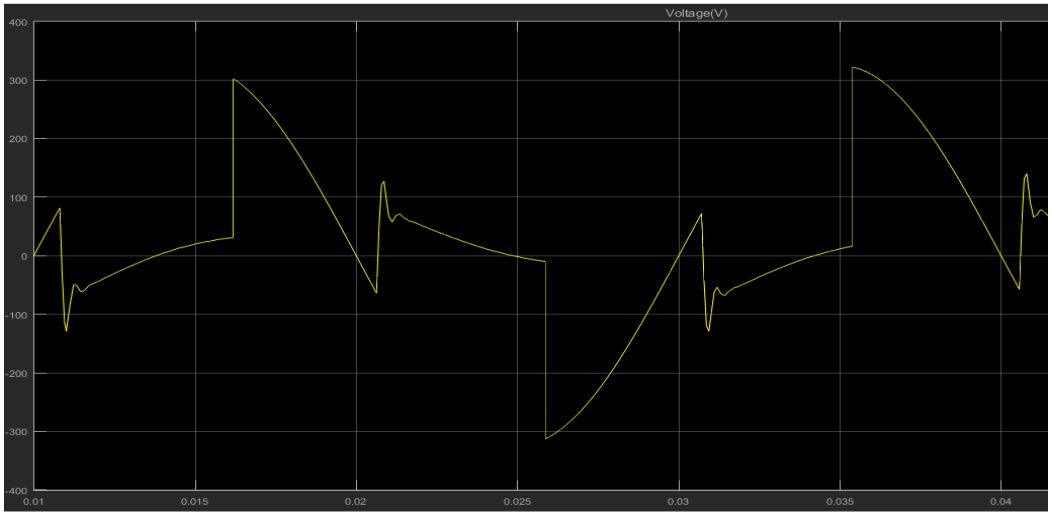

31*Figure 3.5: Load voltage vs. time waveform at 260rpm*

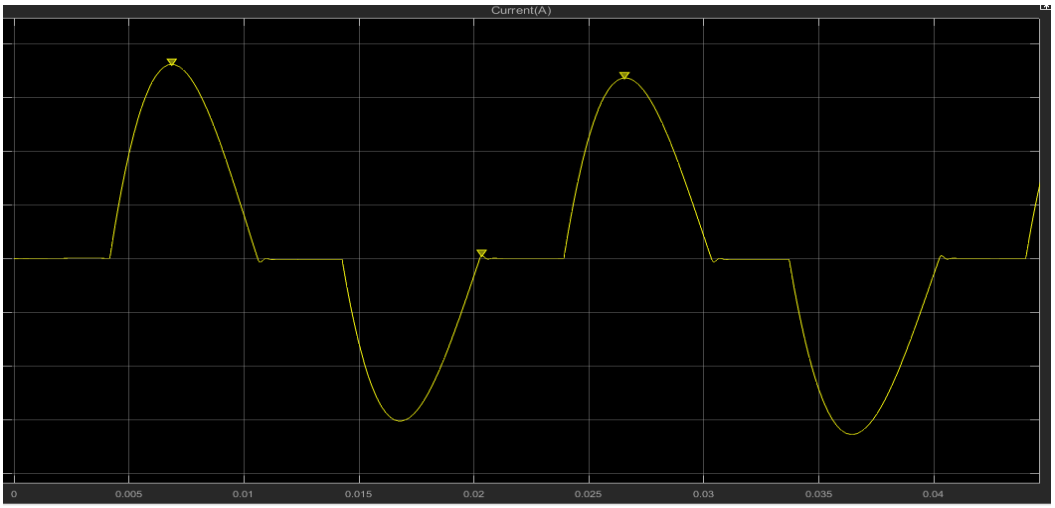

32*Figure 3.6: Load current vs. time waveform at 260rpm*

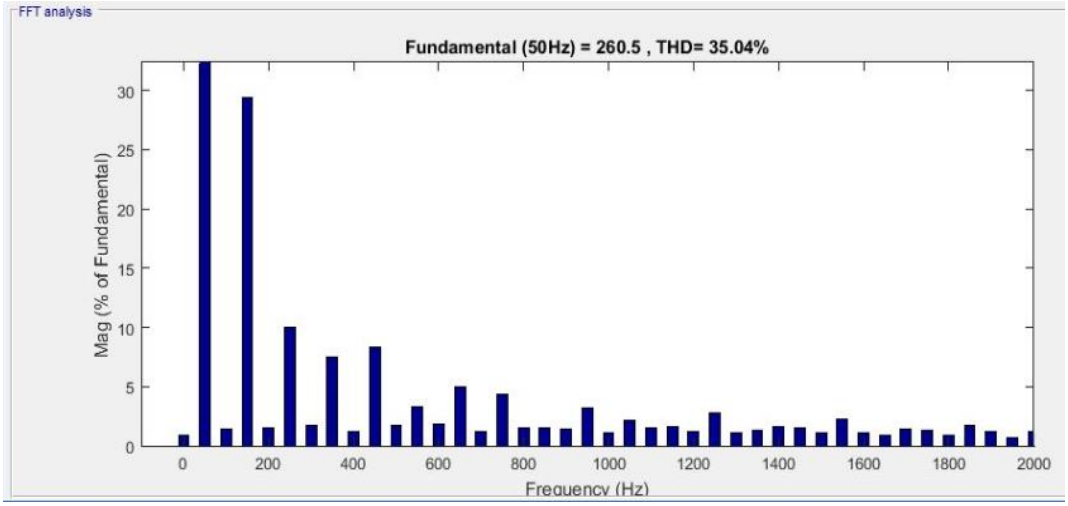

33*Figure 3.7: FFT analysis for load voltage waveform at 260rpm*

3.3.2 Simulation of DC chopper fed controller

In this method, AC signal is chopped using an active switch (MOSFET in simulated circuit) operated by a PWM signal. A bridge rectifier needs to be used since MOSFET is a uni-directional device. This method needs an auxiliary path with an active switch for freewheeling purposes since the load is inductive (MOSFET 1 in figure 3.5). Complementary PWM signals for active switches were given using a PWM generator. 2.5 kHz switching frequency was used in the simulation. By varying the duty cycle given to the PWM generator, effective voltage seen by the fan motor can be adjusted.

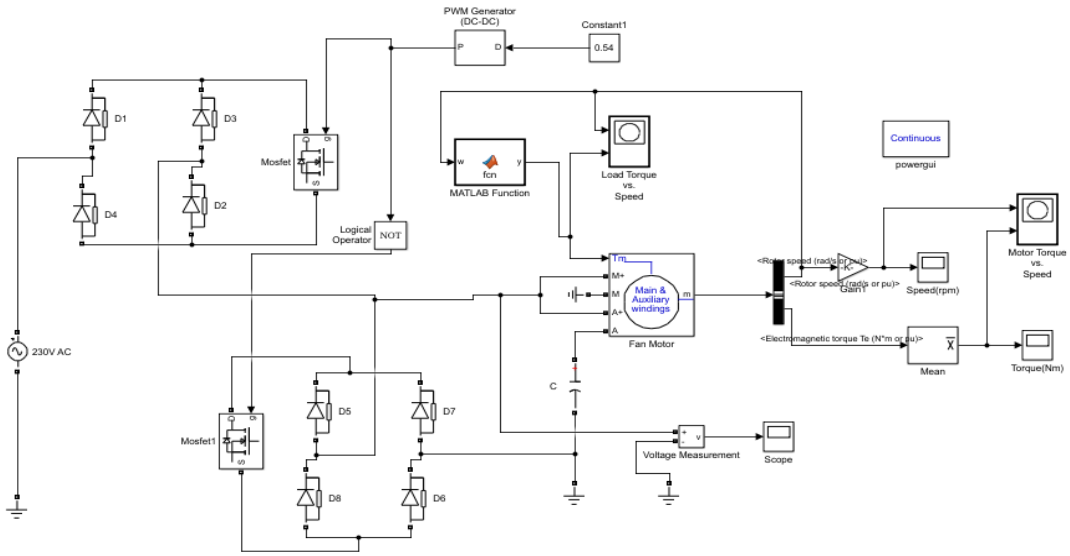

34Figure 3.8: Block diagram of simulated DC chopper fed controller

In this method, AC signal is chopped using an active switch (MOSFET in simulated circuit) operated by a PWM signal. A bridge rectifier needs to be used since MOSFET is a uni-directional

4Table 3.4: Performance of DC chopper fed controller for different speed levels

No.	Speed(rpm)	Stabilization time(s)	THD_I%	Max. I/P current(mA)	THD_V%
1	170	24	0.37	215	8.15
2	200	21	0.29	315	7.59
3	230	19	0.25	360	7.13
4	260	16	0.23	413	6.58
5	288	9	0.01	418	0.01

Figures 3.9, 3.10 and 3.11 shows obtained waveforms and FFT analysis for an arbitrary operating point.

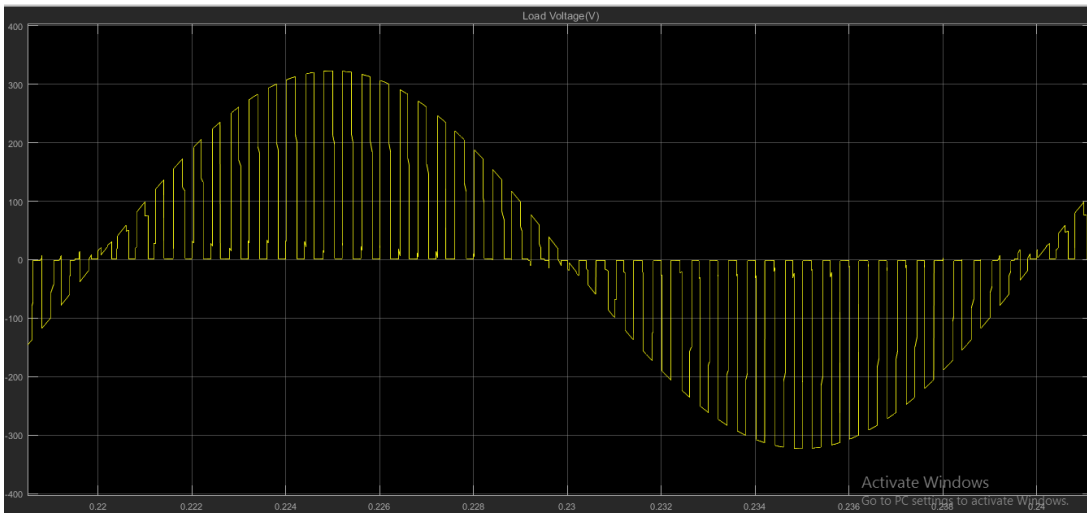

35*Figure 3.9: Load voltage vs. time waveform at D (PWM duty) =0.54*

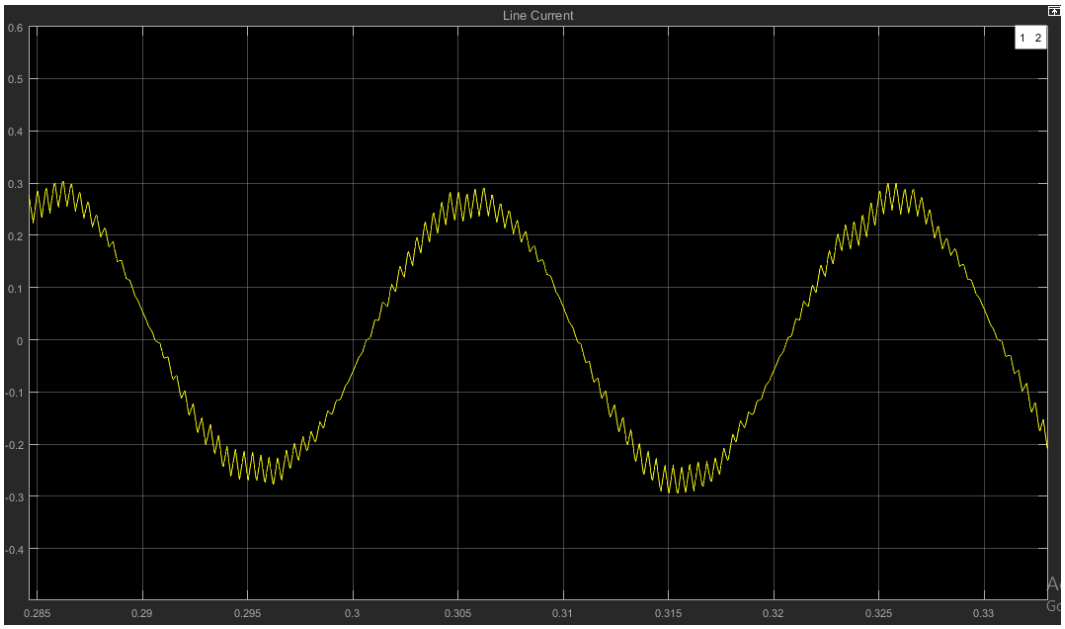

36*Figure 3.10: Load current vs. time waveform at D= 0.54*

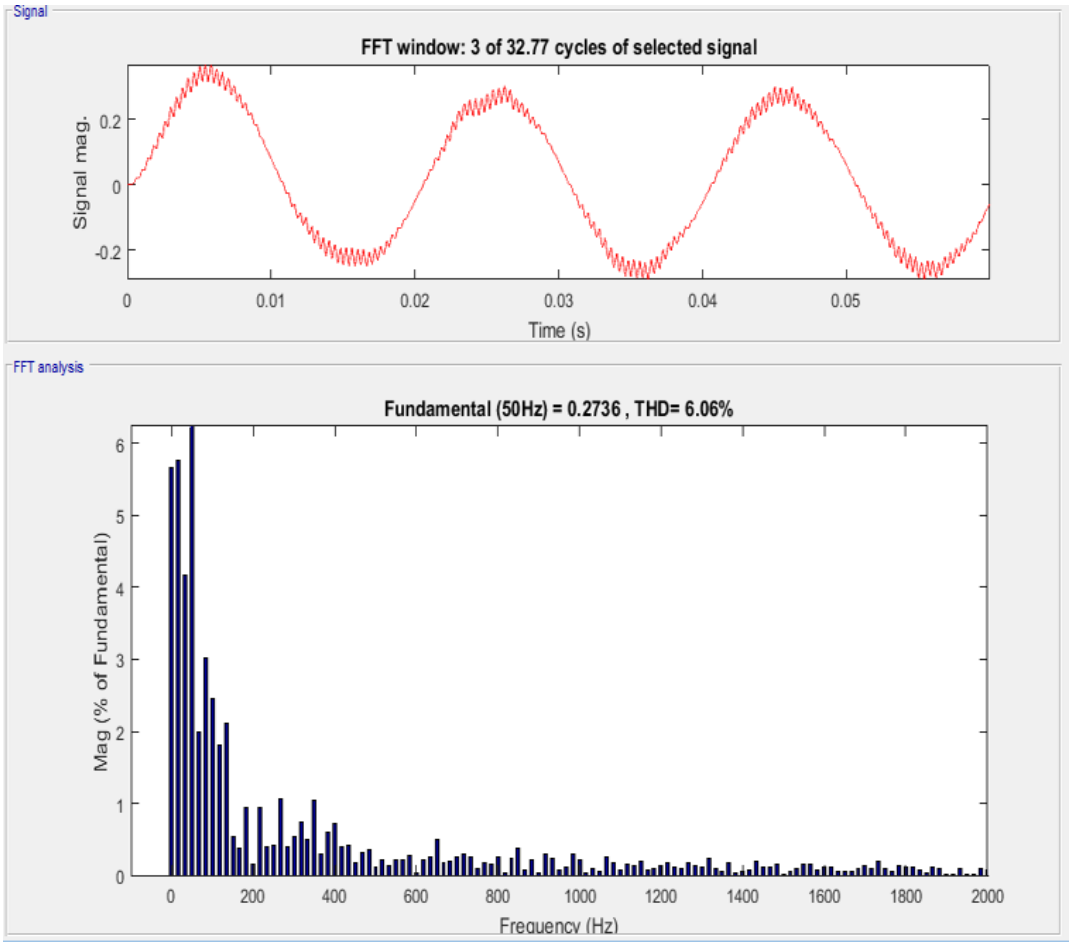

37*Figure 3.11: FFT analysis for load current waveform at D=0.54*

Compared to traditional electronic fan regulator, this method equipped with continuous current supply to the motor. It helps the motor to reduce torque pulsations and thereby achieve reduced speed ripples.

Also, low order load voltage harmonics in this method has been drastically reduced. This can also be advantageous to obtain less mechanical oscillations [10], humming noise [2] and stator losses [10].

3.3.3 Simulation of burst firing method

In order to control the speed of the fan motor, this method uses cycle switching. A zero crossing detector has to be used to determine the starting of a cycle. Block diagram of simulated system is given in figure 3.12. A Matlab function was used to trigger the back-to-back thyristors after detecting a zero crossing point. Developed Matlab function for this purpose is given in appendix - B

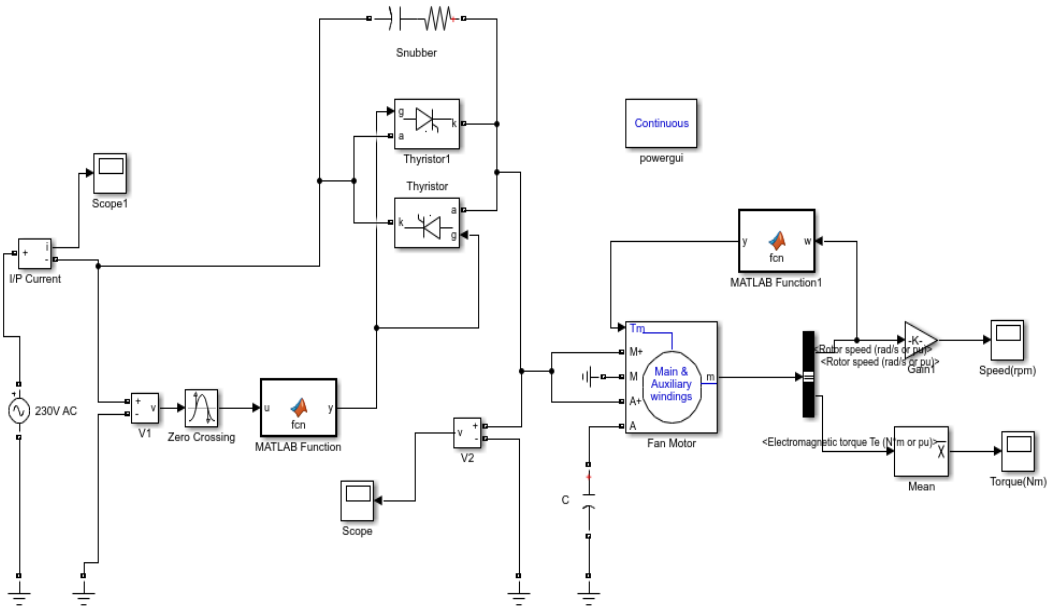

38Figure 3.12: Block diagram of simulated burst firing method

Figure 3.13 shows waveform of load voltage vs. time at 225 rpm. Although it shows pure sinusoidal waveform at the ON period, waveform gets somewhat distorted at the end of the cycle. This happens due to the freewheeling current passing through the main and auxiliary windings of the fan.

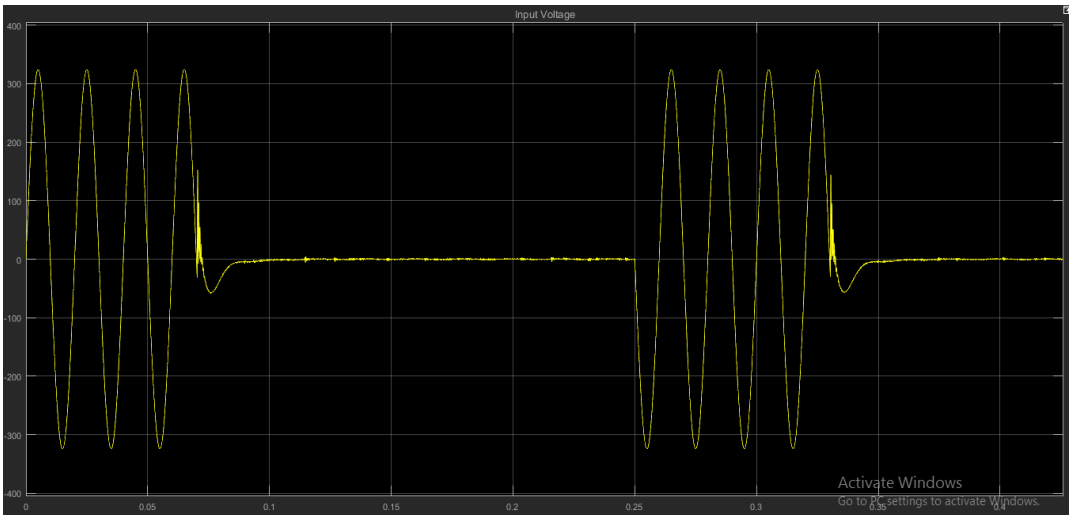

39Figure 3.13: Load voltage vs. time waveform at 225rpm

Figure 3.14 shows waveform of load current vs. time at 225 rpm. There is a high current surge at the beginning of every cycle. Since starter capacitor is not charged at the starting of the cycle and dv/dt is high at the starting point, this graph

shows high starting current at the beginning of the burst. This could result shorter lifetime of the ceiling fan.

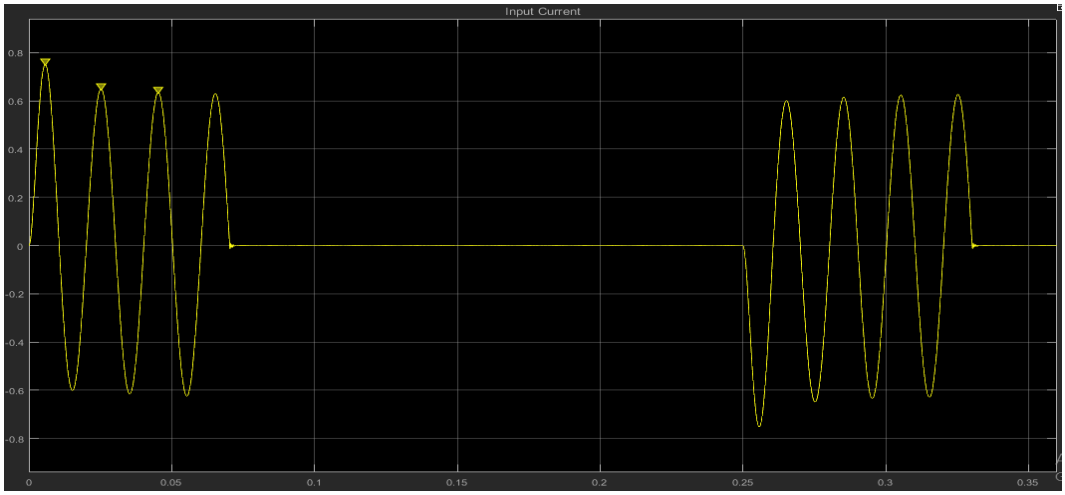

40Figure 3.14: Load current vs. time waveform at 225rpm

Figure 3.15 shows FFT analysis of load voltage while table 3.5 shows performance of burst firing method.

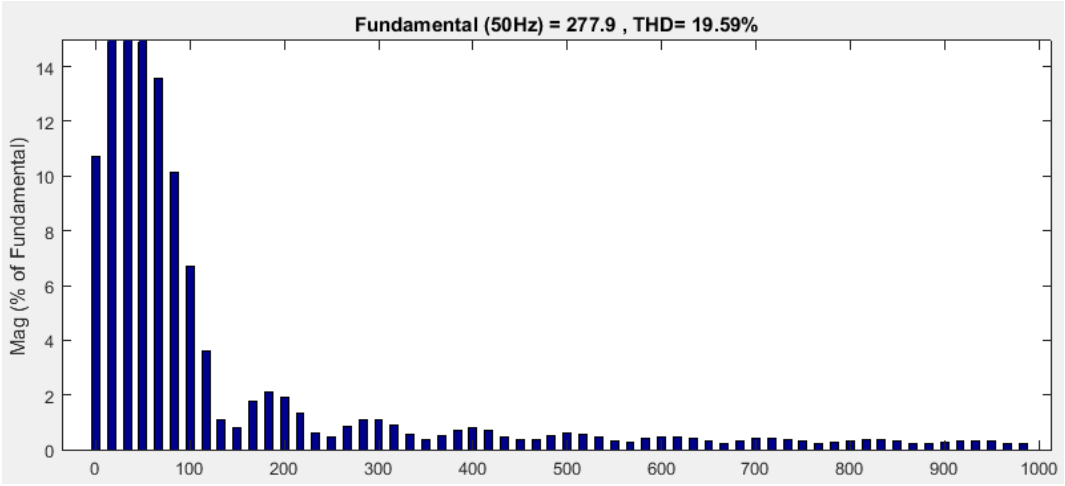

41Figure 3.15: FFT analysis for load voltage waveform at 225 rpm

5Table 3.5: Performance of burst firing method for different speed levels

No.	Speed(rpm)	Stabilization time(s)	THD_I%	Max. I/P current(mA)	THD_V%
1	170	28	5.66	502	19.52
2	200	24	5.32	502	23.52
3	230	22	5.21	502	19.45
4	260	17	5.13	501	19.39
5	288	9	0.01	421	0.18

3.3.4 Simulation of non-conventional cyclo converter method

Figure 3.16 shows Matlab/Simulink model for non-conventional cyclo converter based motor controller. As explained in chapter2, this method needs a separate switching strategy to supply same frequency as in the switching signal generator to the load.

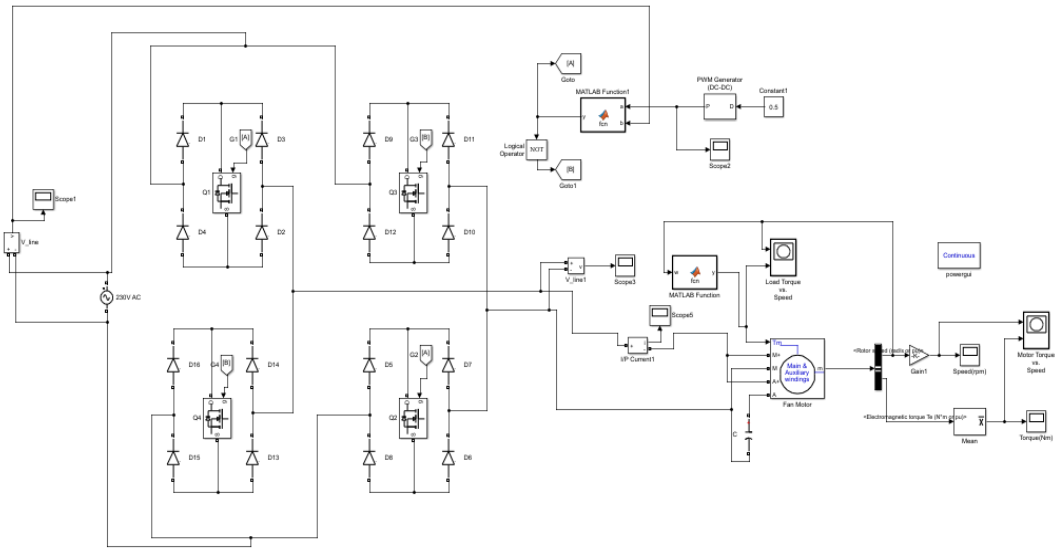

42Figure 3.16: Block diagram of simulated non-conventional cyclo converter

Matlab Function 1 shown in figure 3.16 takes source voltage polarity and output state of frequency generator as inputs to generate correct frequency output. Developed switching strategy for this method is shown in table 3.6 and code for Matlab Function 1 is given in appendix – C.

6Table 3.6: Developed switching strategy

Output state of frequency generator	**Source voltage polarity**	**Output**
1	(+)	Q1, Q2
1	(-)	Q3, Q4
0	(+)	Q1, Q2
0	(-)	Q3, Q4

This switching strategy can be verified using figure 3.17. That was taken at a random duty of frequency generator.

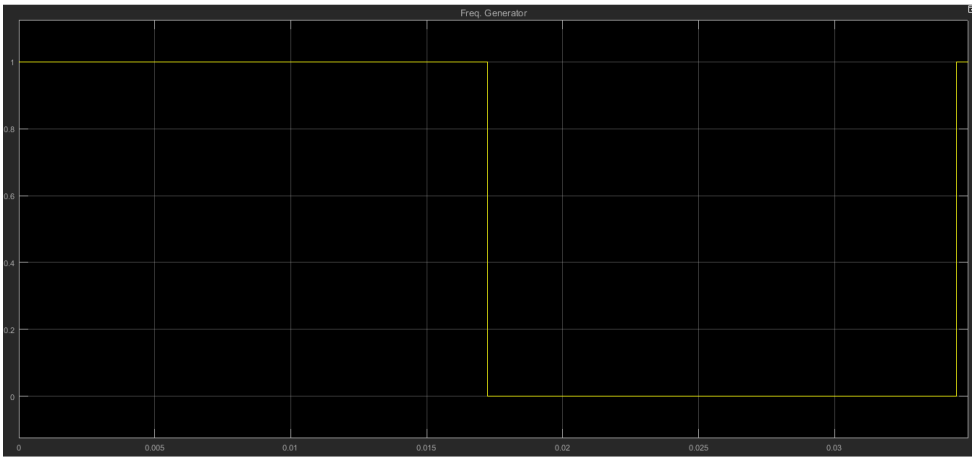

(a)

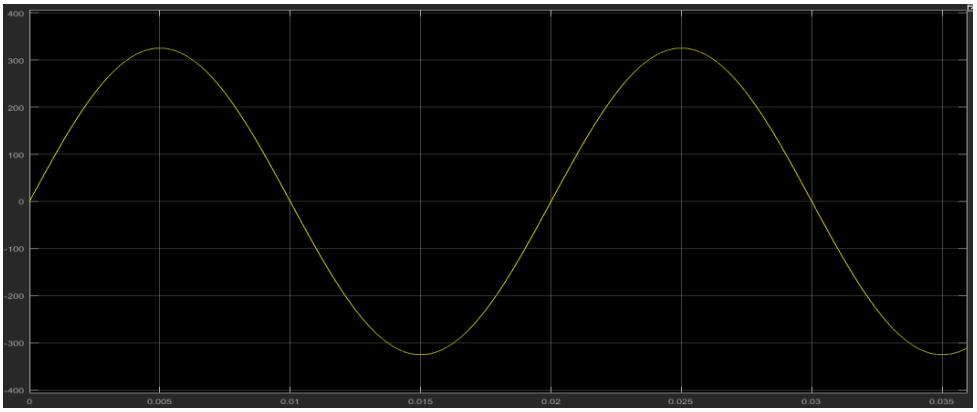

(b)

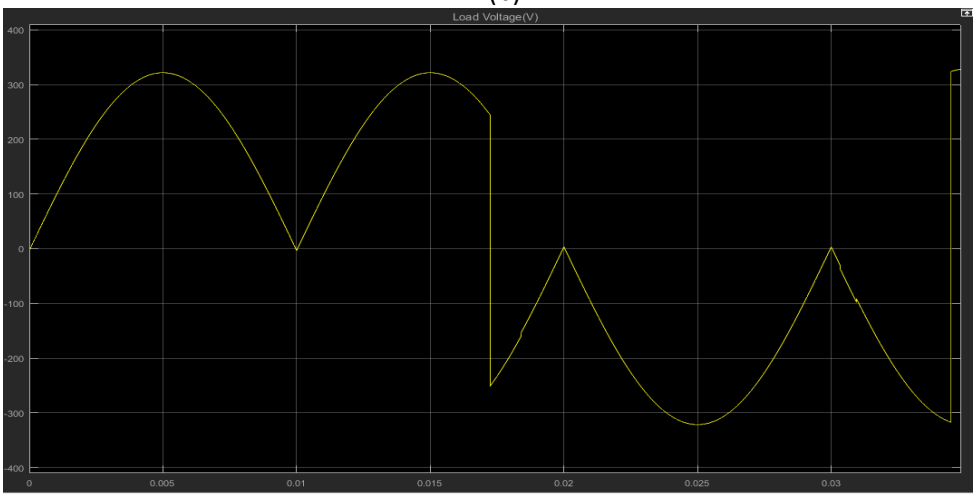

(c)

43 Figure 3.17: (a) Output of frequency generator (b) Output voltage waveform (c) Output voltage to the load

Table 3.7 shows the performance of non-conventional cyclo converter based motor controller for different speed levels. Compared to other methods, this method has very good stabilization times (figure 13.18). However, this controlling method shows very high current and voltage harmonic content compared to previous

methods. Voltage and current waveforms are shown in figure 3.17 (c) and 13. 19 respectively.

7Table 3.7: Performance of non-conventional cyclo converter based controller for different speed levels

No.	Speed(rpm)	Stabilization time(s)	$THD_I\%$	Max. I/P current(mA)	$THD_V\%$
1	170	8	86.54	567	69.9
2	200	11	84.47	582	69.27
3	230	11.5	78.54	519	76.78
4	260	12	33.51	460	49.99
5	288	9	0.01	415	0.59

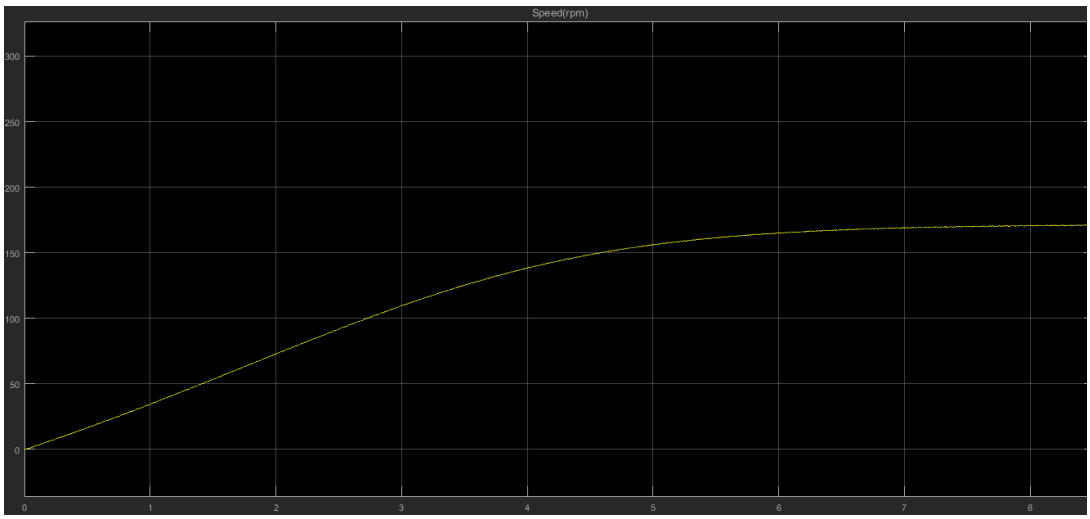

44Figure 3.18: Speed vs. stabilization time graph at 170 rpm

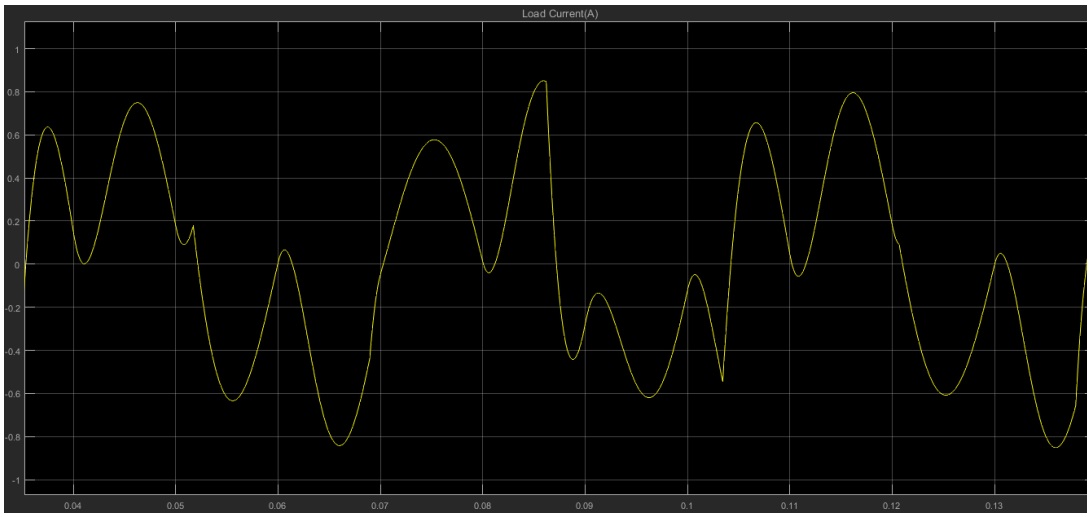

45 Figure 3.19: Load current vs. time waveform at 170 rpm

3.3.5 Simulation of AC-AC buck converter method

Block diagram of simulated AC-AC buck converter is given in figure 3.20. Waveform chopping of positive half cycle is done by MOSFET Q1. MOSFET Q2 is conductive in this period through body diode. MOSFETs Q3 and Q4 were used for freewheeling purposes.

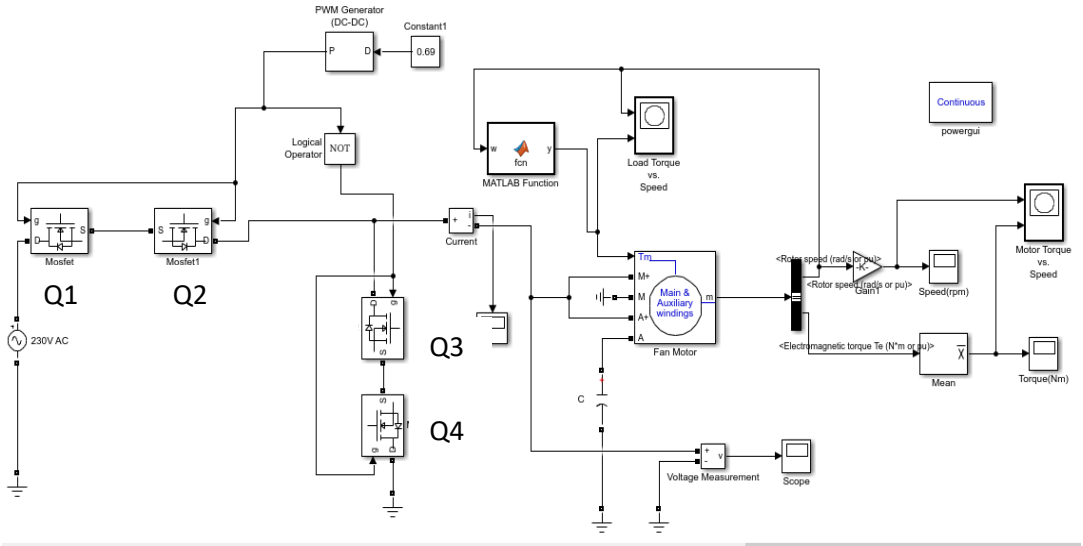

46Figure 3.20: Block diagram of simulated AC-AC buck converter

Switching pattern for this method is given in table 3.7. Switching frequency was set to 2500Hz. Reduced harmonics are some of the attractions in this method. Figure 3.21 shows FFT analysis for load voltage at D=0.62.Table 3.8 shows performance of AC-AC buck converter for different speed levels.

8Table 3.8: Developed switching pattern for AC-AC buck converter method

Q1	Q2	Q3	Q4	V_{load}
1	1	0	0	V_{source}
0	0	1	1	0

9 Table 3.9: Performance of AC-AC buck converter method for different speed levels

No.	Speed(rpm)	Stabilization time(s)	THD_I%	Max. I/P current(mA)	THD_V%
1	170	25	0.38	210	9.13
2	200	21	0.27	301	9.01
3	230	20	0.26	360	6.02
4	260	15	0.25	423	5.13
5	288	9	0.01	420	0.04

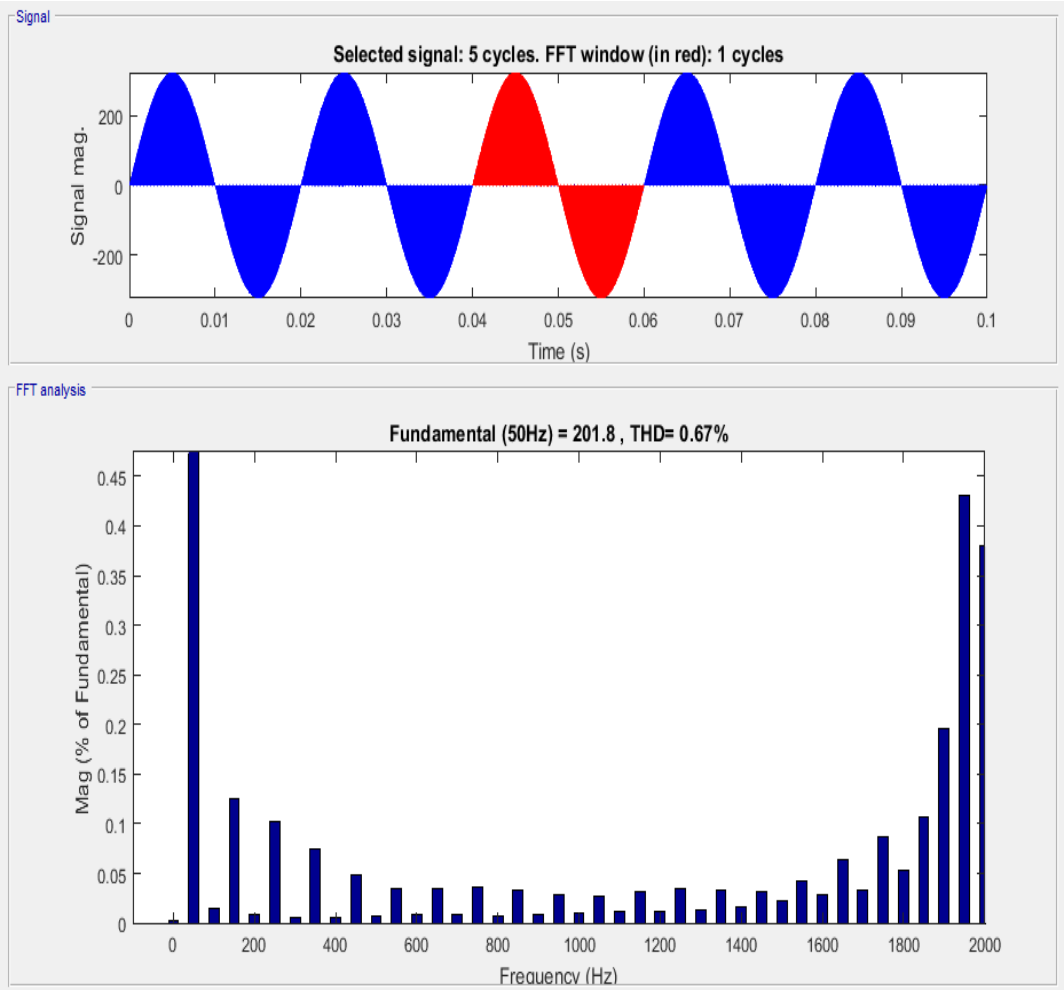

47Figure3.21: FFT analysis for load voltage waveform at D=0.62

3.3.6 Simulation of single phase sinusoidal PWM inverter method

This method uses frequency controlling technique to control the speed of the ceiling fan. Required sinusoidal PWM was generated by comparing a sine wave with a saw tooth waveform. Generated PWM signal was fed to Q1 and Q2 MOSFETs while the complementary was fed to Q3 and Q4 MOSFETs. Specifications for this control is listed as follows:

I. $f_{sw} = 2.5kHz$
II. $m\ (modulation\ index) = 0.66$
III. $p_{\min}(carrier\ ratio, i.e.\frac{f_{sw}}{f_r}) = 50$
IV. $Scheme: Sinusoidal\ PWM(Bipolar)$

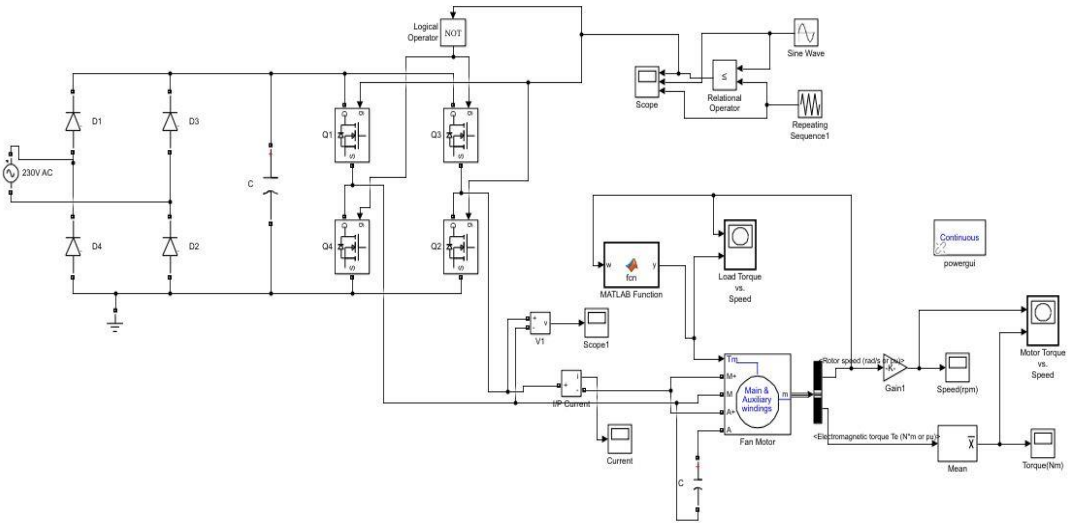

48Figure 3.22: Block diagram of simulated sinusoidal PWM inverter method

Block diagram for this simulation is given in figure 3.22. Switching algorithm, performance, load voltage waveform and FFT analysis for load voltage waveform are shown in table 3.9, table 3.10, figure 3.23 and figure 3.24 respectively. In table 3.9, V_d is the voltage difference between DC rails after bridge rectification. 270uf DC capacitor was used as the smoothing capacitor.

10Table 3.10: Developed switching pattern for sinusoidal PWM inverter method

Q1	Q2	Q3	Q4	V_{load}
1	1	0	0	$+V_d$
0	0	1	1	$-V_d$

11Table 3.11: Performance of sinusoidal PWM inverter method for different speed levels

No.	Speed(rpm)	Stabilization time(s)	THD_I%	Max. I/P current(mA)	THD_V%
1	170	8	16.84	389	16.84
2	200	8	15.86	397	15.86
3	230	8.5	16.82	404	16.82
4	260	11	16.58	411	16.58
5	288	14	15.3	413	15.3

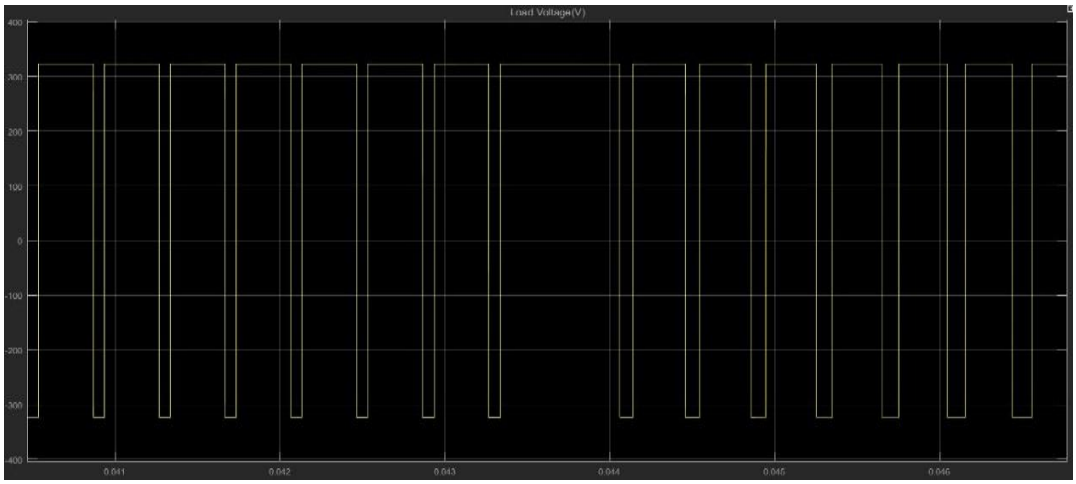

49Figure 3.23: Load voltage vs. time waveform at 200 rpm

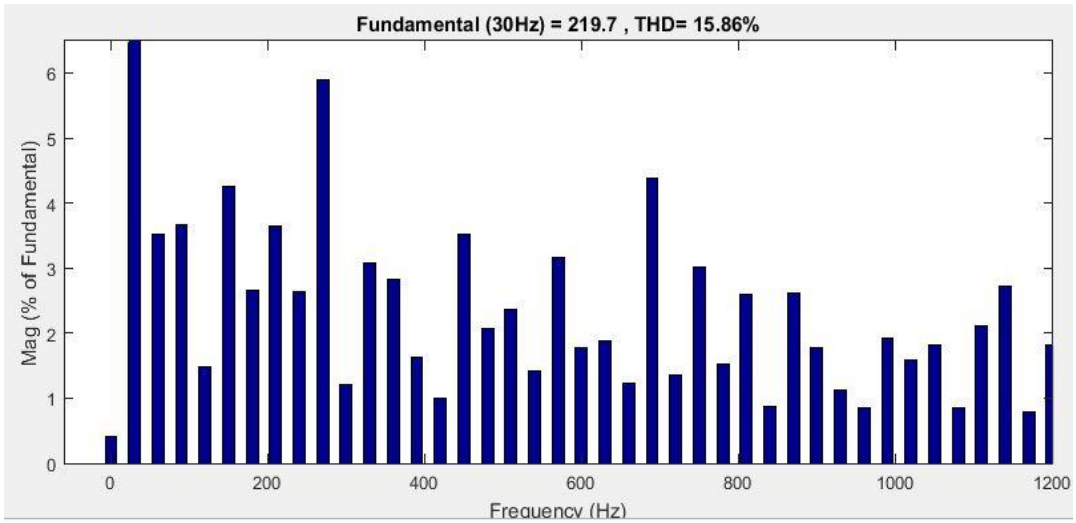

50Figure 3.24: FFT analysis for load voltage waveform at 200 rpm

Compared to other methods, this method has good very good stabilization times. Also this method allows to improve waveform quality further by increasing modulation index or switching frequency. However, when it comes to practical implementation higher switching frequencies can cause more switching losses. Hence there is a tradeoff between waveform quality and switching losses.

3.3.7 Simulation of single phase sinusoidal PWM inverter with half bridge configuration

Figure 3.25 shows block diagram for this simulation. This is also a frequency controlling method. In order to keep the voltage ripple same, capacitor value was chosen as twice the value in the previous method. Same switching signal

generation strategy in single phase sinusoidal PWM inverter method was utilized here too.

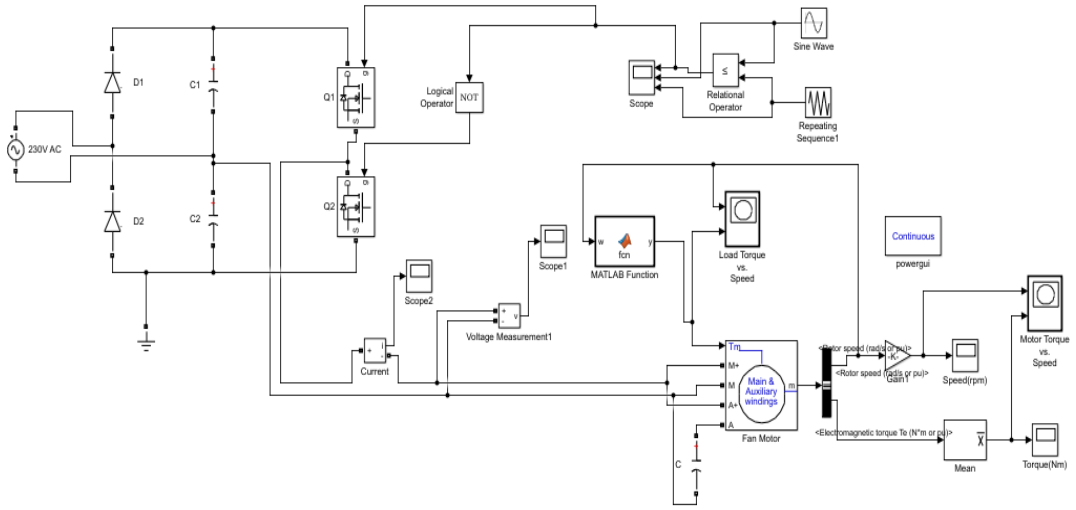

51Figure 3.25: Block diagram of simulated single phase sinusoidal PWM inverter with half bridge configuration

Developed switching pattern and performance of this technique is given in table 3.11 and 3.12 respectively.

12Table 3.12: Developed switching pattern for single phase sinusoidal PWM inverter with half bridge configuration

Q1	Q2	V_{load}
1	0	$+V_d$
0	1	$-V_d$

13Table 3.13: Performance of single phase sinusoidal PWM inverter method with half bridge configuration for different speed levels

No.	Speed(rpm)	Stabilization time(s)	THD_I%	Max. I/P current(mA)	THD_V%
1	170	8	38.06	411	16.85
2	200	8	37.64	407	16.35
3	230	8.5	35.05	285	17.15
4	260	11	36.04	288	15.49
5	288	14	36.02	295	18.48

One of the attractions of this method is the stabilization times. Shape of the current and voltage waveforms are almost similar to the previously discussed method.

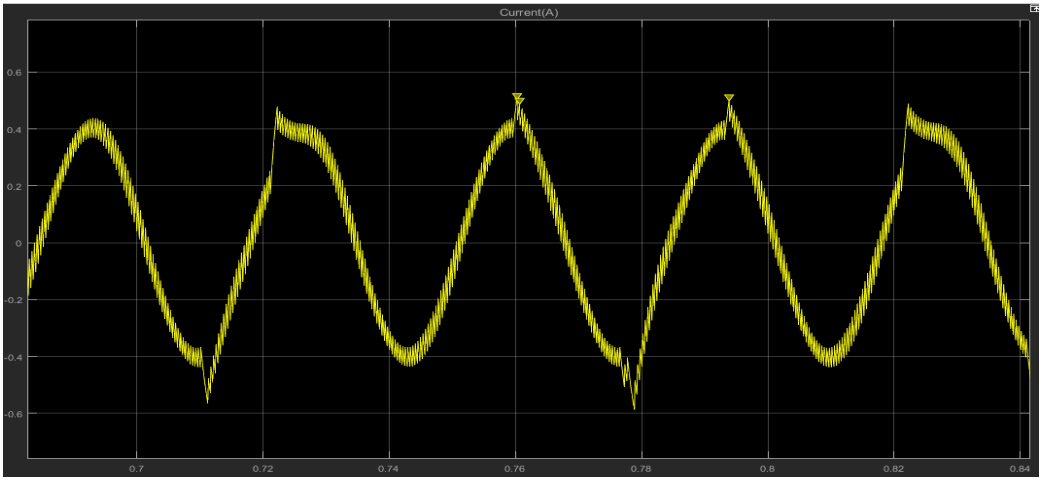

52Figure 3.26: Load current vs. time waveform at 200 rpm

3.4 Cost comparison of fan regulators

Introducing a high performance fan regulator for very high cost can affect its market competitiveness. Hence, another crucial factor needs to consider is cost of the fan regulator. This chapter subsection is dedicated to compare the cost of proposed fan regulators. Furthermore, cost of the traditional fan regulator was also obtained from local market to compare the prices.

Sometimes local electronic shops offer slightly different prices for same component. Hence, cost of each and every component was obtained from one local shop [28]. Some design considerations were also set in order to make the cost estimation more realistic. Those design considerations are as follows:

I. Used same microcontroller for every circuit design
II. Placed snubbers circuit for active switches
III. Same driver method was used to drive all the active switches where possible
IV. Signal-power isolation was considered as a safety requirement

All the fan regulators are expected to be operated using a remote controller kit and the regulator circuit expected to be mounted on the ceiling fan shaft. Hence, developed cost estimation sheets reflect price for remote controller kit and the enclosure used to mount the fan regulator on the ceiling fan shaft.

In order to find out the cost for enclosures, an excel file was developed (table 3.14). It takes number of components of the fan regulator as inputs and outputs necessary volume (i.e. total volume in table 3.14) of the enclosure. 'Required volume for enclosure' gives 3 times higher value to the 'total volume'. This was done to make clearances between components. Enclosure cost per volume was obtained from [28] and calculated the cost of enclosures.

14Table 3.14: Developed cost calculator for enclosures

Item	L(mm)	H(mm)	W(mm)	volume(mm3)	No.	Tot Vol(mm3)
Mosfet	5	20	10	1000	4	4000
Diode	10	4	4	160	22	3520
Resistor(3W)	25	10	10	2500	4	10000
Cap(10nf) 630V polyester	13	10	4	520	4	2080
Resistor(0.25W)	10	4	4	160	17	2720
Inductor	15	15	8	1800	1	1800
Bypass Caps	10	10	3	300	7	2100
Opto isolator(TLP250)	10	10	10	1000	4	4000
Microcontroller	35	10	10	3500	1	3500
Oscillator	12	6	5	360	1	360
DC link cap(270uf,400V)	30	50	30	45000	0	0
DC link cap(680uf,400V)	35	57	35	69825	0	0
Triac	5	20	10	1000	0	0
Zero cross optocoupler	10	10	10	1000	0	0
Comparator IC(LM393)	10	10	10	1000	1	1000
4 pin opto coupler	10	5	8	400	1	400
SMPS	30	30	20	18000	2	36000

Total Volume(mm3)	71480
Required Volume for enclosure(mm3)	214440
Price	248.1944

Switch mode power supplies were used to power up the microcontroller and other low voltage equipment. Those were also added in the cost estimation too. Cost related to soldering, connectors, labor etc. is shown in 'other' category of cost calculation sheets. This was taken as 5% of total cost.

3.4.1 Cost estimation of DC chopper fed controller

Simplified power circuit and gate driver circuit for cost estimation is shown in figure 3.27.

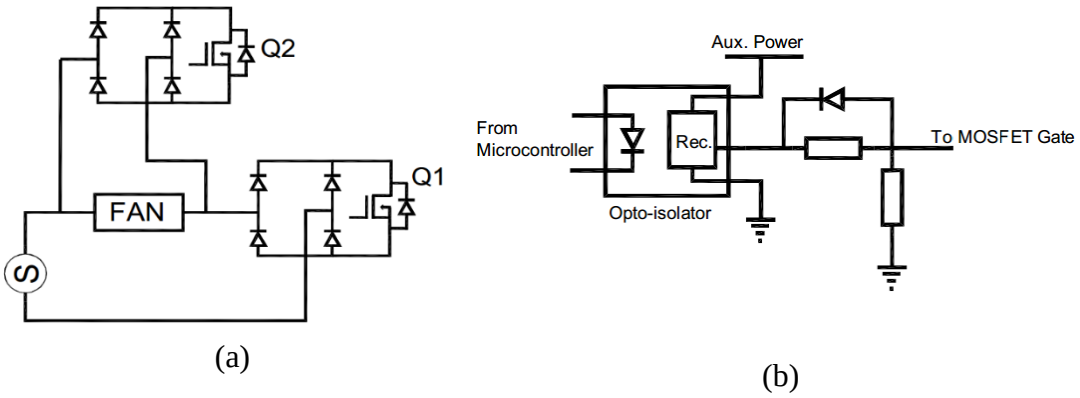

(a) (b)

53Figure 3.27: (a) Simplified power circuit for DC chopper fed controller (b) Gate driver circuit

Two separate gate driver circuits are needed to switch Q1 and Q2 MOSFETs. Complementary switching can be generated from digital pins of the microcontroller. By connecting receiver of the IR remote controller to microcontroller, various duty values can be obtained for switching devices through remote controller action. Developed cost estimation sheet for DC chopper fed controller is shown in table 3.15.

15Table 3.15: Cost estimation of DC chopper fed controller

Item	Part No:	Per Unit Cost	No.	Cost
Mosfets	IRF840	65	2	Rs 130.00
Diodes For Rectification	FR104	5	8	Rs 40.00
Snubber Res	47ohm 3W	8	2	Rs 16.00
Snubber Cap	10nf (polyester)	4	2	Rs 8.00
Pull down Res	68k 0.25W	1	2	Rs 2.00
Gate Res	33ohm 0.25W	1	2	Rs 2.00
Anti-Parallel Gate Diode	FR104	5	2	Rs 10.00
Inductors	441uH	40	2	Rs 80.00
Bypass Caps	100nf	1	3	Rs 3.00
Res. For IR side	390ohm 0.25W	1	2	Rs 2.00
Opto-isolators	TLP250	100	2	Rs 200.00
Microcontroller	Atmega 328P	330	1	Rs 330.00
Reset Res.	10k 0.25W	1	1	Rs 1.00
Oscillator	16Mhz	11	1	Rs 11.00
Caps for Oscillator	20pf	1	2	Rs 2.00
Remote Controller kit	-	180	1	Rs 180.00
1 way 1 gang switch		175	1	Rs 175.00
SMPS	150mA	90	3	Rs 270.00
Enclosure	-	263	1	Rs 263.00
Other	-	86	1	Rs 86.00

Total	
Rs	1,811.00

3.4.2 Cost estimation of burst firing method

As discussed earlier in this chapter, this method needs a zero crossing identification system to trigger the triac. This can be realized using a zero crossing triac output opto-coupler. It not only triggers the triac at zero crossings, but also provides signal-power isolation. Same hot-line switching application circuit (figure 3.28) from MOC304x zero crossing triac output opto-coupler datasheet can be used to drive the triac of the fan controller.

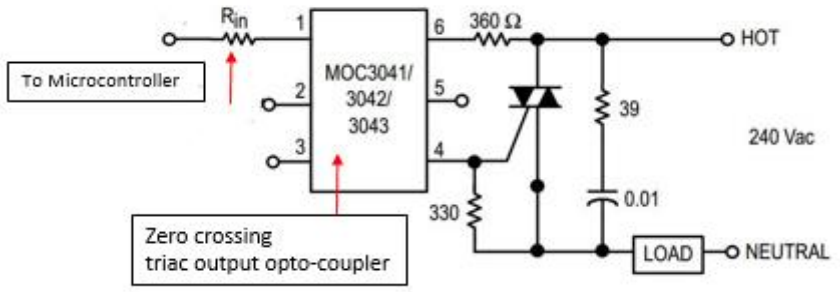

54Figure 3.28: Hot–Line Switching Application Circuit (Source: MOC304X Datasheet)

Developed cost estimation sheet for burst firing method is shown in table 3.16.

16 Table 3.16: Cost estimation of burst firing method

Item	Part No:	Per Unit Cost	No.	Cost
Triac	BT138	55	1	Rs 55.00
Snubber Res	39ohm, 3W	8	1	Rs 8.00
Snubber Cap	10nf (polyester)	4	1	Rs 4.00
Zero crossing Triac output optocoupler	MOC3042	75	1	Rs 75.00
Microcontroller	Atmega 328P	330	1	Rs 330.00
Oscillator	16Mhz	11	1	Rs 11.00
Caps for Oscillator	20pf	1	2	Rs 2.00
Reset Res.	10k 0.25W	1	1	Rs 1.00
Inductor	441uH	40	1	Rs 40.00
Bypass Caps	100nf	1	2	Rs 2.00
Res. For IR side	390ohm 0.25W	1	1	Rs 1.00
Remote Controller kit	-	180	1	Rs 180.00
1 way 1 gang switch		175	1	Rs 175.00
SMPS	150mA	90	1	Rs 90.00
Enclosure		160	1	Rs 160.00
Other		57	1	Rs 57.00

Total	
Rs	1,191.00

3.4.3 Cost estimation of non-conventional cyclo converter method

This method consists of 3 main circuits, namely power circuit, control circuit and circuit to identify source voltage polarity. Design shown in figure 2. 14 was used for power circuit with active switches as MOSFETs. Same gate driver circuit shown in figure 3.27(b) was assumed for driving active switches.

A separate circuit was designed and simulated to obtain source voltage polarity (figure 3.29). Simulated result using Proteus 8 circuit simulation software is shown in figure 3.30.

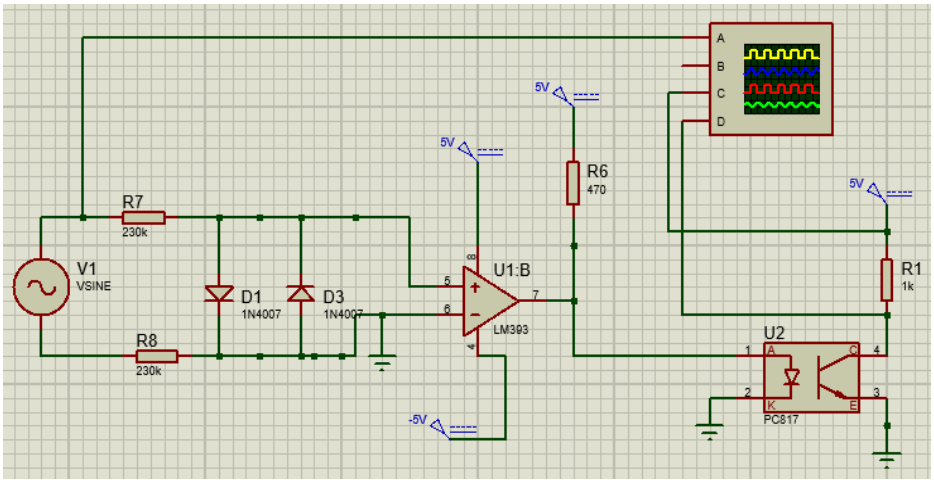

55*Figure 3.29: A circuit to identify source voltage polarity*

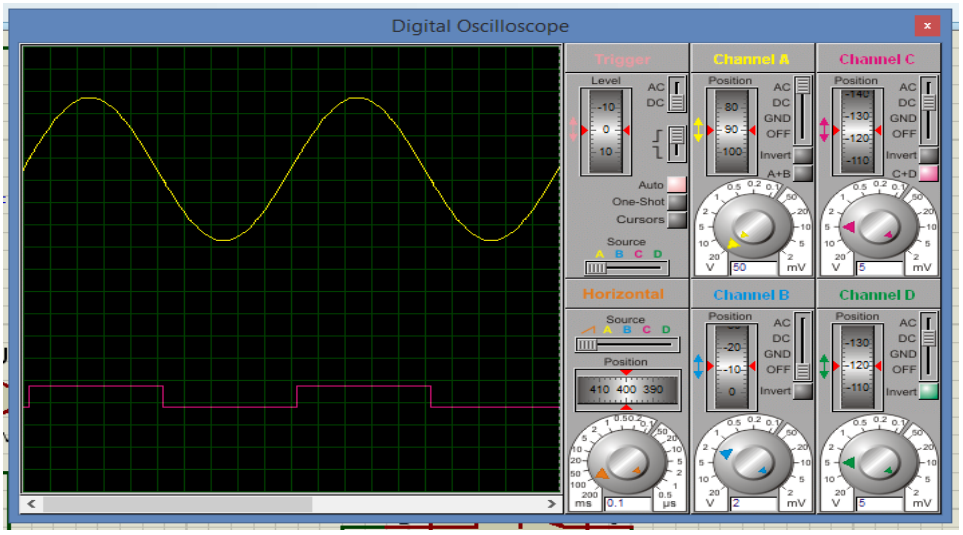

56*Figure 3.30: Digital oscilloscope output of circuit shown in figure 3.29(Yellow: Source voltage, Pink: Voltage through R1)*

Heart of this circuit is voltage comparator U1. R7 and R8 are current limiting resistors. When the voltage is negative, pin 7 of the comparator connects to ground and bypasses IR LED of opto-coupler. Hence 3, 4 will not conduct and voltage across R1 will be 0V. When the source voltage is positive, pin 7 of the comparator disconnects from the ground and allows the current to flow through IR LED. This will turn on the receiver and there will be a voltage drop across R1. This voltage drop across R1 can be used as digital input to the microcontroller to sense source voltage polarity. SMPS can be used to supply DC voltage to this circuit. It also provides isolation between controls and mains. Since maximum frequency is 50Hz, a general purpose opto-isolator was used to isolate the sensing circuit from microcontroller.

Developed cost estimation sheet for non-conventional cyclo converter method is shown in table 3.17.

17Table 3.17: Cost estimation of non-conventional cyclo converter method

Item	Part No:	Per Unit Cost	No.	Cost
Mosfets	IRF840	65	4	Rs 260.00
Snubber Res	47ohm 3W	8	4	Rs 32.00
Snubber Cap	10nf (polyester)	4	4	Rs 16.00
Diodes For Mosfets(Bridge)	FR104	5	16	Rs 80.00
Inductor	441uH	40	1	Rs 40.00
Pull down Res.	68k 0.25W	1	4	Rs 4.00
Gate Res.	33ohm 0.25W	1	4	Rs 4.00
Anti-Parallel Gate Diodes	FR104	5	4	Rs 20.00
Comparator IC	LM393	25	1	Rs 25.00
Res. for comparator IC	220k	1	2	Rs 2.00
Diodes for comparator IC	1N4007	2	2	Rs 4.00
Opto-isolator for LM393	PC817	8	1	Rs 8.00
IR res. For PC817	390 ohm 0.25W	1	1	Rs 1.00
O/P resistor for PC817	1k	1	1	Rs 1.00
Microcontroller	Atmega 328P	330	1	Rs 330.00
Caps for Oscillator	20pf	1	2	Rs 2.00
Oscillator	16Mhz	11	1	Rs 11.00
Reset Res.	10k 0.25W	1	1	Rs 1.00
Bypass Caps	100nf	1	5	Rs 5.00
Opto-isolator	TLP250	100	4	Rs 400.00
Res. For IR side	390 ohm 0.25W	1	4	Rs 4.00
Remote controller Kit	-	180	1	Rs 180.00
1 way 1 gang switch		175	1	Rs 175.00
SMPS module	150mA	90	6	Rs 540.00
Enclosure		498	1	Rs 498.00
Other		132	1	Rs 132.00

Total
Rs 2,775.00

3.4.4 Cost estimation of AC-AC buck converter method

Circuit shown in figure 3.31 was assumed as the AC-AC buck converter's power circuit while keeping the driver circuit and microcontroller as same as other methods. Developed cost estimation sheet for this method is shown in table 3.18.

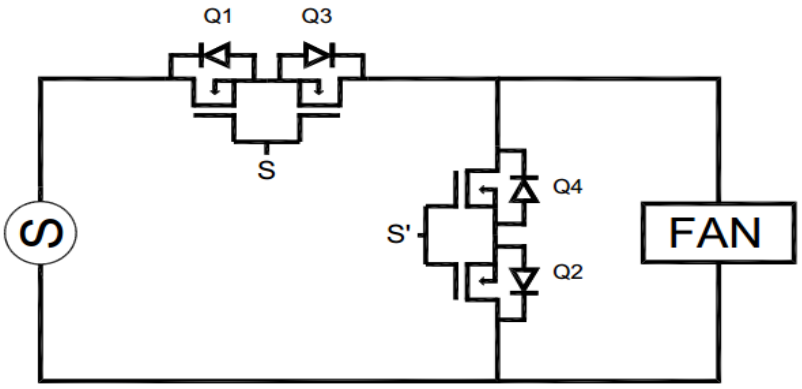

57*Figure 3.31: Simplified power circuit for AC-AC buck converter*

18Table 3.18: Cost estimation of AC-AC buck converter method

Item	Part No:	Per Unit Cost	No.	Cost
Mosfets	IRF840	65	4	Rs 260.00
Snubber Res	47ohm 3W	8	4	Rs 32.00
Snubber Cap	10nf (polyester)	4	4	Rs 16.00
Pull down Res	68k 0.25W	1	2	Rs 2.00
Gate Res	33ohm 0.25W	1	2	Rs 2.00
Anti-Parallel Gate Diode	FR104	5	2	Rs 10.00
Inductors	441uH	40	2	Rs 80.00
Bypass Caps	100nf	1	3	Rs 3.00
Res. For IR side	390ohm 0.25W	1	2	Rs 2.00
Opto-isolators	TLP250	100	2	Rs 200.00
Microcontroller	Atmega 328P	330	1	Rs 330.00
Reset Res.	10k 0.25W	1	1	Rs 1.00
Oscillator	16Mhz	11	1	Rs 11.00
Caps for Oscillator	20pf	1	2	Rs 2.00
Remote Controller Kit		180	1	Rs 180.00
1 way 1 gang switch		175	1	Rs 175.00
SMPS module	150mA	90	3	Rs 270.00
Enclosure		286	1	286
Other	-	93	1	93

Total
Rs 1,955.00

3.4.5 Cost estimation of single phase sinusoidal PWM inverter method

Power circuit shown in figure 3.32 was used to estimate the cost of this method. Developed cost estimation sheet for this method is shown in table 3.19.

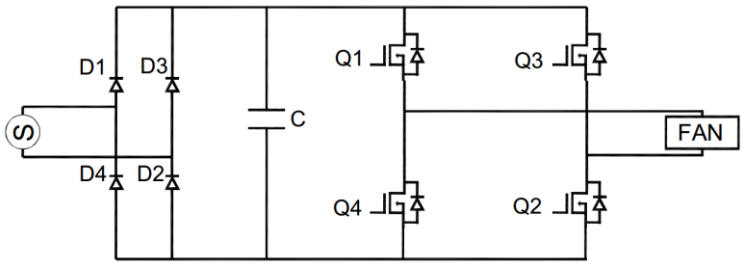

58 *Figure 3.32: Simplified power circuit for single phase sinusoidal PWM inverter method*

19Table 3.19: Cost estimation of single phase sinusoidal PWM inverter method

Item	Part No:	Per Unit Cost	No.	Cost
Mosfets	IRF840	65	4	Rs 260.00
Snubber Res	47ohm 3W	8	4	Rs 32.00
Snubber Cap	10nf (polyester)	4	4	Rs 16.00
Pull down Res.	68k 0.25W	1	4	Rs 4.00
Gate Res.	33ohm 0.25W	1	4	Rs 4.00
Anti-Parallel Gate Diodes	FR104	5	4	Rs 20.00
Inductor	441uH	40	1	Rs 40.00
DC link cap	270uf, 400V	300	1	Rs 300.00
Microcontroller	Atmega 328P	330	1	Rs 330.00
Oscillator	16Mhz	11	1	Rs 11.00
Caps for Oscillator	20pf	1	2	Rs 2.00
Diodes For rectification	FR104	5	4	Rs 20.00
Reset Res.	10k 0.25W	1	1	Rs 1.00
Bypass Caps	100nf	1	4	Rs 4.00
Opto-isolator	TLP250	100	4	Rs 400.00
Res. For IR side	390ohm 0.25W	1	4	Rs 4.00
Remote Controller kit	-	180	1	Rs 180.00
1 way 1 gang switch		175	1	Rs 175.00
SMPS module	150mA	90	5	Rs 450.00
Enclosure		576	1	Rs 576.00
Other		142	1	Rs 142.00

Total
Rs 2,971.00

3.4.6 Cost estimation of single phase sinusoidal PWM inverter with half bridge configuration

Realized power circuit for cost estimation is given in figure 3.33. In order to keep the ripple voltage same, C1 and C2 capacitor values was chosen to be twice the value of the DC link capacitor in the previous method. Since exact 540uf capacitance is not available in the market, 2 x 680uf polarized electrolytic capacitors were assumed for cost estimation. Developed cost estimation sheet for this method is shown in table 3.20.

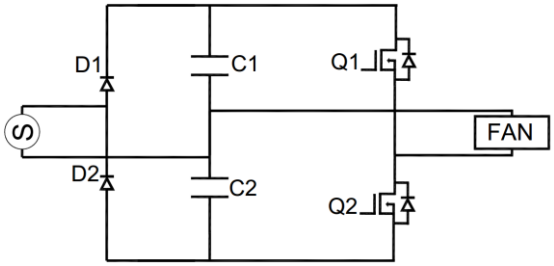

59Figure 3.33: Simplified power circuit for single phase sinusoidal PWM inverter with half bridge configuration

20Table: 3.20: Cost estimation of single phase sinusoidal PWM inverter with half bridge configuration

Item	Part No:	Per Unit Cost	No.	Cost
Mosfets	IRF840	65	2	Rs 130.00
Snubber Res	47ohm 3W	8	2	Rs 16.00
Snubber Cap	10nf (polyester)	4	2	Rs 8.00
Pull down Res.	68k 0.25W	1	2	Rs 2.00
Gate Res.	33ohm 0.25W	1	2	Rs 2.00
Anti-Parallel Gate Diodes	FR104	5	2	Rs 10.00
Inductor	441uH	40	1	Rs 40.00
DC link cap	680uf, 400V	500	2	Rs 1,000.00
Microcontroller	Atmega 328P	330	1	Rs 330.00
Oscillator	16Mhz	11	1	Rs 11.00
Caps for Oscillator	20pf	1	2	Rs 2.00
Diodes For rectification	FR104	5	2	Rs 10.00
Reset Res.	10k 0.25W	1	1	Rs 1.00
Bypass Caps	100nf	1	3	Rs 3.00
Opto-isolator	TLP250	100	2	Rs 200.00
Res. For IR side	390ohm 0.25W	1	2	Rs 2.00
Remote Controller kit	-	180	1	Rs 180.00
1 way 1 gang switch		175	1	Rs 175.00
SMPS module	150mA	90	3	Rs 270.00
Enclosure		495	1	Rs 495.00
Other		144	1	Rs 144.00

Total	
Rs	3,031.00

3.4.7 Cost of traditional electronic fan regulator

Cost of traditional electronic fan regulator was also obtained as the base case to compare the costs of novel methods with traditional one.

One concern arose here was that the different fan regulator manufacturers advertise different prices for their fan regulators. Hence an average cost of 3 fan regulators (triac based) were obtained. Chosen fan regulator designs are shown in figure 3.34. Prices were obtained from [29]. Average selling price for traditional fan regulator was estimated around Rs 1150/=.

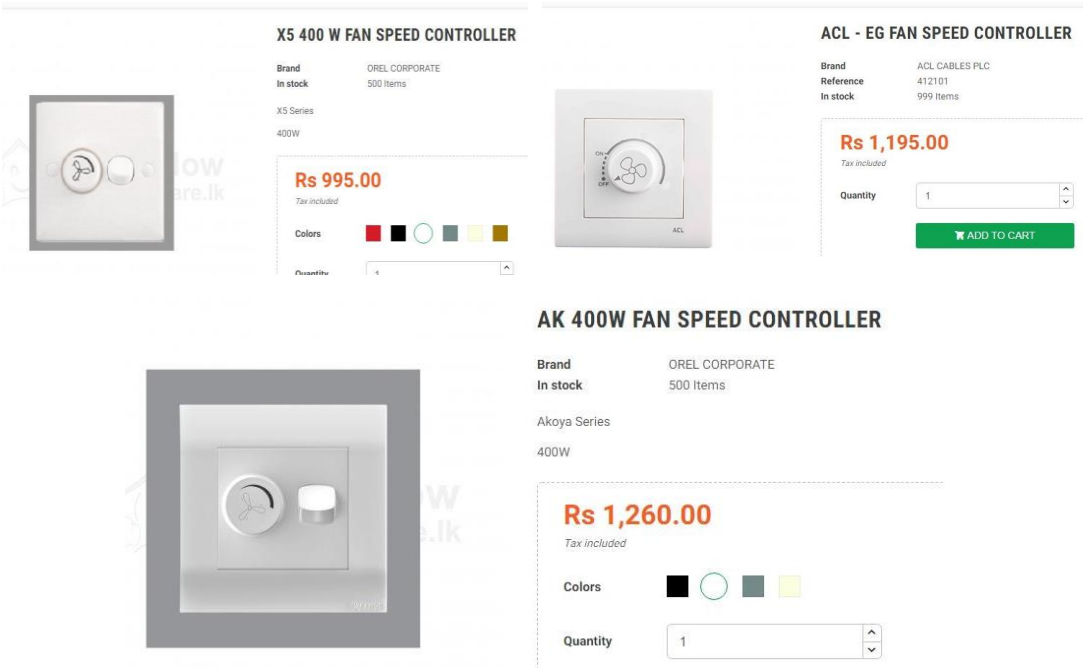

60*Figure 3.34: Costs of market available traditional electronic (triac based) fan regulators*

However, estimations of considered novel methods reflect cost of production while traditional fan regulator gives the selling price. Cost of production should definitely be less than the selling price. An assumption was taken in order to proceed further which the cost of production is 75% of the selling price. With that assumption, average cost of production of traditional fan regulator came around Rs. 862/=.

3.5 Performance and cost comparison

Graphs were developed for THD_v vs. speed (figure 3.35(a)), stabilization time vs. speed (figure 3.35(b)), maximum input current vs speed (figure 3.35(c)) and THD_I vs. speed (figure 3.35(d)) to compare and contrast novel fan regulator control methods vs. traditional electronic fan regulator. Developed graphs are shown below.

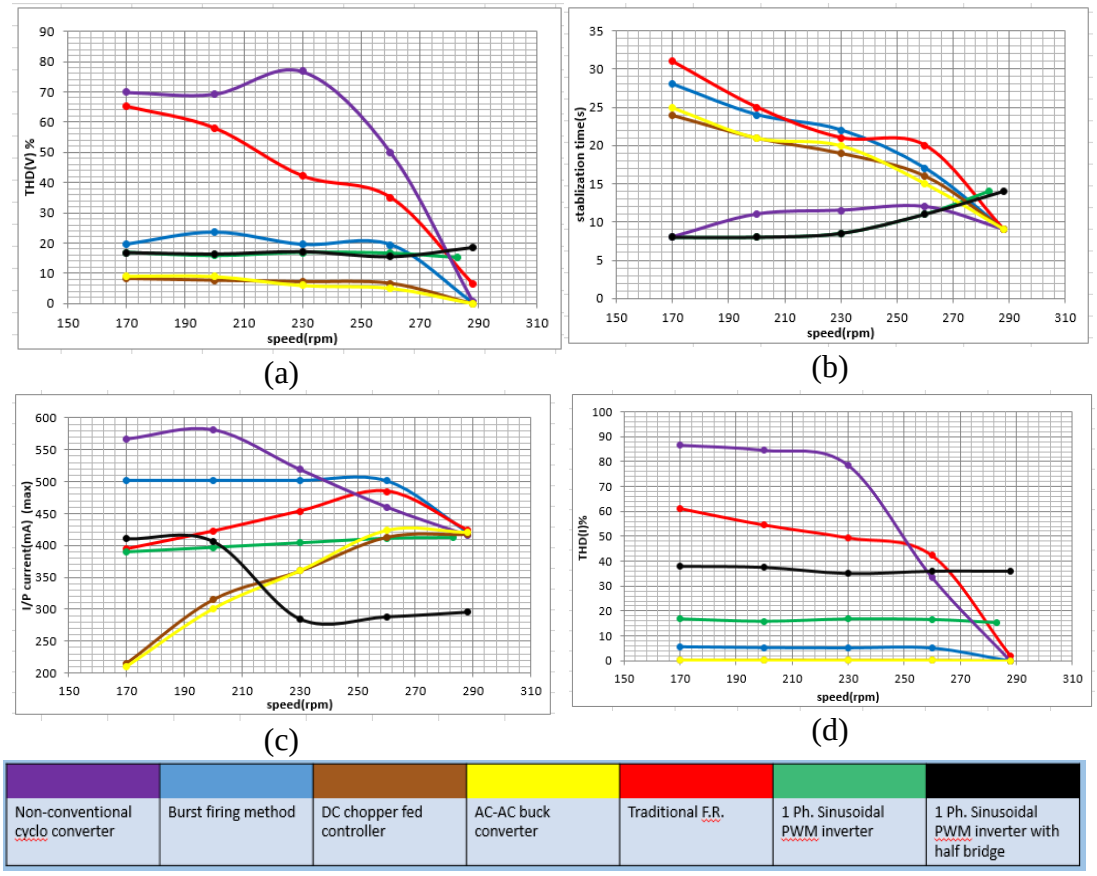

61 *Figure 3.35(a): THD(v) % vs. speed(rpm) (b) Stabilization time(s) vs. speed (rpm) (c) Maximum input current (mA) vs speed (rpm) (d) THD (I) % vs. speed (rpm)*

According to the stabilization time vs. speed graph, it is clearly seen that frequency controlling methods can stabilize quickly than voltage controlling methods. These methods can quickly come to its set voltage even at the low speeds. Afterwards DC chopper fed controller and AC-AC buck converter shows moderate stabilization times. Due to their high intermittent nature of applied voltage to the fan,

burst firing method and traditional fan regulator shows somewhat high stabilization times in lower speed levels.

When it comes to THD(I) and THD(V) graphs, traditional electronic fan regulator and non-conventional cyclo converter methods show high harmonic content compared to other methods. This is the governing reason to eliminate non-conventional cyclo converter as a potentially viable solution.

According to maximum current graph, burst firing method and non-conventional cyclo converter method shows high maximum input current at low speeds. This can cause additional heat generation in the ceiling fan and eventually degrade the insulation of the windings. Also it causes more power losses.

At the very first burst of first cycle, current waveform shows its maximum value in the burst firing method. Since the fan capacitor discharges through main winding during the off time, it quickly tries to charge when the supply is available. Also the rate of change of voltage (dv/dt) is high at the beginning of the cycle. Hence the ceiling fan draws high current.

Although the THD(V) value and THD(I) values are comparatively less in burst firing method, it contains sub harmonics. These are very difficult to filter [14] and also in the practical implementation, sub harmonic content can be little higher than simulations due to computational limitations of tracking zero crossing point.

Due to these two reasons, burst firing method was kept aside and analyzed rest of the methods.

Both single phase sinusoidal PWM inverter method and single phase sinusoidal PWM inverter with half bridge configuration have remarkably good stabilization times. Also compared to traditional fan regulator and some other novel methods these two methods show relatively less harmonic content of their output waveforms. However both of these fan regulators show high production cost in the estimation. This happens mainly due to costly DC link capacitors. Since the average production cost of traditional fan regulator is way less than the above two, analysis went to rest of the other methods.

DC chopper fed controller and AC to AC buck converter methods show less THD(V) and THD(I) content. Maximum input current of these two regulators are also less in lower speeds. Compared to frequency controlling methods, these two methods show moderate stabilization times. Anyway, stabilization time doesn't have to be perfect since ceiling fan is a general household equipment and uses do not expect very quick stabilization times. However, both of these methods show relatively quick stabilization times compared to traditional fan regulator.

When comparing DC chopper fed controller and AC to AC buck converter with regards to production cost, DC chopper fed controller shows somewhat less estimate. This happens mainly due to less active switches and snubbers. However, DC chopper fed controller gives higher cost estimate compared to traditional fan regulator. But it is logical to pick DC chopper fed controller as most viable solution for mentioned problems in chapter 1 with the added technical features.

CHAPTER 4

HARDWARE DEVELOPMENT

Introduction

Simulation and analysis of several key characteristics of novel fan regulators were performed in chapter 3 of this research and identified DC Chopper fed controller as one of the best possible solutions for mentioned concerns in chapter 1.

This chapter provides how the hardware implementation of DC chopper fed controller was carried out by going through microcontroller selection, obtaining complementary switching and dead time, developed algorithm, selection of active switches, gate driver selection and signal-power isolation, mitigation of ringing, input filter design and development of PCB.

4.1 Microcontroller selection

This circuit needs a microcontroller for two purposes. Those are; to generate switching signals for active switches and to enable remote controlling facility. Table 4.1 shows a brief comparison between two Famous microcontroller ICs. Selected microcontroller was based on this comparison.

21Table 4.1: Comparison of PIC16F628A and Atmega328P microcontrollers

Characteristic	**PIC (PIC16F628A)**	**Atmega (Atmega328P)**
Programming Complexity	Hard	Easy
Libraries	Less	More
Memory	14.3KB	32KB
Cost	Low(Rs. 250/=)[30]	Moderate(330/=)[31]

Shown PIC16F628A microcontroller was created by Microchip Technology Inc. and Atmega328P was created by Atmel Corporation before acquired it in 2016 by Microchip Technology Inc. Arduino integrated development environment can be used to program Atmega328P while PIC16F628A uses integrated development environments like MPLAB. Since assembly language is used to program PIC16F628A, code complexity is bit high. However, Arduino IDE uses C++ with some additional functions to program the microcontroller. Compared to previous one, this technique is less complex.

In case if the designer wants to improve the functions, some critical things that need to consider from microcontroller prospective are: inbuilt libraries, I/O pins and microcontroller memory…etc. Atmega328P microcontroller supports more inbuilt libraries, which means that designer can easily add more functionalities to the system. Since memory is also greater, it can store programs with higher capacities. Also this microcontroller offers 14 digital and 6 analog I/O pins (altogether 20 I/O pins) whereas PIC16F628A gives 16 I/O pins. This is critical when attaching external hardware to the microcontroller.

When it comes to price, PIC16F628A is cheaper than Atmega328P. However, Atmega328P stands in front compared to other features. Also the code developed using Arduino IDE can easily be transferred to low power low cost at mega microcontrollers (e.g. ATtiny microcontrollers) if needed. Hence, Atmega328P chip was used as the microcontroller for this project

4.2 Complementary switching and dead time

As explained in chapter 2, two active switches in DC chopper fed controller should work in complementary manner. Since a practical MOSFET has turn rise time, fall time, on time, turn off time…etc, there is a need to introduce a dead time between switching to prevent any shoot-through. This dead time was given to the circuit by implemented algorithm. In order to keep the waveform quality, and also to prevent the shoot-through, two microsecond dead time was set. Figure 4.1 shows complementary output from the microcontroller for two different PWM values.

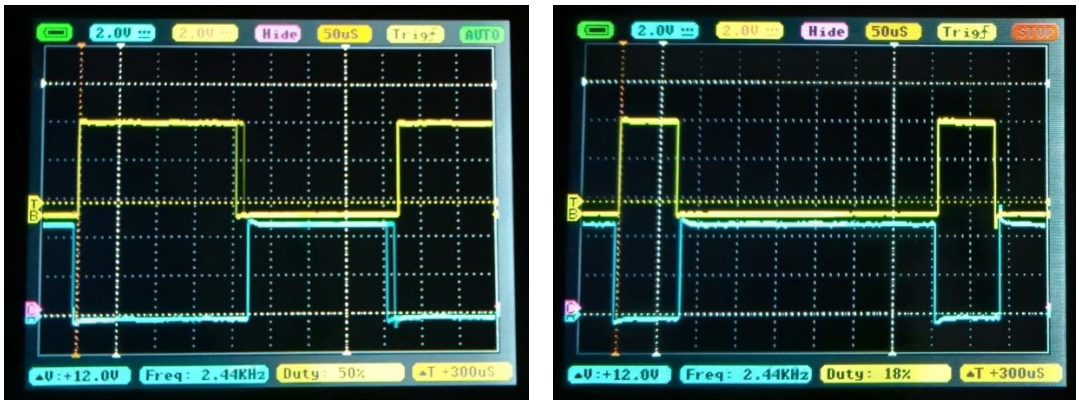

62Figure 4.1: Complementary PWM at D=50 %(right) and D=88 %(left) (Duty - relative to main signal)

[Yellow: Auxiliary signal, Blue: Main signal]

4.3 Algorithm

Figure 4.2 shows developed algorithm for remote controlled DC chopper fed controller using a flowchart. Variable ‘n_time’ is measured in microseconds and starts counting from 0 us when the microcontroller gets power. Period is a constant and its value is 400 us (Since switching frequency is 2.5 kHz). ‘p_time’ variable is used to track multiples of 400(i.e. period). So, if (n_time-p_time) <= period, process can go to latter blocks. Otherwise p_time is replaced by n_time and starts over.

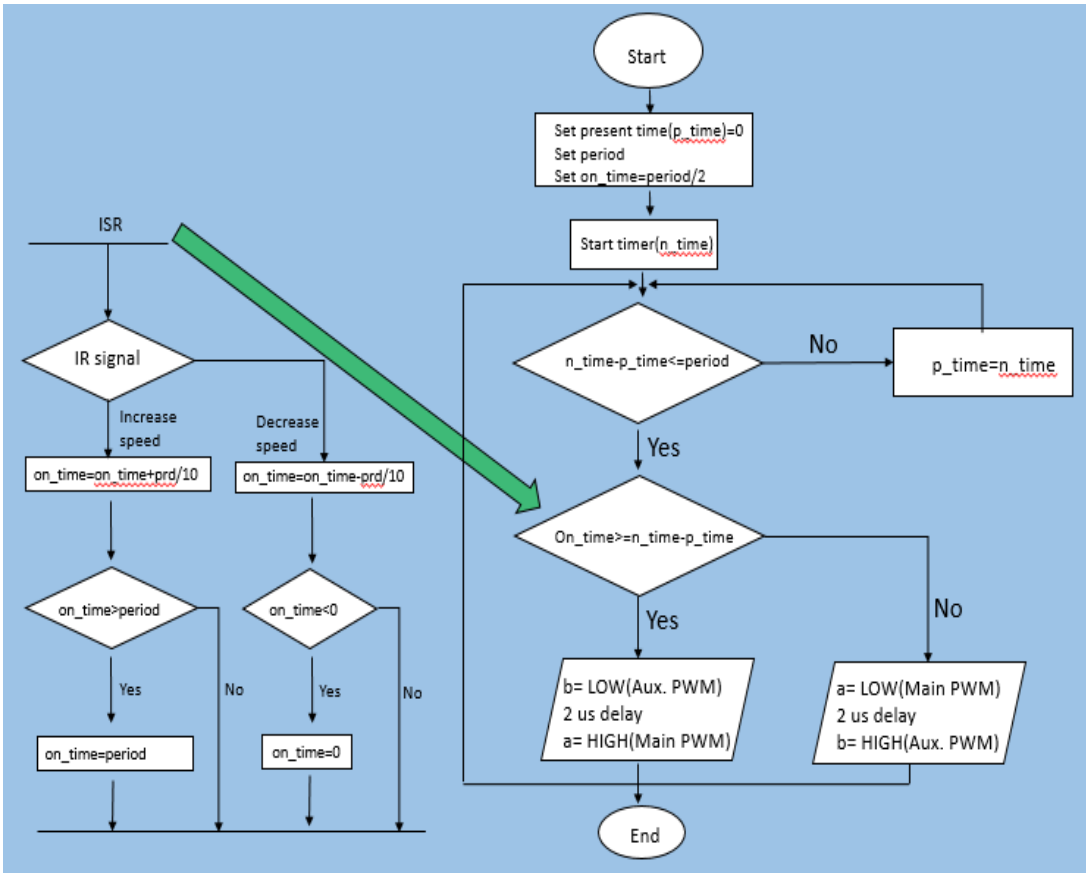

63Figure 4.2: Flowchart of developed algorithm

After checking (n_time-p_time) <= period, it checks whether (n_time-p_time) is less than on_time (figure 4.3). Variable ‘on_time’ gives the time which the MOSFET in main path is active. If (n_time-p_time) <= on_time, controller needs to keep the main MOSFET on while keeping auxiliary MOSFET turned off. In order to preserve safety, switching off of active switches were performed earlier.

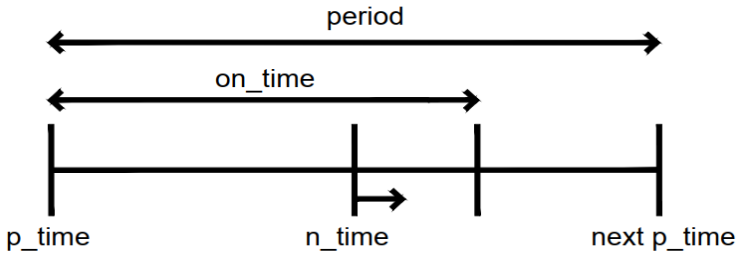

64Figure 4.3: Graphical representation of time variables used in the algorithm

Speed increment/decrement through IR remote controller is introduced as an external interrupt to the algorithm. Speed depends on the value of 'on_time' and initial value of 'on_time' was taken as 200 us (i.e. time period/2). When an IR receiver receives a signal from its transmitter (remote controller), that signal transfers to microcontroller and it checks whether the received signal corresponds to an increment of the 'on_time' or a decrement of the 'on_time'. If it is an increment, 'on time' is increased by 40 microseconds and if it is a decrement, 'on_time' is decreased by 40 microseconds. However, the range of 'on_time' lies between 0 and 400 microseconds. Finally this constant is checked and keep on time between its limit.

Motor controlling code was created in Arduino IDE and it is given in appendix D.

4.4 Active switches

Q1 and Q2 in figure 3.27(a) need to be realized by power electronic switching devices. MOSFETs and IGBTs have lot of attractions nowadays when considering high power active switches. Hence, the choice was made by comparing those two.

22Table 4.2: Comparison between MOSFET and IGBT

Characteristic	MOSFET	IGBT
Voltage rating	High(<1000V)	Very High(>1000V)
Current rating	High(>500A)	High(>500A)
Switching speed	Fast	Medium
Cost	Medium	High

The component to be chosen should theoretically handle nearly 325V peak voltage. According to the simulations done, this component need to handle

295mA rms current and 418mA peak current. Since switching the speed is also moderate and cost is less, MOSFETs were chosen as switching devices for prototype. IRF840 MOSFET gave perfectly fit electrical characteristics for the design. Data sheet of this MOSFET is attached in appendix E for references.

4.5 Gate drivers and signal-power isolation

In order to utilize efficient switching of MOSEFTs and isolate between signal circuit and power circuit, gate drivers were used. There are two main options for isolated gate drivers. Those are pulse transformers and opto-isolated gate drivers.

Compared to opto-isolated gate drivers, pulse transformer option has a noticeable disadvantage. A pulse transformers can't continuously switch on MOSFET attached to it. So, full speed option of the fan can't be achieved. Hence, opto-isolated gate driver option was taken into account.

Chosen TLP250 opto-isolated gate driver meets all the electrical requirements for the operation. Internally set push-pull configuration offers efficient switching of MOSFETs and IR emitter & receiver pair isolates power and signal circuits (figure 4.4).

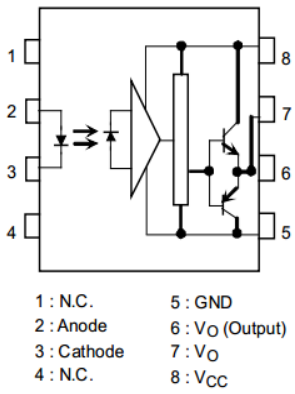

65*Figure 4.4: Internal circuitry of TLP250 opto-isolated gate driver*

A general purpose opto-isolator can’t be used for this kind of an application. It can be concluded by comparing general purpose opto-isolator (e.g. PC817) with special purpose opto-isolator (e.g. TLP250) (see table 4.3). Opto-isolated gate drivers offer much less response time, can handle higher currents and can be operated in much higher frequency.

23Table 4.3: Comparison between a general purpose opto-isolator vs. TLP250 opto-isolator

Characteristic	A general purpose opto-isolator(PC817)	TLP250 opto-isolator
Response time	18us(max)	0.5us(max)
Output current	30mA	1.5A
Max. operating frequency	1kHz	25kHz

4.6 Mitigation of ringing

A series LC circuit is formed when the MOSFET turns off. Inductance exists since the load is inductive and also because of stray inductances. MOSFET output capacitance is responsible for C. This LC circuit causes turn-off ringing. An RC snubber circuit was placed in parallel to MOSFET to dampen this ringing.

When the MOSFET turns on (when the gate goes high), MOSFET requires high gate current to charge its C_{gs} and C_{gd} capacitors (figure 4.5). Hence V_{DS} becomes somewhat higher than its steady state value because of internal source inductance. So, a gate resistor was introduced in between the driver circuit and the MOSFET to charge the gate slowly.

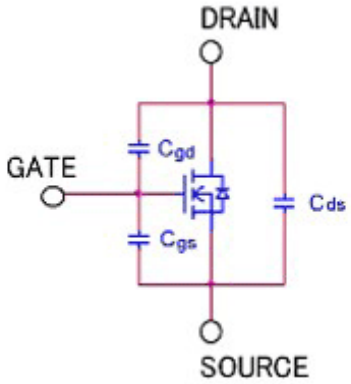

Symbol	Expression	Meaning
Ciss	Cgs +Cgd	Input capacitance
Coss	Cds +Cgd	Output capacitance
Crss	Cgd	Feedback capacitance

66Figure 4.5: Parasitic capacitances of a MOSFET

Moreover, two toroid core inductors were included in the main path and auxiliary path to limit current spikes. Figure 4.6(a) and figure 4.6(b) respectively shows voltage waveforms across the main MOSFET before and after addressing the ringing effect.

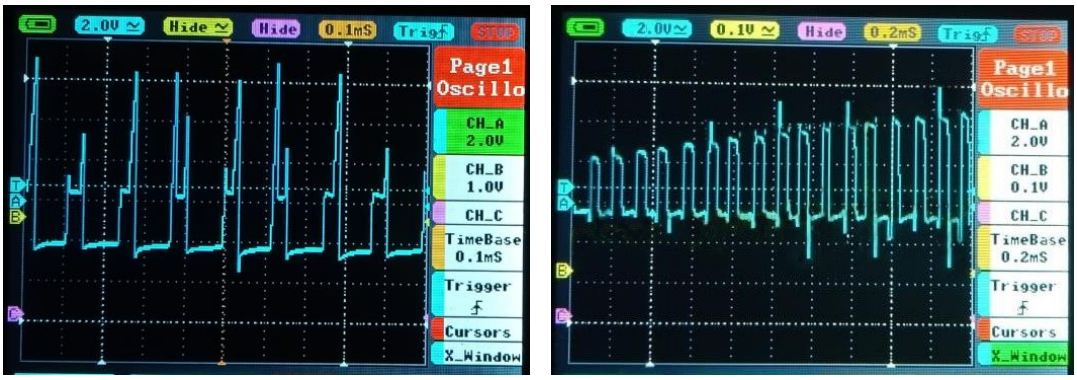

(a) (b)

67Figure 4.6: Voltage waveform through the main Mosfet (a) Before addressing the ringing effect (b) after addressing the ringing effect

4.7 Input filter design

Since this is a chopper circuit, it produces pulsating current at the input. This can cause problems like;

- Disturbance to nearby equipment and
- Decreasing the power quality by drawing harmonic currents from the power source.

An input filter was constructed in order to reduce these effects. Since RC filters are lossy, this was realized using an LC filter (figure 4.7). Specification of the constructed LC filter are as follows:

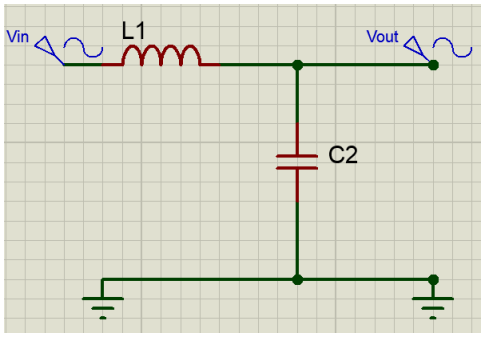

- L1 = 27 mH
- C2 = 150 nf
- f_c = 2500 Hz

68Figure 4.7: Undamped LC filter and specifications

According to $f_c = \frac{1}{2\pi\sqrt{LC}}$ formula [17], corner frequency of 2500 Hz can be achieved from the above mentioned specifications. An Excel based Bode plot

diagram was created afterwards (figure 4.8). However, it shows an asymptotic peak around corner frequency.

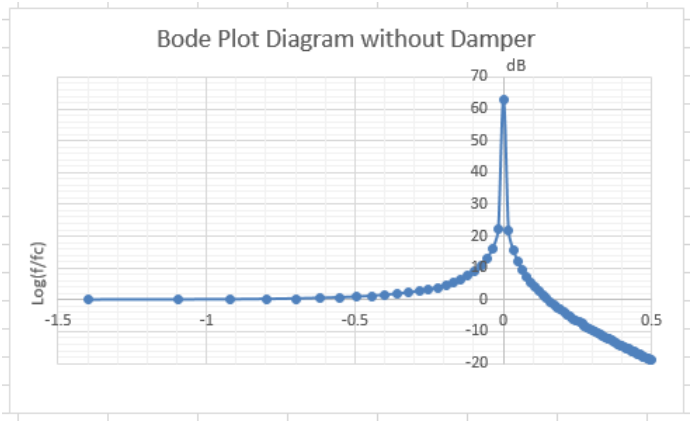

69Figure 4.8: Bode plot diagram of undamped LC filter

This rise can cause huge current peaks. Hence, this LC filter needs to be damped. A damper RC branch was introduced in parallel to existing capacitor C1 [figure 4.9(a)]. Another Excel sheet was constructed to find the damper RC combination. Trial and error method was used to find a suitable value for R' and C'. At the end of the study, 220 ohm valued resistor was chosen for R' and 0.68 uf valued capacitor was chosen for C'.

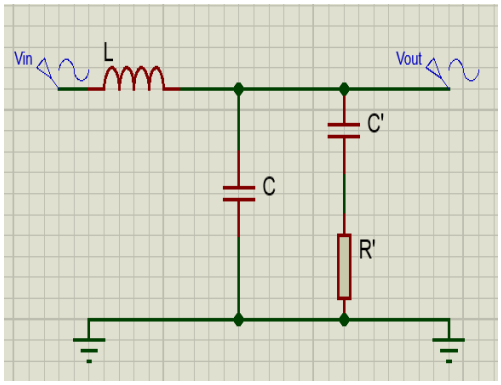

(a)

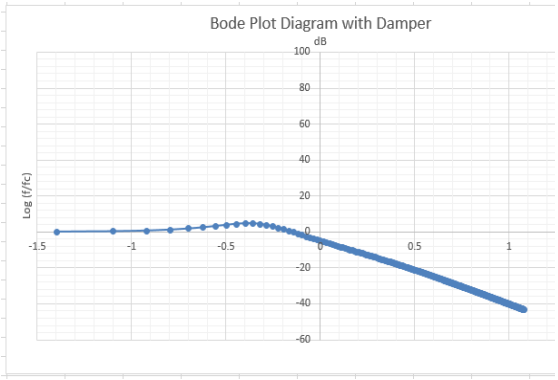

(b)

70Figure 4.9(a): Input LC filter with damper (b) Corresponding Bode plot diagram

Figure 4.9(b) shows corresponding Bode plot diagram for input filter with damper.

4.8 PCB development

Two separate PCBs were developed for power circuit and signal circuit. First, power circuit was tested by prototyping on a breadboard (figure 4.10). Switching signals were given using Arduino Uno board and receiving sides of isolated get drivers were powered using two separate switch mode power supplies and two separate boost converters. 18V signal was given by these boost converters to power up the MOSFET switches. IR receiver was connected to Arduino Uno board and it was used to pick the IR transmitter signal from the remote controller.

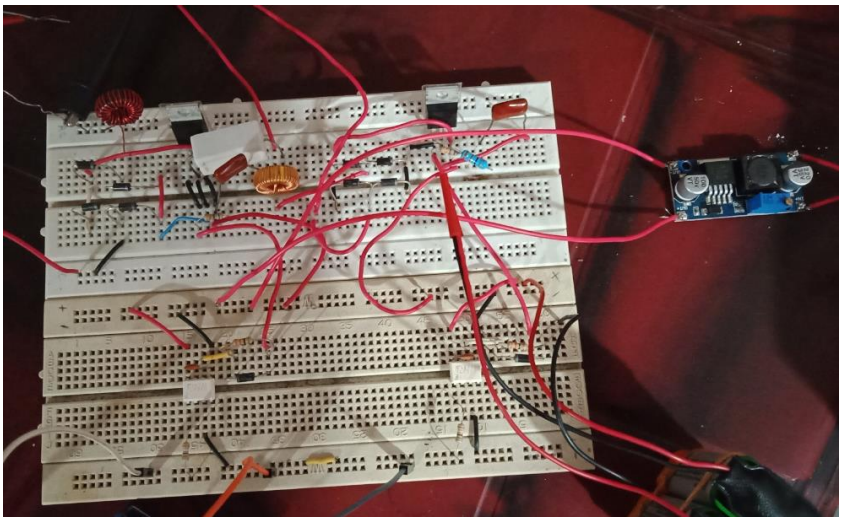

71 *Figure 4.10: Power circuit on a breadboard*

Proteus 8 circuit design software was used to design the PCBs. Figure 4.11 (a), (b) and (c) shows circuit diagram of power circuit, PCB layout and 3D view of the design respectively. In the PCB layout, traces were designed such a way that the stray inductance become minimum.

After constructing the PCB layout, hardware PCB was created using toner transfer method with the help of heat. Etching was done by dissolving the copper board with toner traces in a ferric chloride solution. Final power circuit is shown in figure 4.12.

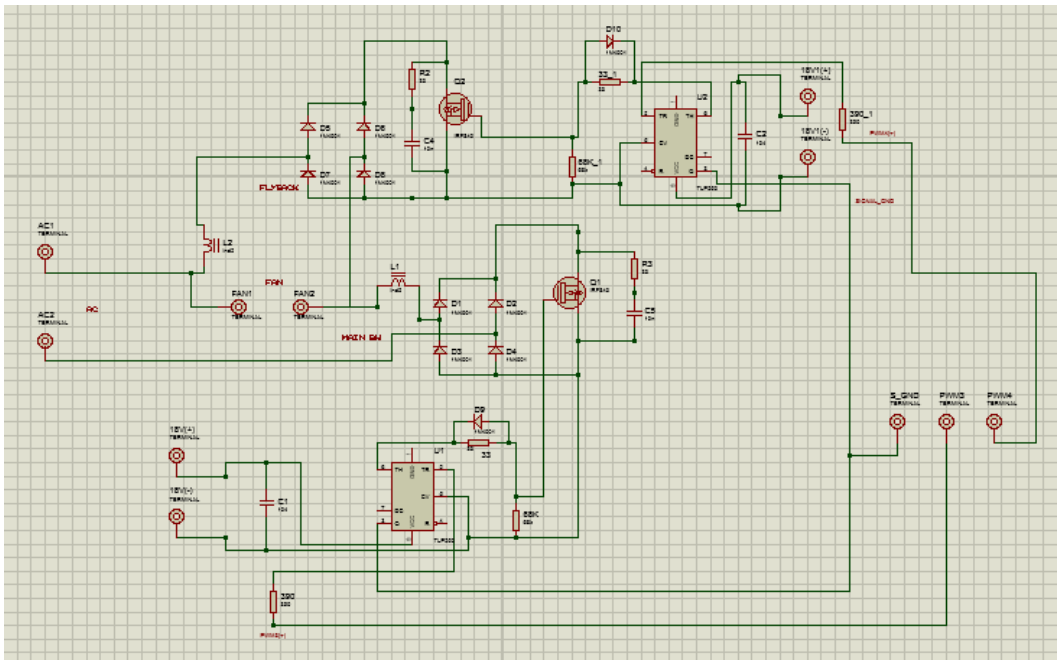

(a)

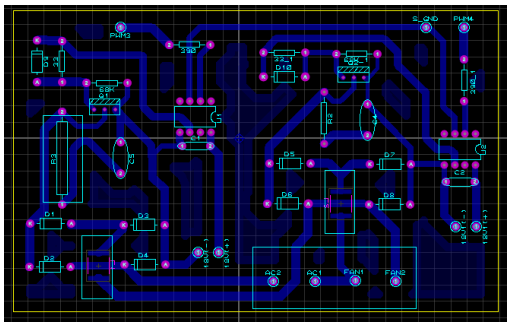

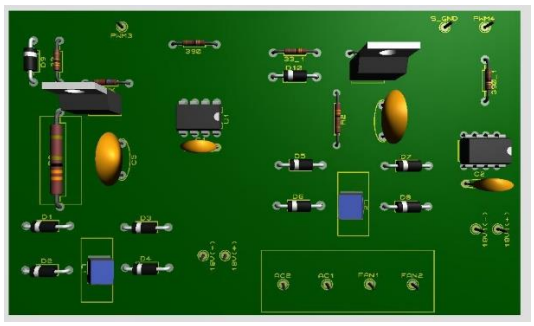

(b) (c)

72*Figure 4.11: Power circuit: (a) Circuit diagram (b) PCB layout (c) 3D view*

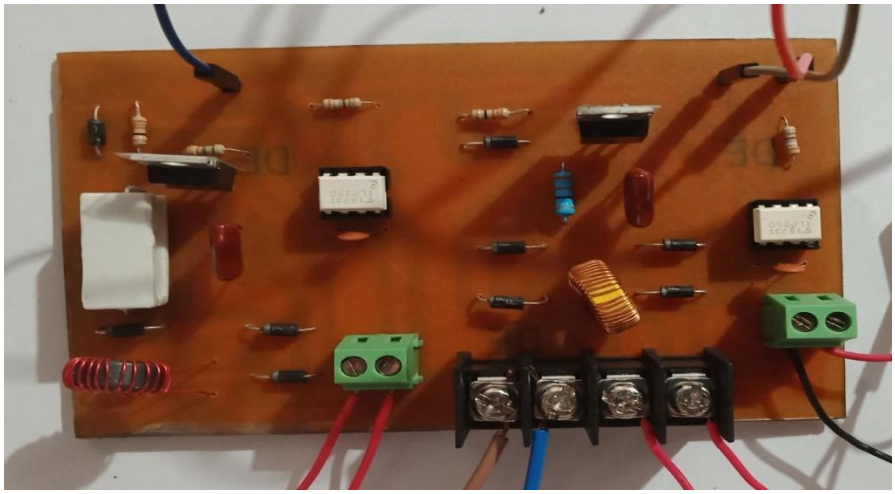

73*Figure 4.12: Built power circuit*

Figure 4.13(a) shows created signal circuit diagram in Proteus. This consists of standalone Atmega 328P chip, 16 MHz crystal oscillator and some passive components. Signal circuit has two inputs and one output. One input is to power the circuit and it is done by connecting 5 volt switch mode power supply. The other input is to receive IR signal from IR sensor. Output is complimentary switching signals which receives to the power circuit to drive two MOSFETs

Figure 4.13(b) and figure 4.13(c) shows designed PCB layout for signal circuit and 3D view of signal circuit respectively.

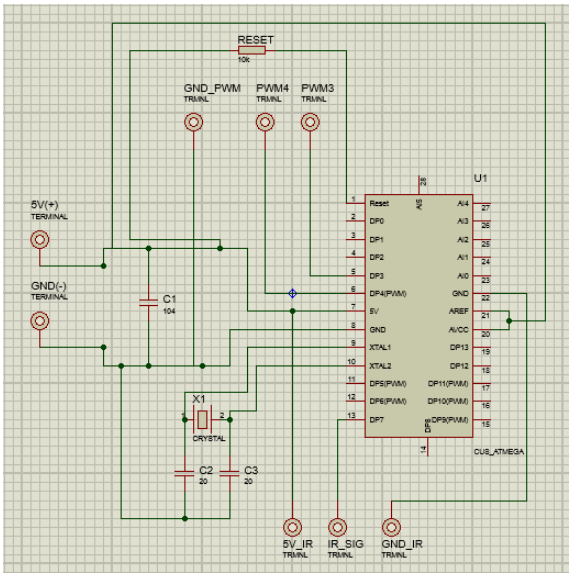

(a)

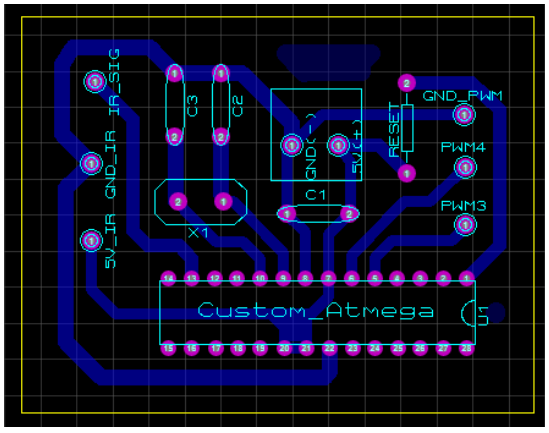

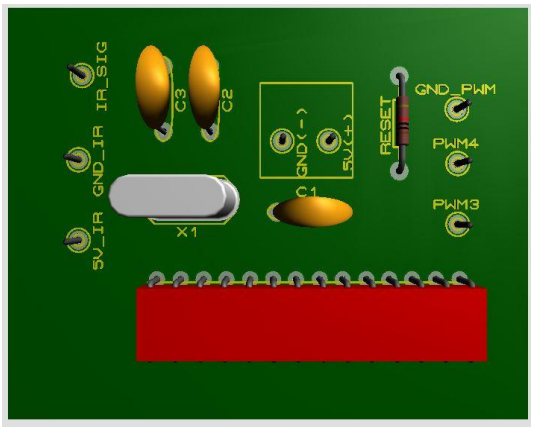

(b) (c)

74Figure 4.13 Signal circuit: (a) Circuit diagram (b) PCB layout (c) 3D view

Hardware PCB of signal circuit was also constructed as same as the way it used to create power circuit PCB. Final signal circuit is shown in figure 4.14.

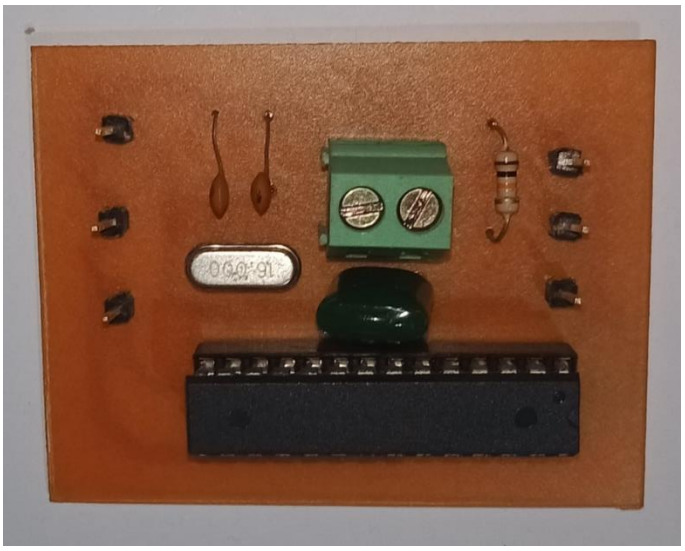

75Figure 4.14: Built signal circuit

Created circuits and power modules were created afterwards. Final circuit of DC chopper fed controller is shown in figure 4.15. This circuit was used to obtain the results shown in chapter 5.

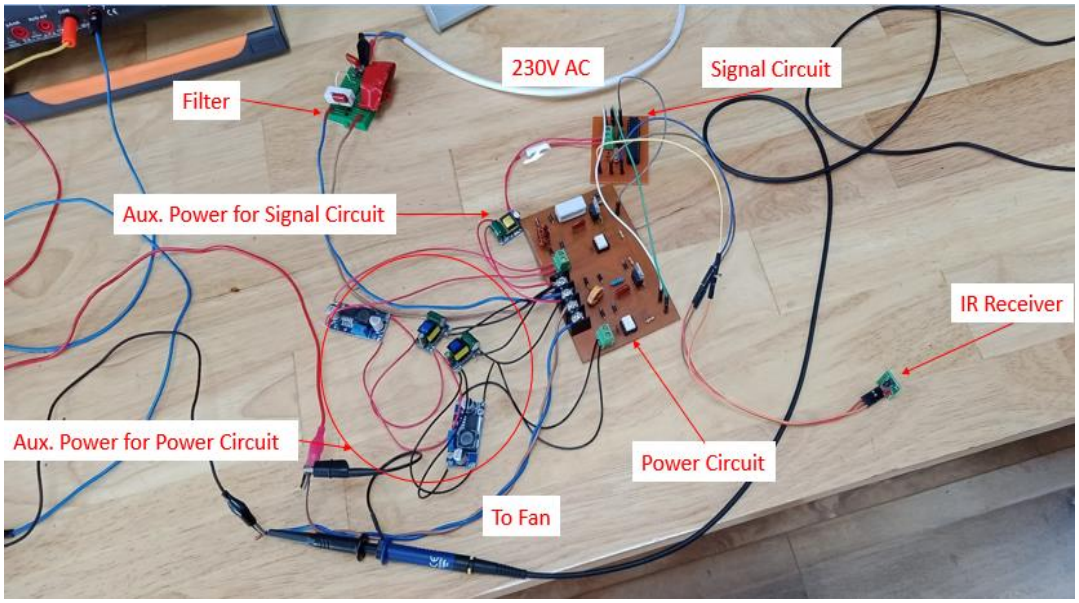

76Figure 4.15: Final circuit of DC chopper fed controller

CHAPTER 5

RESULTS AND DISCUSSION

Introduction

Chapter 4 of this research ended up discussing the final prototype circuit of DC chopper fed controller. This chapter is dedicated to discuss the experimental setup of the investigated systems, results obtained from the prototyped circuit, waveform comparison between traditional fan regulator circuit and DC chopper fed controller.

5.1 Experimental setup

Prototype circuit shown in figure 4.15 was powered up using 230 V AC 50 Hz supply and connected a 70 W ceiling fan as the load. In order to record the performance, two lab bench multi meters (to record load voltage and current) and an oscilloscope (to record the waveforms) was connected (figure 5.1). Speed of the fan was controlled using IR remote controller. Same experimental setup was used to check the performance of traditional electronic fan regulator circuit and compared the results obtained.

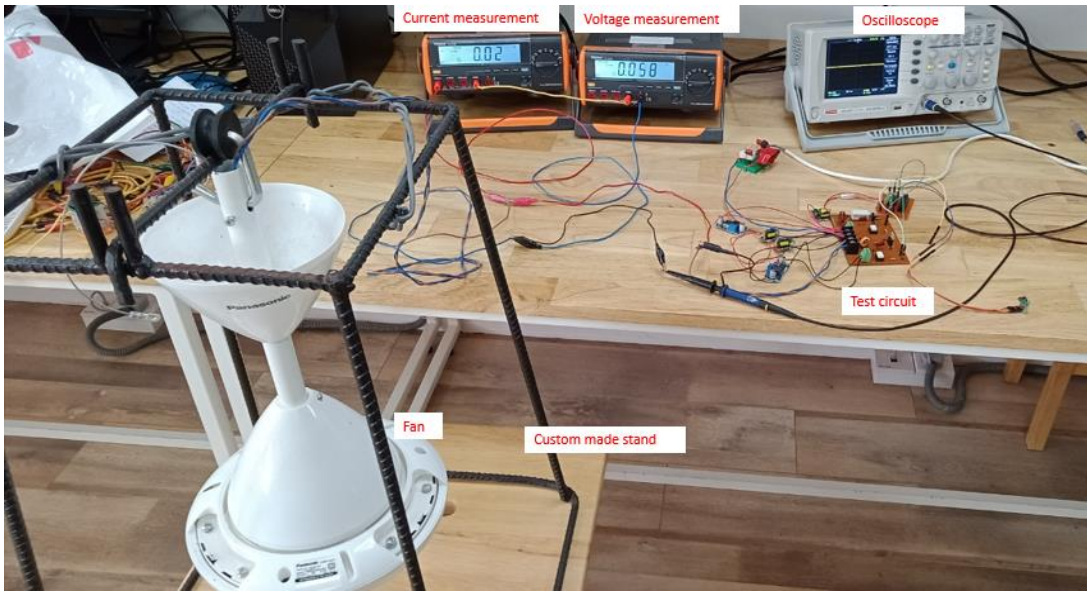

77*Figure 5.1: Experimental setup*

5.2 Comparison of obtained waveforms

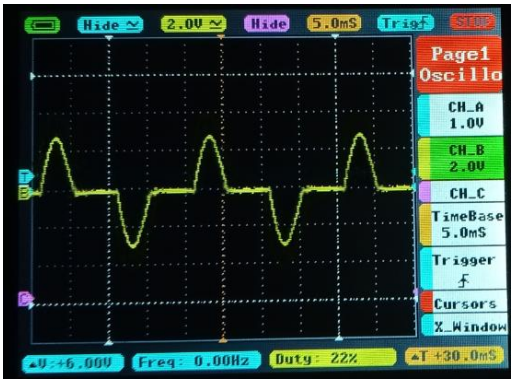

(a)
Load current waveform of traditional FR
@100rpm I(max) = 230mA, 200mA/div

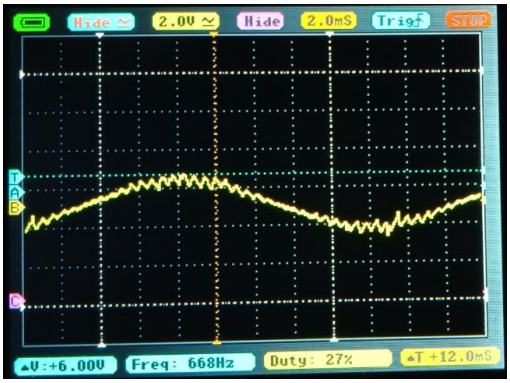

(b)
Load current waveform of proposed circuit
@100rpm I(max) = 140mA, 200mA/div

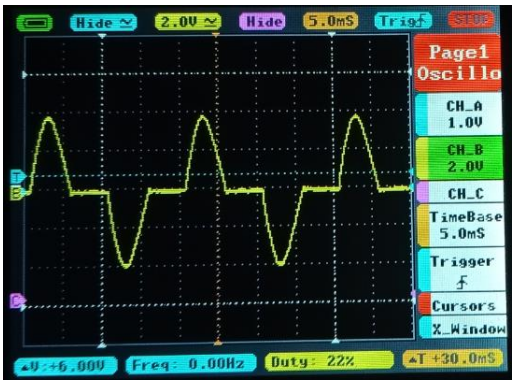

(c)
Load current waveform of Traditional FR
@160rpm I(max) = 380mA, 200mA/div

(d)
Load current waveform of proposed circuit
@160rpm I(max) = 210mA, 200mA/div

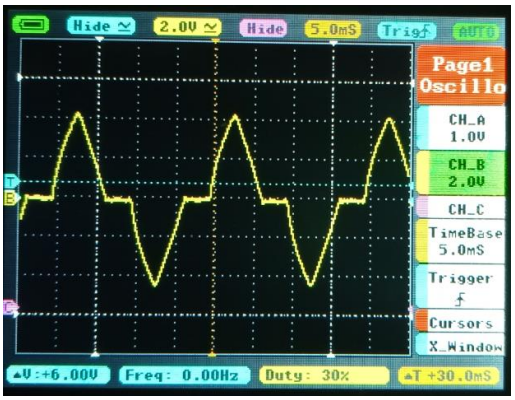

(e)
Load current waveform of Traditional FR
@220rpm I(max) = 400mA, 200mA/div

(f)
Load current waveform of proposed circuit
@220rpm I(max) = 320mA, 200mA/div

78Figure 5.2: Load current variation utilizing traditional fan regulator vs. DC chopper fed controller for low speed levels

Rated speed of the ceiling fan was 288 rpm. Three arbitrary low speeds were considered to check the performance of DC chopper fed controller and traditional

fan regulator. Figure 5.2 shows load current versus time waveforms of about two methods.

According to the obtained waveforms for traditional fan regulator, the load (ceiling fan) receives discontinuous current over time. Since electromagnetic torque produced is proportional to square of the current which is responsible for producing torque, this method suffers from high torque pulsations. Hence it produces speed ripples over time.

However, load receives continuous current when utilizing DC chopper fed controller. Hence the ceiling fan generates slower speed pulsations. This continuous current also responsible for quick speed stabilizations.

Practically obtained load current graphs of traditional fan regulator are almost same as simulation results (figure 3.6). However practically obtained and simulated load current graphs for DC chopper fed controller shows slight discrepancies. More current spikes can be seen in practically obtained waveform. Less accurate inductor value calculations may be one of the reasons behind this.

Figure 5.3 shows load voltage versus time waveforms of three low speed levels of the ceiling fan for two scenarios.

Simulated (figure 3.5) and practically obtained load voltage waveforms for traditional fan regulator have some similarities as well as some discrepancies. Although the general wave shape is similar, practically obtained waveform shows higher oscillations. This may due to the formation of LC oscillator comprised with load (inductive), stray inductances and poorly designed snubber circuit. Both figures exhibits the waveform distortion due to flyback and reverse recovery.

When compared to simulated load voltage waveform (figure 3.9) with practically obtained waveforms, some additional voltage spikes can be seen in practically obtained result. Most of the times in positive half cycle, falling edge has gone beyond 0V. Also in negative half cycles, falling edge has gone above 0V. This could be due to introduced dead time to the complementary switching circuit.

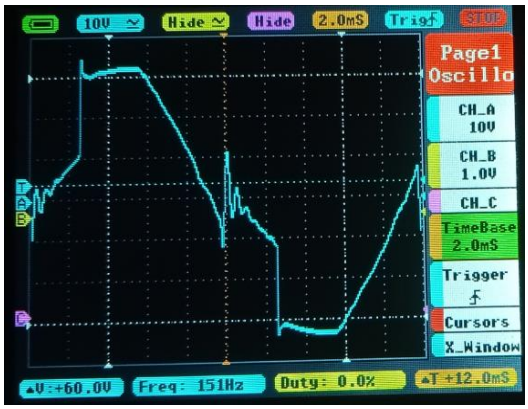

(a)
Load voltage waveform of Traditional FR @220rpm 100V/div (x10)

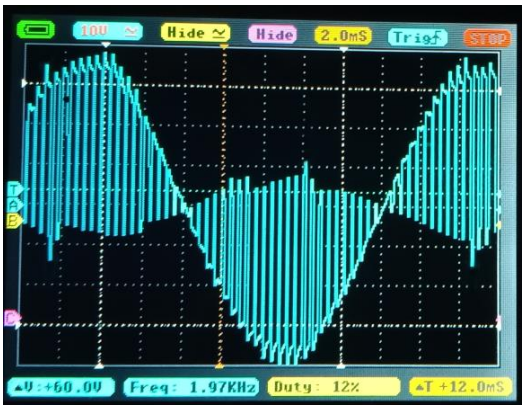

(b)
Load voltage waveform of proposed circuit @220rpm 100V/div (x10)

(c)
Load voltage waveform of Traditional FR @160rpm 100V/div (x10)

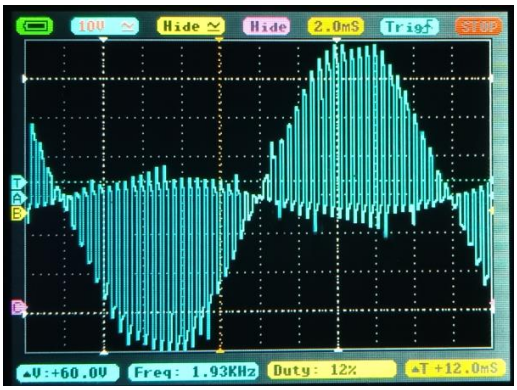

(d)
Load voltage waveform of proposed circuit @160rpm 100V/div (x10)

(e)
Load voltage waveform of Traditional FR @100rpm 100V/div(x10)

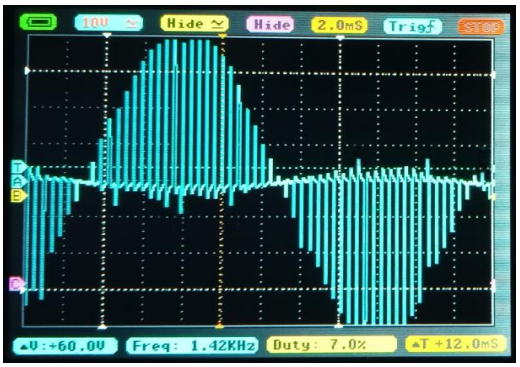

(f)
Load voltage waveform of proposed circuit @100rpm 100V/div (x10)

79*Figure 5.3: Load voltage variation utilizing traditional fan regulator vs. DC chopper fed controller for low speed levels*

5.3 FFT analysis of waveforms

Figure 5.4 shows FFT analysis for load voltage of DC chopper fed controller and traditional fan regulator. It is clearly seen that the traditional fan regulator gives higher number of low order harmonics while DC Chopper fit controller drastically eliminates them. So, proposed circuit gives much more hope in terms of quality output voltage to the fan.

However there are some discrepancies between simulated FFT analysis and practically obtained FFT analysis. Waveform oscillations of traditional fan regulator circuit, voltage spikes seen in the DC chopper fed controller…etc. could be the reason for this divergence.

(a)
Load voltage waveform of traditional EFR @100rpm 200V/div

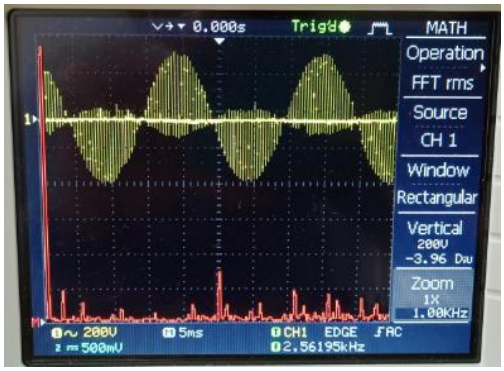

(b)
Load voltage waveform of proposed circuit @100rpm 200V/div

(c)
Load voltage waveform of Traditional EFR @185rpm 200V/div

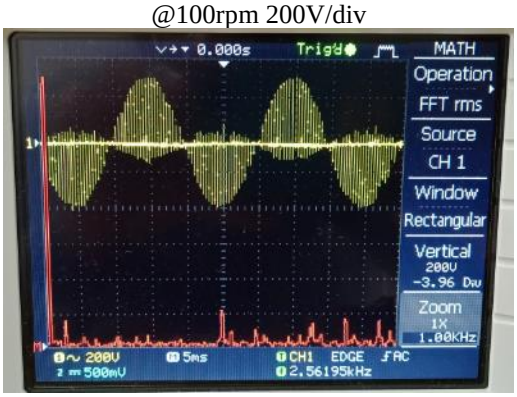

(d)
Load voltage waveform of proposed circuit @185rpm 200V/div

80*Figure 5.4: FFT analysis of load voltage*

Figure 5.5 shows FFT analysis for load current of DC chopper fed control and traditional fan regulator. Since higher content of current harmonics exists in traditional fan regulator, it generates more copper losses than the proposed circuit.

Obtained current waveform for DC chopper fed controller is almost sinusoidal. Some notice can be seen in the peaks and valleys of this waveform. Since load experiences high voltage variances in peaks and valleys, di/dt is high at this portion. Hence, notches exist($\frac{V}{L} = \frac{di}{dt}$).

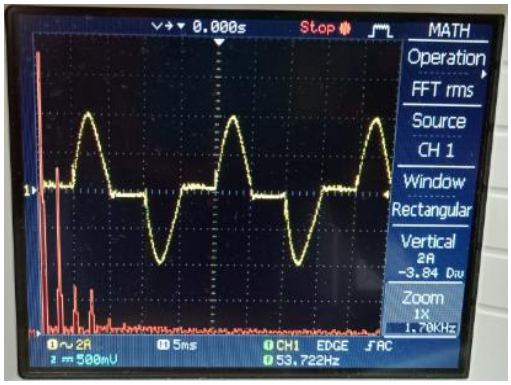

(a)
Load current waveform of Traditional EFR @160rpm 200mA/div

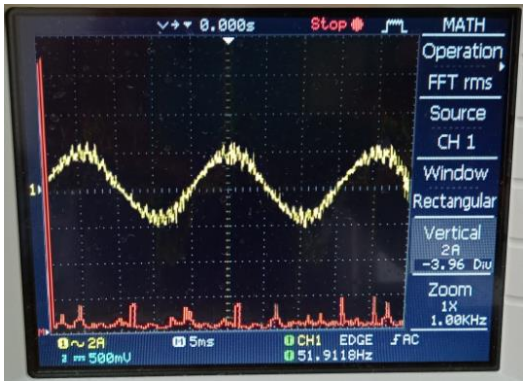

(b)
Load current waveform of proposed circuit @160rpm 200mA/div

(c)
Load current waveform of Traditional EFR @100rpm 200mA/div

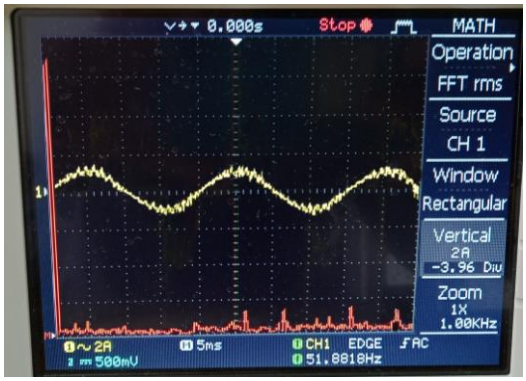

(d)
Load current waveform of proposed circuit @100rpm 200mA/div

81Figure 5.5: FFT analysis of load current

As explained in chapter 4 - subsection 7(input filter design), proposed circuit causes pulsating current at the input. Hence an input filter was designed and constructed. Input waveforms (figure 5.6) were also captured and compared to investigate how each regulator interacts with its nearby equipment and how much harmonic current it draws from the power supply.

As same as in the previous situation, FFT of traditional fan regulator consist of higher number of low order current harmonics. These low order current

harmonics are difficult to filter using low-cost input filters. Proposed circuit itself also generates harmonic currents too. However, these harmonious can easily demarcate from the power frequency and easy to eliminate by utilizing low cost input filters. Figure 5.6(b) shows input current waveform of the proposed circuit with damped input filter. Although it shows some noises, it roughly gives sinusoidal waveform at the input. This result can be improved by accounting ESR value of capacitors, internal resistance of inductors…etc. into the filter design calculations.

(a)
Input current waveform of traditional EFR @100rpm 200mA/div

(b)
Input current waveform of proposed circuit @100rpm 100mA/div

82*Figure 5.6: FFT analysis of input current*

CHAPTER 6

CONCLUSION

Introduction

Chapter 5 of this research was dedicated to compare the performance of DC chopper fed controller against traditional electronic fan regulator in different aspects. This chapter explains how the proposed fan regulator met the aim and objective of this study, its importance and recommendation for future work.

6.1 Conclusion remarks

As explained in chapter 1, the aim of this research was to develop an affordable electronic fan regulator with reduced harmonics and ripple free speed. Out of six different power electronic based control methods, DC chopper fed controller showed comparatively most viable solution. Unlike traditional fan regulator, DC chopper fit controller feeds current continuously to the load. Hence it minimizes speed ripples. FFT results in chapter 5 suggested the reduced load current and voltage harmonic content compared to traditional electronic fan regulator. Also this fan regulator generates much less input current harmonics with damped filter. Since the input current harmonics generated were not multiples of power frequency, low cost input filters can be utilized too. Also the efficiency of this chopper circuit was calculated too. According to the calculations, it shows 81% efficiency. However, this could be improved by better PCB designs, tuning input filter, snubber and gate resistor circuits etc.

However compared to traditional fan regulator, cost of DC chopper fed controller shows somewhat high cost of production. Compared to other five methods, this controller stays second lowest in price. Also this controller needs two auxiliary power supply for active switches and one for power up the microcontroller.

Moreover, the developed prototype uses software coded PWM for MOSFET switches. This is another reason for discrepancies between simulated and practically obtained results. However, more cleaner waveforms could be acquired from microcontrollers having hardcoded peripherals for power electronic PWM.

Apart from that, DC chopper fed controller shows some other merits over traditional fan regulator too. It improves the lifetime of electronic components by having freewheeling path and less amount of ringing. It also offers a smooth controlling by having less reverse recovery times and less amount of ringing.

After carrying out this research, a novel electronic fan regulator was identified having smooth control capabilities, less humming noises, less mechanical oscillations and less internal heating of the fan compared to traditional electronic fan regulator. Ceiling fan industries can develop this product with less production cost by utilizing double sided PCB with SMD components, multi-output SMPS for auxillary power etc.

6.2 Recommendations for future work

Since the fan controller unit utilizes a microcontroller, this can easily be integrated to modern smart homes and use voice-activated device control methods (Ex: Google assistant) to operate.

Proposed circuit utilizes MOSFETs as active switches. However by selecting active switches like IGBTs and proper cooling methods, same design could be used to control high power single phase induction motors.

REFERENCES

[1] S.J. Chapman, "Electric Machinery Fundamentals", 4th edition, New York: McGraw-Hill, 2003, pp. 656-657.

[2] M.D.A.K Wijerathna, "Remote Control Hum Less Fan Controller Unit", MSc thesis, Electrical Engineering, University of Moratuwa, 2010.

[3] S. Waghare, D. R. Tutakne, A. Deshmuk, M. Mardikar, "PWM controlled high power factor single phase Fan regulator", Proceedings of the Third International Conference on Electronics Communication and Aerospace Technology, IEEE Xplore ISBN: 978-1-7281-0167-5.

[4] K. Ambhorkar, A.K. Rana, P. Jain, D.R. Tutakne, "Single Phase AC-AC Converter with Improved Power Factor for Efficient Control of Fan Motors", 7th India International Conference on Power Electronics (IICPE), Nov, 2016.

[5] A. Julian, R. Wallace and P.K sood, "Multi-speed control of single phase induction motors for blower applications", IEEE Transactions on Power Electronics, Vol. 10, No.1, January 1995.

[6] M. S. J. Asghar, "Smooth speed control of single-phase induction motors by integral-cycle switching," IEEE Transactions on Energy Conversion, Vol. 14, Issue 4, Dec. 1999, pp. 1094-1099.

[7] D. Yildirim and M. Bilgic, "PWM AC chopper control of single phase induction motor for variable-speed fan application", 2008, 34th Annual Conference of IEEE Industrial Electronics.

[8] C. Young, C.Liu and C.Liu, "New inverter-driven design and control method for two phase induction motor drives", IEE proceedings on electric power application, Vol 143, No. 6, Nov 1996, pp. 458-466.

[9] D. G Holmes, and A. Kotsopoulos, "Variable speed control of single and two phase induction motors using a three phase voltage source inverter", Proceedings of IEEE conference, 1993, pp 613-620.

[10] Q. Kabashi, M. Limani, N. Caca, M. Zabeli, "The impact of sampling frequency and amplitude modulation index on low order harmonics in a 3-phase SV-PVM voltage source inverter", Turkish Journal of Electrical Engineering & Computer Sciences, January 2017, pp 184-199

[11] D. Ishak, T.L. Tiang , S.K. Choy, “Performance Evaluation of Permanent Split Capacitor Single-Phase Induction Motor for Ceiling Fan Application”, 18th International Conference on Electrical Machines and Systems(ICEMS), Oct 25-28, 2015.

[12] M. F. Rahman and L. Zhong, "A Current-Forced Reversible Rectifier Fed Single-phase Variable Speed Induction Motor Drive, “Proceedings of IEEE Conference, 1996,pp. 114-119.

[13] M. F. Rahman and L. Zhong, "A Singlemwo-Phase, Regenerative, Variable Speed, Induction Motor Drive with Sinusoidal Input Current," Proceedings of IEEE Conference, 1995, pp. 584-590.

[14] I. Badran, A. Lateef and M. T. Lazim “Harmonics Phase Shifter for a Three-Phase System with Voltage Control by Integral-Cycle Triggering Mode of Thyristors”, American Journal of Applied Sciences, Nov, 2008.

[15] M. F. Rahman and L. Zhong, "A Variable Speed Single Phase Induction Motor Drive using a Smart Power Module, Proceedings of the 1996 IEE Power Electronics and Variable Speed Drives Conference, 23-5 Sept. 1996, Conference Publication No. 429, pp. 407-412.

[16] M. B. R. Correa, C. B. Jacobina, A. M. N. Lima, E. R. C. Lima and E.R.C. da Silva, " Rotor-Flux-Oriented Control of a Single-phase Induction Motor Drive", IEEE Transactions on Industrial Electronics, Vol. 47, No. 4, August 2000, pp. 832- 841.

[17] R. W. Erickson, “Optimal Single Resistor Damping of Input Filter”, IEEE Applied Power Electronics Conference and Exposition, APEC ’99, Vol. 2, 14-18 March 1999, pp.1073 - 1079.

[18] T. J. E. Miller, J. H. Gliemann, C. B. Rasmussen, D. M. Ionel, “Analysis of a tapped-winding capacitor motor,” International Conference on Electrical Machines (ICEM 98), Istanbul, Turkey, Sep. 2-4, 1998, pp. 581-585

[19] K. Sundareswaran and P. S. Manujith, “Analysis and performance evaluation of triac-voltage controlled capacitor run induction motor,” Electric Power Components and Systems, 2004, pp. 913-925

[20] V. Thanyaphirak , V. Kinnares and A. Kunakorn, “PWM AC Chopper Control Schemes for Energy Saving of Single-Phase Induction Motors”, 10th International Power & Energy Conference (IPEC), Dec. 2012, pp. 82 – 87.

[21] K. Samidurai; G. S. Ilango and K. Thanushkodi “Performance Comparison of Single-Phase Power Electronic Controllers”, 4th International Power Engineering and Optimization Conference (PEOCO), June 2010, pp. 107-111.

[22] S. Manias, “Power Electronics and Motor Drive Systems”, 1st edition, Massachusetts: Academic Press, 2016, pp 183-269.

[23] A. Maamoun, “Development of Cycloconverters”, Canadian Conference on Electrical and Computer Engineering (IEEE CCECE), 2003, pp. 521 – 524.

[24] T. Islam, H. H. Fayek, E. Rusu and F. Rahman, “Triac Based Novel Single Phase Step-Down Cycloconverter with Reduced THDs for Variable Speed Applications”, Applied Sciences, Vol 11, No. 18, 2021.

[25] S. A. Nasar, “Theory and Problems of Electrical Machines and Electro Mechanics, 2nd edition, New York: McGraw-Hill, 1997, pp 154 – 156.

[26] A. S. Ba-Thunya, R. Khopkar, K. Wei and H.A. Toliyat, “Single phase induction motor drives - A literature survey” , IEEE International Electric Machines and Drives Conference, 2001, pp. 911 - 916

[27] R. K. Rao, P. Srinivas, M. V. S. Kumar, “Design and Analysis of Various Inverters Using Different PWM Techniques”, The International Journal of Engineering and Science (IJES) 2014, pp. 41-51

[28] https://nilambaraelectronics.com (Accessed on: May. 24, 2021)

[29] https://www.orelstore.lk (Accessed on: May. 24, 2021)

[30] https://scionelectronics.com/product/pic16f628a-original/

[31] https://www.microchip.lk/product/atmel-atmega328p-pu-atmega-328p-pu-microcontroller-dip-28/ (Accessed on: May. 24, 2021)

[32] https://www.dialog.lk/smart-fan-controller (Accessed on: June. 1, 2021)

APPENDICES

Appendix A: Matlab code for DB3 diac

```
function [S1,S2]  = fcn(u)

if u>32 || u<-29  %DB3 taken, breakover=32V breakover symmetry=3V
    S1=1;
    S2=1;

else
    S1=0;
    S2=0;
end
```

Appendix B: Matlab code for triggering back-to-back thyristors after detecting a necessary zero crossing point

```
function y = fcn(u)
persistent k;        %%k is local.retains value between calls
if isempty(k)
   k=0;
end
if u==1
    k=k+1;
end
    if(k<=9)
        y=5;
    elseif (k>=10 && k<=16)
        y=0;
    else
        k=0;
        y=0;
    end
end
```

Appendix C: Matlab code for switching of non-conventional cyclo converter

```
function y = fcn(a,b) %% y is output,
                      %%'a' is for i/p of PWM
                      %%b gives source voltage polarity

    if (a==1 && b>=0)
        y=1;
    elseif (a==1 && b<0)
        y=0;
    elseif (a==0 && b<0)
        y=1;
    elseif (a==0 && b>=0)
       y=0;
    else
        y=0;
    end

end
```

Appendix D: Arduino code for DC chopper fed controller

```
#include <IRremote.h>


unsigned long p_time=0,n_time;
int a=3,b=4;
const int prd=400;  //period in micro seconds
int on_time=prd/2;
int x=2;  //arbitary val to check the code has gone into increase speed or decrease


int receiver = 7; // Signal Pin of IR receiver to Arduino Digital Pin 7
IRrecv irrecv(receiver);     // create instance of 'irrecv'
decode_results results;      // create instance of 'decode_results'


void setup()
{
  irrecv.enableIRIn();      // Starts the receiver
  pinMode(a,OUTPUT);        //main switching signal
  pinMode(b,OUTPUT);        //aux. switching signal
   delay(500);
}
```

```
void loop()
{

    if (irrecv.decode(&results))
     {
         IR();
         irrecv.resume();
     }
  n_time = micros();

     if (n_time - p_time <=prd )          //prd
     {

                          if(on_time>=(n_time - p_time))      //on time
                         {
                         digitalWrite(b,LOW);
                         delayMicroseconds(2);
                         digitalWrite(a,HIGH);
                          }
                              else                    //off time
                             {
                         digitalWrite(a,LOW);
                         delayMicroseconds(2);
                         digitalWrite(b,HIGH);
                             }
      }
```

```
      else                //when micros exceeds 400us do this
        {
         p_time=n_time;
        }


}
void IR()    //increment and decrement
{
           if(results.value==0xFFA857 || (results.value==0x57D22309&&x==1))
            {
                 on_time = on_time+prd/10;
                  if( on_time >= prd ) //prd
                   {
                      on_time=prd; //prd
                   }
            x=1;
            }


             if(results.value==0xFFE01F || (results.value==0x57D22309&&x==0))
            {
                 on_time = on_time-prd/10;
                   if( on_time <= 0 )
                   {
                     on_time=0;
                    }
            x=0;
            }
}
```

Appendix E: Datasheet of IRF840

IRF840

RoHS-compliant Product

Advanced Power Electronics Corp.

N-CHANNEL ENHANCEMENT MODE POWER MOSFET

- ▼ Ease of Paralleling
- ▼ Fast Switching Characteristic
- ▼ Simple Drive Requirement

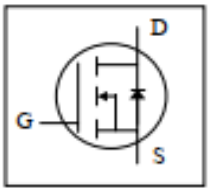

BV_{DSS}	500V
$R_{DS(ON)}$	0.85Ω
I_D	8A

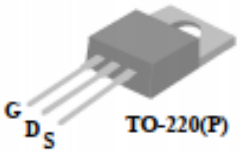

Description

APEC MOSFET provide the power designer with the best combination of fast switching , lower on-resistance and reasonable cost.

The TO-220 and package is universally preferred for all commercial-industrial applications. The device is suited for switch mode power supplies ,DC-AC converters and high current high speed switching circuits.

Absolute Maximum Ratings

Symbol	Parameter	Rating	Units
V_{DS}	Drain-Source Voltage	500	V
V_{GS}	Gate-Source Voltage	±20	V
I_D@T_C=25℃	Continuous Drain Current, V_{GS} @ 10V	8	A
I_D@T_C=100℃	Continuous Drain Current, V_{GS} @ 10V	5.1	A
I_{DM}	Pulsed Drain Current[1]	32	A
P_D@T_C=25℃	Total Power Dissipation	125	W
	Linear Derating Factor	1	W/℃
E_{AS}	Single Pulse Avalanche Energy[2]	320	mJ
I_{AR}	Avalanche Current	8	A
T_{STG}	Storage Temperature Range	-55 to 150	℃
T_J	Operating Junction Temperature Range	-55 to 150	℃

Thermal Data

Symbol	Parameter		Value	Unit
Rthj-c	Thermal Resistance Junction-case	Max.	1.0	℃/W
Rthj-a	Thermal Resistance Junction-ambient	Max.	62	℃/W

Electrical Characteristics@T_J=25°C(unless otherwise specified)

Symbol	Parameter	Test Conditions	Min.	Typ.	Max.	Units
BV_{DSS}	Drain-Source Breakdown Voltage	V_{GS}=0V, I_D=1mA	500	-	-	V
$R_{DS(ON)}$	Static Drain-Source On-Resistance	V_{GS}=10V, I_D=4.8A	-	-	0.85	Ω
$V_{GS(th)}$	Gate Threshold Voltage	V_{DS}=V_{GS}, I_D=250uA	2	-	4	V
g_{fs}	Forward Transconductance	V_{DS}=10V, I_D=4.8A	-	4.2	-	S
I_{DSS}	Drain-Source Leakage Current (T_J=25°C)	V_{DS}=500V, V_{GS}=0V	-	-	25	uA
	Drain-Source Leakage Current (T_J=125°C)	V_{DS}=400V, V_{GS}=0V	-	-	250	uA
I_{GSS}	Gate-Source Leakage	V_{GS}=±20V	-	-	±100	nA
Q_g	Total Gate Charge[3]	I_D=8A	-	45	72	nC
Q_{gs}	Gate-Source Charge	V_{DS}=400V	-	7	-	nC
Q_{gd}	Gate-Drain ("Miller") Charge	V_{GS}=10V	-	25	-	nC
$t_{d(on)}$	Turn-on Delay Time[3]	V_{DD}=250V	-	12	-	ns
t_r	Rise Time	I_D=8A	-	31	-	ns
$t_{d(off)}$	Turn-off Delay Time	R_G=9.1Ω,V_{GS}=10V	-	48	-	ns
t_f	Fall Time	R_D=31Ω	-	33	-	ns
C_{iss}	Input Capacitance	V_{GS}=0V	-	1250	2000	pF
C_{oss}	Output Capacitance	V_{DS}=25V	-	270	-	pF
C_{rss}	Reverse Transfer Capacitance	f=1.0MHz	-	85	-	pF
R_g	Gate Resistance	f=1.0MHz	-	1.6	2.4	Ω

Source-Drain Diode

Symbol	Parameter	Test Conditions	Min.	Typ.	Max.	Units
V_{SD}	Forward On Voltage[3]	T_j=25℃, I_S=8A, V_{GS}=0V	-	-	1.5	V
t_{rr}	Reverse Recovery Time[3]	I_S=8A, V_{GS}=0V,	-	515	-	ns
Q_{rr}	Reverse Recovery Charge	dI/dt=100A/μs	-	8.6	-	uC

Notes:

1.Pulse width limited by Max. junction temperature.

2.Starting T_j=25°C , V_{DD}=50V , L=10mH , R_G=25Ω

3.Pulse test

THIS PRODUCT IS ELECTROSTATIC SENSITIVE, PLEASE HANDLE WITH CAUTION.

THIS PRODUCT HAS BEEN QUALIFIED FOR USE IN CONSUMER APPLICATIONS. APPLICATIONS OR USE IN LIFE SUPPORT OR OTHER SIMILAR MISSION-CRITICAL DEVICES OR SYSTEMS ARE NOT AUTHORIZED.

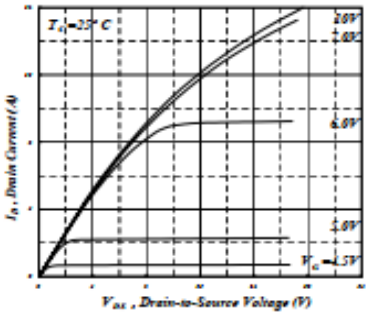

Fig 1. Typical Output Characteristics

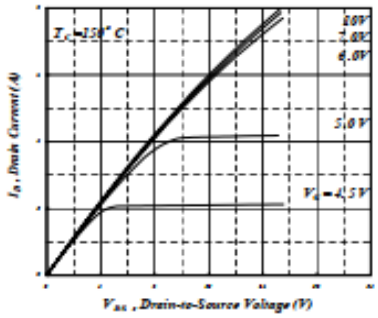

Fig 2. Typical Output Characteristics

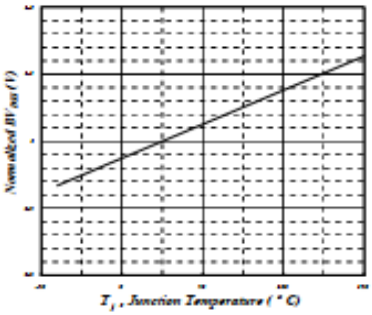

Fig 3. Normalized BV_{DSS} v.s. Junction Temperature

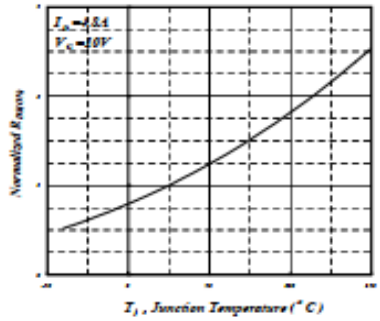

Fig 4. Normalized On-Resistance v.s. Junction Temperature

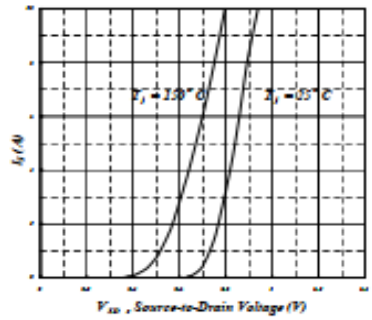

Fig 5. Forward Characteristic of Reverse Diode

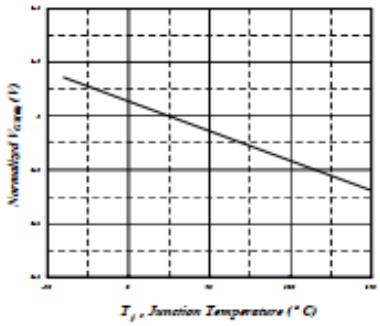

Fig 6. Gate Threshold Voltage v.s. Junction Temperature

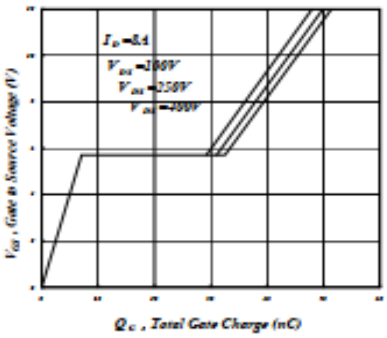

Fig 7. Gate Charge Characteristics

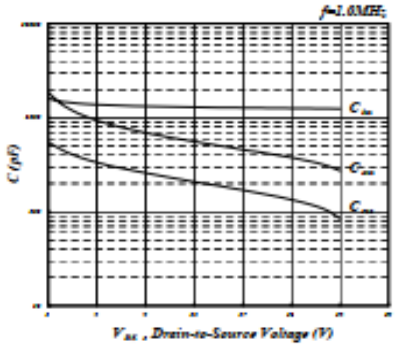

Fig 8. Typical Capacitance Characteristics

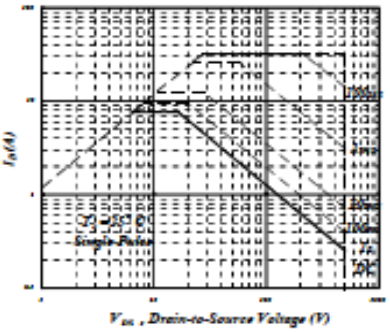

Fig 9. Maximum Safe Operating Area

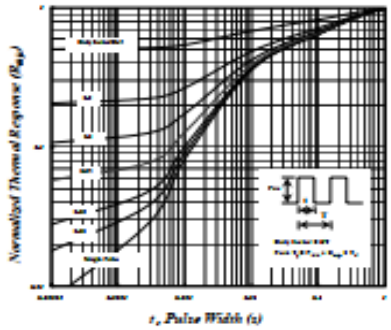

Fig 10. Effective Transient Thermal Impedance

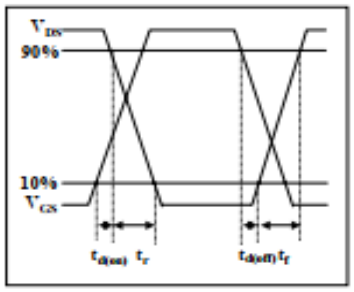

Fig 11. Switching Time Waveform

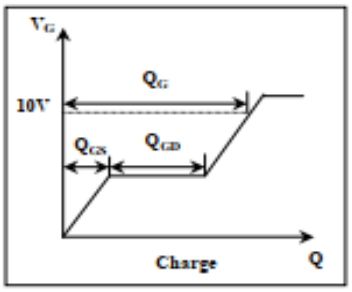

Fig 12. Gate Charge Waveform